The Effects of GMS Immunity-Related GTPases on Guanylate-Binding Proteins, Protein Aggregate Formation, and Macroautophagy

by

Maria Traver

Department of Molecular Genetics and Microbiology
Duke University

Date:_____

Approved:

_____
Gregory Taylor, Supervisor

_____
Raphael Valdivia

_____
Jörn Coers

_____
Patrick Seed

_____
David Pickup

Dissertation submitted in partial fulfillment of
the requirements for the degree of Doctor
of Philosophy in the Department of
Molecular Genetics and Microbiology in the Graduate School
of Duke University

2013

ABSTRACT

The Effects of GMS Immunity-Related GTPases on Guanylate-Binding Proteins, Protein Aggregate Formation, and Macroautophagy

by

Maria Traver

Department of Molecular Genetics and Microbiology
Duke University

Date:_____

Approved:

_____
Gregory Taylor, Supervisor

_____
Raphael Valdivia

_____
Jörn Coers

_____
Patrick Seed

_____
David Pickup

An abstract of a dissertation submitted in partial
fulfillment of the requirements for the degree
of Doctor of Philosophy in the Department of
Molecular Genetics and Microbiology in the Graduate School of
Duke University

2013

Abstract

The Immunity-Related GTPases (IRGs) are a family of dynamin-like proteins found in vertebrates that play critical roles in cell-autonomous resistance to bacteria and protozoa. The IRGs are divided into two subfamilies, with the GMS IRGs exerting a regulatory function over the GKS IRGs, affecting GKS IRG expression, localization, and ultimately function. The profound loss of host resistance seen in mice lacking the GMS protein Irgm1 suggests that GMS IRGs may additionally have broader functions beyond the regulation of GKS IRGs, though the nature of these functions remains poorly understood. In this dissertation, we address the regulatory functions of GMS IRGs in mouse cells.

We first addressed regulation of GKS IRGs (Irga6 and Irgb6) by GMS IRGs (Irgm1 and Irgm3). We found that in both fibroblasts and macrophages lacking these GMS IRGs, that the GKS IRGs relocalized to form punctate structures that were ubiquitin-, p62-, and LC3-positive. A biochemical analysis indicated that the GKS IRGs were directly ubiquitinated through K63 linkages. Collectively, these results suggested that GMS IRGs regulate aggregation of GKS IRGs and their transfer to autophagosomes through one of at least two possible mechanisms -- by the direct association of GMS IRGs with GKS IRGs to block their aggregation that subsequently leads to autophagic removal, and/or by directly promoting autophagic removal of spontaneously forming GKS aggregates. The latter hypothesis was addressed using a series of complementary

assays, which ultimately showed that absence of Irgm1 has no effect on the maturation of autophagosomes in fibroblasts, and only a very small and statistically insignificant effect in macrophages. Thus, we conclude that the major mechanism through which GMS IRGs regulate GKS IRGs is by directly inhibiting their aggregation, rather than through general effects on autophagic initiation or maturation of GKS IRG-containing autophagosomes.

We also addressed the possibility of broad regulatory functions of GMS IRGs beyond the regulation of GKS IRGs by examining whether GMS IRGs can affect another family of dynamin-like GTPases, the guanylate-binding proteins (GBPs). Despite no previous evidence of interactions between these two protein families, we found that the absence of GMS IRGs had striking effects on the localization of the murine Gbp2, leading it to colocalize with GKS IRG aggregates formed as a consequence of GMS IRG deficiency. We further demonstrated that unlike the GKS IRGs, Gbp2 was not tagged with K63-linked ubiquitin chains, which might have targeted it for specific macroautophagy, implying that Gbp2 is not aggregating in the absence of Irgm1. We then showed both that Gbp2 forms puncta in the presence of generic protein aggregates, and that guanylate-binding proteins including Gbp2 promote the degradation of GKS IRG protein aggregates. These findings suggest that GMS IRGs do not exert direct control over GBPs, but rather that GBPs are involved in the macroautophagic

degradation of protein aggregates as a primary function, and are thus influenced indirectly by GMS IRGs.

In total, our experiments contribute to the understanding of regulatory interactions among GMS IRGs, GKS IRGs, and GBPs. These results will be important in establishing the mechanisms through which these important families of proteins influence eradication of bacterial and protozoan pathogens through key innate immune mechanisms.

Dedication

This work is dedicated to the memory of Dr. Moisés Galí Sanchez (1925-2011), who first introduced me to true scientific inquiry.

Contents

List of Tables

List of Figures

List of Abbreviations

ANOVA : analysis of variance

Apgy : autophagy

Baf : bafilomycin A1

BMM : bone marrow-derived macrophage

C/EBP-β : CCAAT / enhancer-binding protein β

CSF : colony-stimulating factor

CTL : control

DNA : deoxyribonucleic acid

ER : endoplasmic reticulum

ERK : extracellular signal regulated kinase

FACS : fluorescence-activated cell sorting

GAP : GTPase activating factor

GAS : γ-activated sequences

GATE : gamma-interferon-activated transcriptional element

GBP : guanylate-binding protein

Gbp$^{(Chr\ 3)}$KO : knockout of all Gbp genes found on chromosome 3

GeLC – MS/MS : gel liquid chromatography tandem mass spectrometry

GFP : green fluorescent protein

GKS : glycine-lysine-serine

GMS : glycine-methionine-serine

GTPase : guanosine tri-phosphatase

HSD : honestly significant difference

IFN : interferon

IFNAR : interferon alpha/beta receptor

IFNGR : interferon gamma receptor

IP : immunoprecipitation

IRF : interferon regulatory factor

IRG : immunity-related GTPase

ISGF : interferon-stimulated gene factor

ISRE : interferon-stimulated response element

JAK : Janus-activated kinase

K63 : lysine 63

KO : knockout

LC3 : light-chain 3

LIR : LC3 interacting region

LPS : lipopolysaccharide

MAPK : mitogen-activated protein kinase

MEF : mouse embryonic fibroblast

MEK : mitogen-activated protein kinase / ERK protein kinase

mTOR : mammalian target of rapamycin

NBR1 : neighbor of BRCA1 gene 1

PI3K : phosphoinositide-3-kinase

PKC : protein kinase C

PLSD : protected least significant difference

siRNA : small interfering ribonucleic acid

SLR : sequestosome-like receptor

SNP : single nucleotide polymorphism

SQSTM1 : sequestosome 1 (p62)

STAT : signal transducer and activator of transcription

tf-LC3 : tandem fluorescent LC3

TUBE : tandem ubiquitin binding entity

WT : wild-type

Acknowledgements

With the knowledge that "No man is an island" (John Donne), a maxim which is increasingly true for scientific researchers, there are many people whom I would like to thank for enabling the completion of this body of work.

First and foremost, the principal investigator of this project, Dr. Gregory Taylor, was crucially and inextricably involved at every point of this work, from conception through experimentation and analysis to manuscript preparation and presentation. His countless hours of patient guidance at every stage of this project were essential to its intellectual development and eventual fruition. Even more than his tireless efforts to help achieve the goals of this work, however, I appreciate Dr. Taylor's emphasis on my own personal professional development, ensuring that I received the opportunities needed to mature intellectually as a scientist and safeguarding my sanity through the typical turbulence of the research endeavor. I will be forever grateful for the incredible opportunity he provided me, and I wish him every success in his future work.

I also need to thank Dr. Jörn Coers and Dr. Raphael Valdivia for contributing significant time and effort in raising the intellectual level of this work. Whenever I reached a significant hurdle in this research, whether technical or scholarly, these two outstanding scientists volunteered their time to provide essential critical analyses, excellent suggestions on key future experimentation, and often generously donated research materials and equipment to further the aims of this project. Their help played a

vital role at key junctures in this process, and they deserve much credit for the eventual outcome of this project.

I would never have completed the work presented here were it not for my coworker and extraordinary friend Stanley "Chuck" Henry, a masters level microbiologist and technician extraordinaire in the Taylor lab. His technical expertise in the fine details of experimental design, and the vast quantities of time he spent instructing me in proper benchwork have been invaluable to my scientific development. More importantly, however, he has been the glue that held my sanity together throughout my graduate career, always ready with a sympathetic ear and a reassuring comment, or an ego-popping and soul-crushing but necessary kernel of truth when I most needed it. Chuck taught me the true meaning of resiliency, which is perhaps the most important skill I have learned these past few years. After a long and extremely successful career, Chuck is retiring at the end of this year, and I wish him a peaceful and fulfilling retirement.

I also need to thank my other more recent coworkers, Viviana Cantillana and Elyse Schmidt, for their help in completing this project. Viviana's no-nonsense approach with suppliers always ensured that I had the proper reagents when I needed them, and she always had a valuable and unique perspective when I presented my data during lab meetings. Elyse brought much-needed humor to my days and was always ready to

provide sympathy and understanding and a sense of a shared burden, for which I will be forever grateful.

There are several other scientists throughout the Duke community whom I need to thank for their contributions to this work. First, Dr. Yasheng Gao of the Duke light microscopy core facility provided excellent, personalized instruction in the use of the Leica SP5 confocal instrument for my tandem-fluorescent experiments, and always took the time to check in with me and ensure I was doing well. Dr. Will Thompson of the Duke proteomics core facility aided the development of the TUBE1 precipitation proteomic assay and ensured, even through his inordinately busy workload and the technical hurdles which surfaced, that this experiment was successfully completed. And finally, I need to thank Dr. Theodore Slotkin of the Duke Pharmacology department for his superior instruction in statistical analysis and the time he volunteered helping to analyze several of the experiments presented in this work.

Finally, I would like to acknowledge the many friends and family who have contributed, knowingly or unknowingly, to my health and well-being during the long graduate school years. Dr. Mark Happel, who paved the way for my own doctoral studies, always had excellent advice, and who taught me the most important rules for succeeding in graduate school, which for the sake of my career I will not repeat here. The greater North Carolina Irish dance community, including the Inis Cairde school and Rince Diabhal, who gave me an important athletic and creative outlet and the

extraordinary gift of their friendship. My extended family, who called on a regular basis, made me laugh, always listened, and made sure I took time off when I needed to. And finally, and most importantly, my husband, Clay, who is always there for me, in good times and bad. Even if he can't tell a gene from a protein, or tissue culture media from fish food, he still always respected me and my work enough to make incredible sacrifices to ensure the success of this project. He is the love of my life and the light of my soul, and words simply aren't enough to express my gratitude.

1. Introduction

1.1 Interferon-mediated innate immunity

1.1.1 The role of interferons in the innate immune response

In 1957, a substance was discovered which conferred a protective effect against viral infection on cells [1]. This protein was dubbed "interferon" for its ability to interfere with viral replication. The subsequent discovery of related cytokines, and the addition of *in silico* analyses of entire genomes, led to the realization that the original interferon was a member of a large family of pro-inflammatory cytokines that induce immune responses.

Interferons (often abbreviated as IFNs) can be divided into two categories, type I interferons and type II interferons. Type I interferons can be further divided into related subfamilies, including the more commonly studied IFN-α's and IFN-β, along with the more recently characterized IFN-ε, IFN-κ, and IFN-ω (all found in *Homo sapiens*) and other families found in other species (compiled and described by ref [2]). Type I interferons are vital to mounting a response to viral challenges; once pathogen-associated molecular patterns, such as viral envelope proteins or double stranded RNA, are detected by Toll-like receptors, signaling pathways are induced that activate the transcription factor NF-kappaB, which induces expression of innate immune cytokines such as type I interferons [3]. In contrast, there is only one type II interferon, IFN-γ, and this cytokine is expressed largely by T lymphocytes, in response to presented antigens,

and natural killer cells, in response to other cytokines [4], including IFN-γ itself [5]. The type II interferon response is most relevant to the work presented in this dissertation, and will be the focus of this discussion.

The cellular response to interferon induction is immediate and profound. Interferons function to promote the transcription of hundreds of genes with anti-pathogen activity, including antimicrobials and antivirals, chemokine/cytokine signalers, and antigen presentation pathways, while simultaneously repressing transcription of anabolic pathways such as lipid metabolism and the cell cycle [6-8]. As much as 25% of the overall macrophage transcriptome is affected by the interferon response [6]. In some cases, even cells which are not normally involved in immunity, such as astrocytes, can be induced by interferons to exhibit immune functions [9]. The signaling pathways which mediate these powerful changes in overall transcription within interferon-stimulated cells will be outlined in the next section.

1.1.2 Interferon signaling pathways

1.1.2.1 The canonical type I interferon signaling pathway

All of the many kinds of type I interferons bind the same cell surface receptor, called the type I cell surface receptor [2]. This receptor is composed of two subunits, IFNAR1 and IFNAR2; each of these subunits is associated with separate members of the Janus-activated kinase (JAK) family -- IFNAR1 with TYK2 and IFNAR2 with JAK1 [10]. Upon binding a type I interferon ligand, IFNAR1 and IFNAR2 dimerize and

autophosphorylate [10], which leads to activation of the two associated JAK proteins [11]. The JAK kinases then activate several other downstream signaling cascades.

The canonical and most-studied of these downstream pathways is mediated by STAT (signal transducer and activator of transcription) proteins. STATs 1-6 are all facilitators of the type I interferon response [12], although some are restricted to certain cell types [13-16]. JAK kinases phosphorylate STAT proteins in response to interferon stimulation, whereupon phosphorylated STAT proteins form homo- or hetero- dimers, which may also complex with other cofactors [10]. These complexes serve as transcription factors that recognize and bind to specific elements upstream of the promoters of interferon effector proteins [17]. The canonical STAT complex, called the ISGF3 complex (interferon-stimulated gene factor 3), contains a heterodimer of STAT1-STAT2 bound with the cofactor IRF9 [18,19]; this complex binds the sequence called the interferon-stimulated response element (ISRE) found upstream of many interferon-induced genes [17].

1.1.2.2 The canonical type II interferon signaling pathway

The canonical type II interferon signaling pathway is very similar to that of type I interferons, involving a separate cell surface receptor which also activates the signaling cascade of JAK kinases followed by STAT protein complexes. The cell surface receptor involved in the type II interferon response also consists of two subunits, IFNGR1 and IFNGR2; these associate with the kinases JAK1 and JAK2, respectively [11,20-22].

Similarly to the type I cell surface receptor, IFNGR1 and IFNGR2 dimerize and autophosphorylate in the presence of the interferon-γ ligand, which activates the two JAK proteins [10,21]. In contrast to the type I signaling pathway, however, activation of JAK1 and JAK2 leads to phosphorylation of only STAT1, on Tyr701, which then forms a homodimer [4,12,17]. This STAT1 homodimer acts as a transcription factor which binds a specific sequence call the gamma-activated sequence, or GAS [4,17,23]. Thus, in contrast to type I interferons which induce transcription of genes with many kinds of upstream elements, type II interferon STAT-mediated signaling specifically and only induces transcription of genes with upstream GAS elements.

1.1.2.3 STAT serine 727 phosphorylation pathways

While the canonical JAK-STAT signaling pathway is sufficient for inducing transcription of interferon-stimulated genes, a stronger transcriptional response can be engendered by the phosphorylation of STAT proteins on their serine 727 residue [24,25]. Mice engineered with a STAT1-S727A mutation succumb more readily to *Listeria monocytogenes* infection, indicating that this phosphorylation event plays an important role in innate immunity to bacterial infection [26]. The mechanisms of Ser727 phosphorylation are currently poorly understood, but in the case of interferon-γ signaling are known to involve the activation of a cascade beginning with JAK1/2 which eventually causes activation of PI3K, which ultimately activates PKC-δ, which is necessary for phosphorylation of STAT1 Ser727 [27-29]. The activation of PI3K by the

interferon signaling pathway is intriguing, as PI3K plays an important role in a variety of signal transduction pathways, including being an upstream activator of mTOR [30,31], a signal integrating protein which upregulates anabolic pathways while inhibiting catabolism [32,33]. mTOR and PI3K will be discussed further in section 1.4 of this dissertation, concerning the process of macroautophagy.

1.1.2.4 Non-canonical interferon signaling pathways

It is worth mentioning that in addition to the STAT-mediated signaling pathways just described, interferons also promote alternative signaling pathways which are independent of STAT activation, and in some cases independent of JAK kinases. These pathways are just beginning to be fully described, and may involve CRK proteins, p38 mitogen-activated protein kinases (p38 MAPKs), or PI3 kinases (for a review, see ref [34]). One non-canonical pathway relevant to the work discussed in this dissertation is a JAK-independent interferon-γ signaling cascade which has been shown to play a role in bacterial defense [35-37]. This cascade involves the MEK-ERK signaling pathway, which activates the transcription factor CCAAT/enhancer-binding protein-β (C/EBP-β) [35]. This protein binds to an enhancer sequence (separate from the canonical GAS sites) called the gamma-IFN-activated transcriptional element, or GATE [36]. Interestingly, STAT1 is necessary for this process, although the mechanism is unknown [35]. The C/EBP-β – GATE pathway may be important to the induction of macroautophagy [37], and will be discussed further in section 1.4 of this dissertation.

In summary, type I and type II interferons are important pro-inflammatory cytokines which upregulate the transcription of hundreds of effector proteins in response to viral and bacterial challenges, while repressing cell growth pathways. Interferon signaling pathways usually involve JAK kinases that promote the formation of STAT-containing transcription factors which bind specific enhancer sequences found upstream of promoters. Future work in the field of interferon signaling will continue to uncover novel signaling pathways, as well as elucidate the complex crosstalk between pathways activated by interferon cell surface receptors.

1.2 Immunity-related GTPases

1.2.1 Genetic and proteomic features of the IRG family

Among the many effector proteins induced by interferons is a family of ~47kDa GTPases known as the Immunity-Related GTPases, or IRGs. Members of this family have been found in mammals and some fish, though the number of genes per species varies widely, from 2 (in *Homo sapiens*) to 23 (in the C57Bl/6 strain of *Mus musculus*) [38,39]. Most of the known members are transcriptionally induced by interferon signaling pathways via multiple interferon-stimulated response elements (ISREs) and γ-activated sequence (GAS) elements in their promoter regions [38,40]. Notable exceptions which are not induced by interferon include members of the C subfamily [38] (see section 1.2.3, IRG subfamilies) and the human gene IRGM [39,41], all of which are constitutively expressed; additionally, members of the murine M subfamily are

constitutively expressed at very low levels but undergo strong expression when induced by interferon-γ (Taylor lab, unpublished data). Intriguingly, some IRG genes of the B subfamily in *Mus musculus* are expressed together on tandem transcripts (Irgb1-Irgb2 and Irgb4-Irgb5), although it is unknown if these transcripts are translated into one or two polypeptide chains [38].

The crystal structure of Irga6 is the only currently solved IRG protein structure, but it is thought to be a good model for other IRGs. This structure contains mainly alpha-helices, and consists of three domains: a short three-helix N-terminal domain, a GTP-binding domain, and an eight-helix C-terminal domain [42]. It should be noted that the most conserved domain across species is the G domain [38]; certain family members, most notably human IRGM, encode very truncated N-terminal and C-terminal domains [38].

1.2.2 IRGs belong to the dynamin superfamily

The dynamins are a superfamily of GTPases which share similar biochemical functions. These include involvement in vesicle formation, vesicle trafficking, and other aspects of lipid membrane remodeling, due to the ability of dynamins to bind and alter lipid membranes in various intracellular membrane-bound compartments, often after forming self-dimers and/or oligomers [43-45]. These abilities may be related to the unique functionality of the GTP-binding domain of dynamins. G domains are commonly thought of as biochemical "switches," with GTP-bound proteins being in the

biologically "active" state, while GDP-bound proteins are in an "inactive" state [46]; the canonical example is the Ras family of signal transducers. The dynamins, however, while still demonstrating some switch-like activity [47], are thought to primarily employ their GTP-binding ability differently. Instead of utilizing GTP only as a biochemical on/off switch, dynamins are thought to exploit the energy of GTP hydrolysis to undergo conformational changes which are necessary to their biological function, thus classifying them as "mechanoenzymes" [48]. Thus, the GTP-bound state of a dynamin can be thought of both as an "on" state, and as a "ready" state which can be quickly activated to perform necessary functions.

These characteristic features of dynamins are in fact mirrored in immunity-related GTPases, thus placing them functionally in the dynamin superfamily (though it should be noted there is little sequence homology outside of the G domain). The G domain of the immunity-related GTPases has been shown to possess GTPase functionality [49,50], although often only after dimerization, implying that IRGs share the dynamin penchant for self-oligomerization [42,49]. Additionally, localization of IRG proteins within the cell is, like dynamins, largely confined to intracellular membranes, a trait which is mediated both by lipidation sites found in certain family members [38][Taylor lab, unpublished data], and by amphipathic alpha-helices in the C-terminal domain (e.g. the αK helix of Irgm1) [51]. The lipidation sites which have so far been discovered include N-terminal MGxxxS myristolation sequences in eleven murine IRG

proteins [38,52]; of these, Irga6 is confirmed myristolated *in vitro* [53]. Additionally, murine Irgm1 has been identified as possibly being S-acylated [54], and has been confirmed both to be palmitoylated near the C-terminal domain αK helix, and that this motif is necessary for proper membrane localization (Taylor lab, unpublished data).

While IRGs share mechanisms of localization, the specific membranes to which they migrate differ by family member in *Mus musculus*. For instance, Irgm1 and Irgm2 localize to the Golgi apparatus [51,55,56], and Irgm1 is also seen very weakly on mitochondrial and lysosomal membranes [51,57,58]. In contrast, Irgm3 localizes strongly to the endoplasmic reticulum (ER), to discrete vesicles in the near vicinity of the ER, and to lipid droplets [50,59]. Irga6 and Irgb6, like Irgm3, appear predominately ER localized [51,60]. Presumably, these difference cellular locations instruct discrete cellular functions.

Interestingly, a functional GTPase domain is not necessary for correct initial localization of any of these IRGs [50,51], and thus activation of these proteins is unnecessary for proper initial localization. This finding implies that these membranes may be "holding pens" for inactive IRGs, and raises the interesting question of whether activated, GTP-hydrolyzing IRGs might relocate to other membranes. This has been found to be the case, as in cells containing membrane-bound pathogens, many IRGs relocate to pathogen-containing compartments, where they are thought to modulate membrane processing [55,61,62]. This processing, in turn, is postulated to impact the

survival of membrane-bound pathogens. We will further discuss these influences of IRGs on innate immunity in section 1.2.4; however, before we can fully discuss this topic, it is necessary to describe the various subfamilies of IRGs.

1.2.3 IRG subfamilies

Members of the IRG family are divided into nine subfamilies (named with the letters A-G, M, and Q) based on sequence similarities (Table 1) [38]. Note that IRG names are derived from the stem Irg + subfamily name + number (for example, Irgm3 is the third member of the M subfamily of IRGs). As mentioned above, IRGs are members of the dynamin superfamily, whose G domain is thought to be very important to their overall function; thus, major sequence differences in the G domain are the primary basis for the IRG subfamily classification [38].

There are two subfamilies of IRGs which contain striking sequence variations in their G domain. One of these, the Q (or quasi-) subfamily, has no members with GTP-binding motifs in their G domains, and thus its members are not well-studied [38]; this subfamily is not relevant to this dissertation and will not be further discussed. The other subfamily with a significant sequence variation in the G-domain is the M subfamily. In this group, a canonical peptide sequence in the p-loop of switch I of the conventional dynamin GTP-binding domain, glycine-lysine-serine, a sequence which is responsible for stabilizing the bound nucleotide, has been changed to a glycine-methionine-serine sequence [40]. Members of the M subfamily of IRGs are often referred to as GMS IRGs,

while IRGs containing the conventional p-loop sequence are called GKS IRGs; this terminology will often be used in this dissertation.

This unique p-loop modification of GMS IRGs is thought to impact their GTP-binding capabilities as compared to GKS IRG subfamilies, a hypothesis which is supported by studies of the murine proteins Irgm3 and Irga6. Irgm3 is a member of the GMS IRG subfamily and contains the non-canonical p-loop sequence; it has been found to be greater than 90% GTP-bound *in vivo* [50]. In contrast, Irga6, which contains the conventional GKS p-loop sequence, displays a marked preference for binding GDP [49]. Utilizing the dynamin GTP-binding model, wherein GTP-bound dynamins can be readily activated, these findings imply that GMS IRGs are nearly always active within the cell, whereas GKS IRGs are largely inactive, but activatable by changing cellular conditions. The implications of this finding on the roles of these two types of IRGs in innate immunity will be discussed further in section 1.2.4.

The GKS IRGs comprise the remaining seven subfamilies of IRGs. Four of these subfamilies are not relevant to this dissertation, and will only be briefly described here for completeness. These subfamilies include subfamilies E – G, which have only been found in fish [38] and are thus not relevant to the mammalian systems utilized in this work; and the C subfamily, which exhibits no obvious functional relationship to other IRGs, is not induced by interferon, has only been found to be expressed in male testes, and is isolated on a separate chromosome from the other two IRG loci [38]. Since this

Table 1: IRG Subfamilies. Information summarized from ref. [38].

P-loop sequence	Subfamily Name	Species	Notable Features	Relevant to this work?
GMS	**M**	*Mus musculus* *Canis familiaris* *Pan troglodytes* *Homo sapiens*	Non-canonical sequence in GTP-binding domain	Yes
GKS	**A**	*Mus musculus*		Yes
	B	*Mus musculus* *Canis familiaris*		Yes
	C	*Mus musculus* *Canis familiaris* *Pan troglodytes* *Homo sapiens*	Constitutively expressed in male testes	No
	D	*Mus musculus* *Canis familiaris*		Yes
	E	*Danio rerio*		No
	F	*Tetraodon nigriviridis* *Fugu rubripes* *Danio rerio*		No
	G	*Danio rerio*		No
GVS, GSS, GLV, or none	**Q**	*Danio rerio* *Mus musculus* *Homo sapiens*	G domain lacks GTP-binding motifs	No

subfamily is not thought to play a role in innate immunity, it will not be discussed further.

The three subfamilies of GKS IRGs which are relevant to this work include subfamilies A, B, and D, which have been found in both *Mus musculus* and *Canis familiaris*, but notably not in *Pan troglodytes* or *Homo sapiens* [38]. More on the functions of these subfamilies, along with the GMS IRGs, in innate immunity will be discussed in section 1.2.4.

1.2.4 The IRG family in innate immunity

1.2.4.1 Innate resistance to membrane-bound pathogens

As we have discussed above, the immunity-related GTPases are a family of small, interferon-inducible, functional GTPases belonging to the dynamin superfamily of membrane-processing proteins. The induction of IRGs by cytokines which induce innate immune responses, along with their localization to membranes, suggest that IRGs might be involved in immune defense against intracellular membrane-bound pathogens. This has been found to be true, as absence of murine Irgm1, a member of the GMS IRGs, leads to a striking susceptibility to multiple membrane-bound intracellular organisms, including *Toxoplasma gondii* [55,63], *Salmonella typhimurium* [64], *Listeria monocytogenes* [63], *Chlamydia trachomatis* [65,66], and *Mycobacterium* species [67,68]. Loss of Irgm3 also leads to susceptibility against *Toxoplasma gondii* [69,70]. However, no consensus has been reached on the mechanism by which IRGs confer this resistance.

One hypothesis describing the mechanism of IRG action involves direct modulation of pathogen-containing membranes by IRGs. Many of the murine GKS

IRGs have been shown to converge on the pathogen-containing membranes. Irga6, Irgb6, and Irgd were shown to localize *Toxoplasma gondii*-containing phagosome; this localization was correlated with stripping of the phagocytic membrane, exposing the parasite to the cytoplasmic environment and resulting in its death [61]. Irga6 localized to this compartment only when it was GTP-bound, implying that it must be activated for this localization to occur [71]. In the case of infection with *Chlamydia trachomatis* (though notably not *Chlamydia muridarum*), Irga6, Irgb6, and Irgd all localized to chlamydial inclusion membranes, but instead of stripping the membrane, these proteins appeared to target the inclusion to the macroautophagic pathway [72]. Macroautophagy is a lysosomal degradation pathway important to innate immunity, and will be discussed further in section 1.4.6 of this dissertation.

Additionally, certain GMS IRGs may also localize to phagosomes and inclusions. Upon engagement of a latex bead (which is used as a model pathogen with no defense mechanisms) with the phagocytic system, Irgm1 and Irgm3 have been shown to relocate to the phagocytic cup of the plasma membrane, and remain associated with the maturing phagosome [51,55]. Irgm2 and Irgm3 were additionally found to colocalize to *Chlamydia trachomatis* inclusion membranes [72]. Some controversy exists, however, about the ability of GMS IRGs to localize to pathogen-containing compartments. For example, Irgm1 has not been seen on compartments containing certain live pathogens,

including *Toxoplasma gondii* [55,73], *Mycobacterium tuberculosis* [57], *Listeria monocytogenes* [57], and *Chlamydia trachomatis* [73].

A second hypothesis ascribing a mechanism to IRG-mediated innate immune resistance utilizes findings relating the immunity-related GTPases to control of macroautophagy, a lysosomal degradative process with innate immune functions, such as the above-mentioned targeting of *Chlamydial* inclusions to lysosomes via this pathway. This hypothesis will be further explored in section 1.4.6 of this dissertation, after a discussion of the basic mechanisms of macroautophagy.

1.2.4.2 The GMS IRGs regulate the GKS IRGs

Intriguingly, absence of the GKS IRG proteins Irgd or Irga6 in mice results in relatively weak susceptibility phenotypes to intracellular pathogens as compared to GMS IRG deficiency [55,61,63]. One possible explanation for this difference is the previously mentioned finding that the p-loop sequence difference of GMS IRGs leads to its members being largely GTP-bound, and thus perpetually activated or in a "ready" state, whereas GKS IRGs are preferentially GDP-bound and thus are largely inactive. This hypothesis assumes, however, that IRGs play a largely redundant role in resistance, and thus the constitutively active forms play a greater role. Evidence contrary to this supposition, however, was demonstrated previously by our lab and others, all of whom found that the GMS IRGS have the ability to regulate the expression, localization, and activation of GKS IRG proteins [60,62,64]. For instance, in Irgm1- and Irgm3-deficient

cells, Irga6 and Irgb6 form large aggregate-like structures, decreasing their localization to pathogen-containing compartments [60,62]. This aggregation appears to largely consist of GTP-bound protein, raising the question of whether GMS IRGs prevent premature activation of GKS IRGs [62]. This ability of GMS IRGs to regulate GKS IRGs was further supported by yeast two-hybrid studies and GST-pulldowns which indicated direct interactions between GMS and GKS IRGs [62]. Additionally, a recent paper indicates that GMS IRGs collect on "self" membranous compartments, but not pathogen-containing vacuoles, and block the localization of GKS IRGs to these compartments [73]. Taken together, these findings have led to a model of IRG protein function in which GMS IRGs initially interact with and hold inactive the GKS IRGs, until direct infection of the cell; infection which triggers GKS IRG release and activation, trafficking specifically to the pathogen-containing vacuole (which does not contain GMS IRGs), and subsequent modulation of this membrane to promote immune functions.

In summary, the immunity-related GTPase protein family is a conserved family found throughout vertebrate species that plays an important role in interferon-induced innate immunity to pathogenic intracellular microbes. The GMS subfamily of IRGs contains a p-loop sequence difference which leads its members to be largely active; their functions appear to involve regulation of the typically inactive GKS IRGs. The specific functions of these proteins in innate immunity include modulation of pathogen-containing membranes and/or regulation of membrane trafficking processes such as

macroautophagy. Further research is necessary to fully determine all the mechanisms whereby this family enables innate immunity.

1.3 Guanylate-binding proteins

1.3.1 Genetic and proteomic features of the GBP family

A second family of GTPases which are induced by interferon-γ are the guanylate-binding proteins, or GBPs. Genes with at least 40% identity with a canonical GBP (in *Mus musculus*) have been found in a wide variety of vertebrate species, from zebrafish to primates, and the genomes of most species encode multiple GBPs [74-76]. These proteins have been studied most extensively in mice and humans. In *Mus musculus*, there are eleven GBP genes clustered on two chromosomes [74,77]; all of these proteins have ISREs and/or GAS elements near their promoters [74] and are induced very strongly by interferon signaling, and some are additionally induced by IL-1β and TNF-α [40,78-80]. In *Homo sapiens*, there are six GBPs and one GBP pseudogene in a cluster on chromosome 1, but similarly to the IRG family in humans, not all of these genes have ISREs or GAS elements upstream, indicating that several of these genes are likely not interferon-inducible [74]. Unlike the IRGs, guanylate-binding proteins have not been subdivided into subfamilies, and thus are named only with the root name Gbp and a number. It should be noted that the numbers assigned to genes do not necessarily correlate between species; thus, murine Gbp1 and human Gbp1 should not be assumed to be orthologues.

The crystal structure of human Gbp1 has been solved, and reveals a protein structure that resembles that of IRGs, minus the N-terminal helical domain [81]. In GBPs, a globular N-terminal G domain is followed by a C-terminal helical domain, although the helices are generally longer than those found in IRGs [81]. The G domain is very unique in several ways. Firstly, the domain lacks a N(T)KXD motif, which is typically required for specificity to guanine nucleotide binding, as opposed to adenosine nucleotide binding; nevertheless, the G domain appears to bind exclusively to guanine nucleotides, and does not bind or hydrolyze ATP, UTP, or CTP [82,83]. Additionally, the G domain of GBPs binds with nearly equal affinity to GTP, GDP, and GMP [82], and is the only known G domain which can catalyze hydrolysis of GTP to GMP [83]. Furthermore, a crystal structure of Gbp1 bound to a non-hydrolyzable GTP analogue reveals a unique GTP-binding site structure that prevents access of other proteins to the bound GTP, preventing the possibility of GAP-protein-induced hydrolysis [84]. Despite this extensive knowledge of the uniqueness of the G domain structure of GBPs, however, the effects of this uniqueness on GBP protein function are unknown.

Like the IRGs, GBPs contain motifs which indicate likely associations with membranes, including amphipathic helices [81,85] and lipid modification sites such as C-terminal isoprenylation motifs (CaaX) [81,85-87]. However, the exact localization sites of guanylate-binding proteins are not well elucidated. Several human GBPs, including human Gbp1, Gbp3, and Gbp5, and murine Gbp1, appear to be evenly distributed

throughout the cytoplasm [88,89]; the human GBPs Gbp2 and Gbp4 are localized to the nucleus in addition to the cytoplasm [88]. Other GBPs, including the murine Gbp2, appear to localize to cytoplasmic vesicles of unknown origin or function [89]. However, activation of the human GBPs Gbp1 and Gbp2 via aluminum fluoride treatment leads to the relocalization of these proteins to the Golgi apparatus [87,88], indicating that activation of GBPs leads to their relocalization, which may affect their functions. Additionally, human Gbp1 is able to attract Gbp2 and Gbp5 to the Golgi in a heterodimerization-dependent manner [86], indicating that membrane-associated GBPs can induce membrane association of others via complex formation.

1.3.2 The GBPs in innate immunity

The IRG family, as described previously, exhibits antimicrobial activity only towards bacteria and protozoa; no known anti-viral properties of these proteins have been described. In contrast, the GBP family is important to direct, cell-autonomous innate immunity against bacteria, protozoa, and viruses. Additionally, specific GBPs are important in assembly and function of inflammasomes, which promote inflammatory cytokine secretion and induce pyroptosis. We will briefly describe the role of GBPs in each of these three innate immune functions, with particular emphasis on their anti-bacterial roles, as this function has the most relevance to the work discussed in this dissertation.

One of the first functions ascribed to GBPs was a role in anti-viral activity. Both human and murine GBPs have demonstrated anti-viral activity against vesicular stomatitis virus and encephalomyocarditis virus [90,91]. Additionally, recent studies have ascribed antiviral properties to human GBPs in response to hepatitis C [92] and influenza [93]. Exact mechanisms of the anti-viral properties of GBPs are only beginning to be understood, but they appear to vary depending on the particular viral challenge based on differing needs for functional GTP hydrolysis [90-93]. Further work is necessary to determine exactly what role GBPs play in innate immunity against viruses.

More recent studies have discovered potent anti-microbial activities exhibited by GBPs in response to a variety of bacteria. Four seminal studies were particularly important to ascertaining the nature of these responses. The first study, in addition to identifying a number of murine GBPs, demonstrated that Gbp1, Gbp2, Gbp3, Gbp5, Gbp7, and Gbp9 colocalized with *Toxoplasma gondii*-containing vacuoles, but not vacuoles containing a highly virulent strain; this study was the first to identify a possible anti-microbial role for the GBP family [77]. In the second study, it was demonstrated that human Gbp1 and Gbp2 localize to *Chlamydia trachomatis* inclusions and, alone, inhibit their growth in a small but statistically significant manner; however, they have a greatly increased negative effect on *Chlamydia* proliferation in the presence of the rest of the interferon-γ-mediated response, indicating that GBPs likely work with other interferon-induced proteins to mediate innate immunity [94]. The third study involved

loss-of-function screens against each member of the murine GBP family, utilizing siRNA, dominant-negative mutations, and chromosomal deletion techniques, to determine which are important to defend against *Listeria monocytogenes* and/or *Mycobacterium bovis* (Mb BCG) [85]. The researchers found that Gbp1, Gbp5, Gbp6, Gbp7, and Gbp10 were all necessary to control growth of these bacterial species in macrophage-like cell lines [85]. The authors further demonstrated that Gbp1, Gbp3, Gbp7, and Gbp10 localized to pathogen-containing compartments via association with small vesicles which then fused with the pathogen-containing compartment [85]. They additionally showed that Gbp7 is important for assembly of NADPH oxidase, which generates superoxide species involved in the killing of pathogenic bacteria, and that Gbp1 and Gbp7 may be involved in macroautophagy [85], which will be discussed further in section 1.4.6 of this dissertation. Finally, the authors of the fourth study generated mice deficient for all five GBP genes found on the murine chromosome three, including Gbp1, Gbp2 (which has two splice forms), Gbp3, Gbp5, and Gbp7 [95]. They demonstrated that these mice were highly susceptible to *Toxoplasma gondii* infection, and that reintroduction of Gbp1, Gbp5, or Gbp7 partially restored wild-type resistance [95]. Additionally, they showed that in the absence of these GBPs, Irgb6 was unable to be recruited to *Toxoplasma gondii*-containing vacuoles, indicating an interplay between these two families in innate immunity [95]. Together, these four studies indicate important

anti-microbial roles for certain members of the guanylate-binding protein family, and link them to other proteins induced by interferon-γ signaling.

In addition to their roles in innate immunity to viral and bacterial/parasitic challenges, a role has been established for specific guanylate-binding proteins in mediating the NLRP3 inflammasome response. This inflammasome stimulates the activity of caspase-1, which cleaves the inactive forms of the inflammatory cytokines IL-1β and IL-18 to their active forms and additionally stimulates pyroptosis [96]. A recent study indicated that both human and murine Gbp5 promoted the assembly of the NLRP3 inflammasome, and thus caspase-1 and IL-1β/IL-18 activity [97]. Intriguingly, Gbp5 only promoted this activity in response to certain microbes or microbial components, but not to non-biological agonists or adjuvants, revealing novel specificity in NLRP3 inflammasome regulation [97]. Additional research is currently being done to address the roles of Gbp5 in regulating other inflammasome activities (Pilla and Cöers, presentation).

In summary, the guanylate-binding protein family is a conserved family found throughout vertebrate species that plays an important role in innate immunity to bacteria, parasites, and viruses. Their specific functions, though known to be varied, are only just beginning to be fully elucidated; these involve cell-autonomous functions such as superoxide generation and macroautophagy, and induction of inflammatory

responses via inflammasome signaling. Further research is necessary to fully determine all the mechanisms whereby this family enables innate immunity.

1.4 Macroautophagy

1.4.1 The importance of degradative processes

The breakdown of excess, unnecessary, and/or defective cellular components into their basic parts is a necessary process for homeostasis. Changing conditions within the cell require the creation of different protein networks to maintain appropriate physiological conditions, which requires that previous protein networks be degraded and recycled. In the case of nutrient deprivation, when anabolic processes are inhibited by a lack of building material, it becomes even more imperative that the cell be able to recycle unimportant components to create anabolic building blocks. Additionally, in certain signaling networks, the cell utilizes the rapid breakdown of signal-transducing elements to either prevent the premature activation of a response pathway or downregulate an active response. And finally, proteins and organelles which have been damaged by various cellular stressors need to be cleared before they develop toxic characteristics which are detrimental to cellular function. Thus, the process of protein and organelle degradation is a necessary component to the overall functioning of the cell.

There are two organelles within the cell whose purpose is to degrade cellular elements into their component parts: the proteasome and the lysosome. It should be

noted that the descriptions of proteasomal and lysosomal degradation outlined in the following paragraphs are largely focused on their homeostatic functions; however, these organelles also participate in processes outside of protein maintenance, for instance, in antigen presentation.

As its name suggests, the proteasome degrades proteins and peptides, and is responsible for the majority of protein turnover in the cell [98]. This organelle consists of a cylindrical protein core (the 20S subunit) between two regulatory protein subunits (the 19S regulatory particles) [99]. The 20S core is responsible for proteolysis via threonine- and water- dependent nucleophilic attack [100], while the regulatory particles are responsible for recognizing proteins tagged for destruction [99]. Because the proteolytic core channel of the proteasome is narrow, these regulatory particles also function to partially unfold the targeted protein and feed it into the proteolytic interior in an ATP-dependent manner, a process called translocation [99,101].

In order to differentiate those proteins destined for destruction via the proteasome, the cell tags the protein with a chain of a small (8.5 kDa) protein called ubiquitin. Ubiquitin is conjugated to proteins via lysine resides or the N-terminal amino group; once the first ubiquitin is conjugated, more ubiquitin proteins are conjugated to the first to form long ubiquitin chains [102]. Ubiquitin chains can be of any length, and linked through any of its five lysines or N-terminus, with each linkage conferring a unique chain conformation; for example, K48-linked ubiquitin chains form are tightly

compact globules, whereas K63-linked chains adopt a looser, "beads-on-a-string" conformation [102]. Chains can be homogenous in linkage type, consist of several different linkages, or even include multiple branched chains, leading to millions of possible ubiquitin-derived signals, each conferring a different fate on its substrate [102]. Not all types of ubiquitin chains lead to degradation of the tagged protein; some can affect localization, signaling pathways, or enzymatic function [102]. The ubiquitin signal which signals proteasomal degradation nearly always consists of a polyubiquitin chain in which ubiquitins are ligated through lysine 48 [103] (although it should be noted that some proteins can be degraded by the proteasome in a ubiquitin-independent fashion [104,105]).

Importantly, the proteasome is a protein-based organelle, and thus the size of the catalytic channel is fixed. Cellular components which cannot fit inside the proteasomal core are not able to be broken down by this organelle. In contrast, the lysosome is a membranous compartment within the cell, meaning it can fuse with other membranous compartments, including other lysosomes, in order to increase in size to accommodate large structures destined for degradation. Lysosomes maintain an acidic interior environment (approximately pH 5) via proton pumps and chloride ion channels in order to maintain conditions necessary for the function of the approximately sixty degradative enzymes found in the lysosomal lumen which can digest any biological macromolecule, including nucleic acids, lipids, polypeptides, and carbohydrates (note that the lysosomal

membrane is protected from these digestive enzymes by a thick glycocalyx) [106]. Thus, while the proteasome is a delicate and controlled degradative organelle specifically designed for cleaving designated peptide bonds, the lysosome is a powerful and multi-functional garbage disposal site for the cell, capable of handling large volumes of cellular junk of varied composition. Additionally, in the event of proteasomal inhibition or blockage, the lysosome can serve as a compensatory degradation system [107].Because of the formidable degradative internal environment of the lysosome, the cell must carefully safeguard the integrity of the compartment while ensuring that targeted macromolecules can reach the lumen. The process of transferring cellular components to the interior of the lysosome is referred to as *autophagy*, or self-eating. There are several types of autophagy. The first, microautophagy, involves the invagination of the lysosomal membrane around a portion of cytoplasm, much the same as phagocytosis, followed by vesicle scission into the lysosomal lumen (reviewed in [108]). A second type of autophagy, chaperone-mediated autophagy, involves the recognition of soluble substrate proteins by chaperones, which then shuttle the unfolded protein directly across the lysosomal membrane via specific lysosomal channel proteins (reviewed in [109]). (Note that this is the only form of autophagy which does not require the formation of a vesicle to transfer components to the interior of the lysosome.) Neither microautophagy nor chaperone-mediated autophagy are important to the work presented in this presentation, and thus will not be discussed in further detail.

Consequently, we will turn to a detailed examination of the third type of autophagy, called macroautophagy.

1.4.2 Macroautophagy

In contrast to micro- and chaperone-mediated autophagy, which are responsible for the degradation of small, specific substrates, macroautophagy is responsible for bulk degradation of cellular components. It involves the formation of a double-membraned vesicle around a portion of the cytoplasm, which can contain whole organelles, large protein aggregates, long-lived proteins, or other random cellular components. This vesicle, termed an autophagosome, is then trafficked to and fuses with lysosomes in a process called maturation, delivering its contents to the degradative lysosomal environment. The terms macroautophagy and autophagy are often used interchangeably, and this process will be referred to by both names for the remainder of this dissertation.

The molecular machinery that regulates autophagosome formation, cargo selection, and maturation can be divided into three groups: the upstream autophagic signallers, the core autophagic machinery, and selective autophagy adaptors, each of which we will discuss in further detail in the next sections. Though much of the work done to elucidate the autophagosomal machinery was performed in yeast, we will focus on what is known of mammalian autophagy because it is the most relevant to the work presented in this dissertation.

1.4.3 Upstream regulation of macroautophagy

The process of macroautophagy occurs constitutively at low levels to ensure turnover of long-lived proteins and organelles and safeguard proper homeostasis of the cytoplasmic environment. However, levels of autophagy can be modulated in response to a diverse array of cellular conditions, including starvation, infection, growth factor signaling, DNA damage, and apoptotic processes. Because of this variety, the signaling pathways which modulate levels of macroautophagy are numerous and extremely complex, and the interplays between pathways are only just beginning to be understood. The pathways which are described below are diagrammed in Figure 1, which is very helpful for understanding the complex systems of activation and repression that eventually lead to control of autophagy.

The "gateway" to control of mammalian autophagy levels is a protein called mammalian target of rapamycin, or mTOR [32,33]. This serine/threonine kinase exists in two separate protein complexes, one of which, mTORC1, serves as an inhibitor of autophagy by causing the phosphorylation and thus inactivation of the autophagy-initiating ULK complex [110-112]. Signaling pathways which modulate levels of autophagy within the cell nearly all modify mTORC1 functioning as their endpoint. mTORC1 is itself activated by the small GTPase Rheb in its active, GTP-bound state [113]; Rheb is inhibited by its GAP (GTPase activating factor) called the TSC1/TSC2 complex [31,113-116].

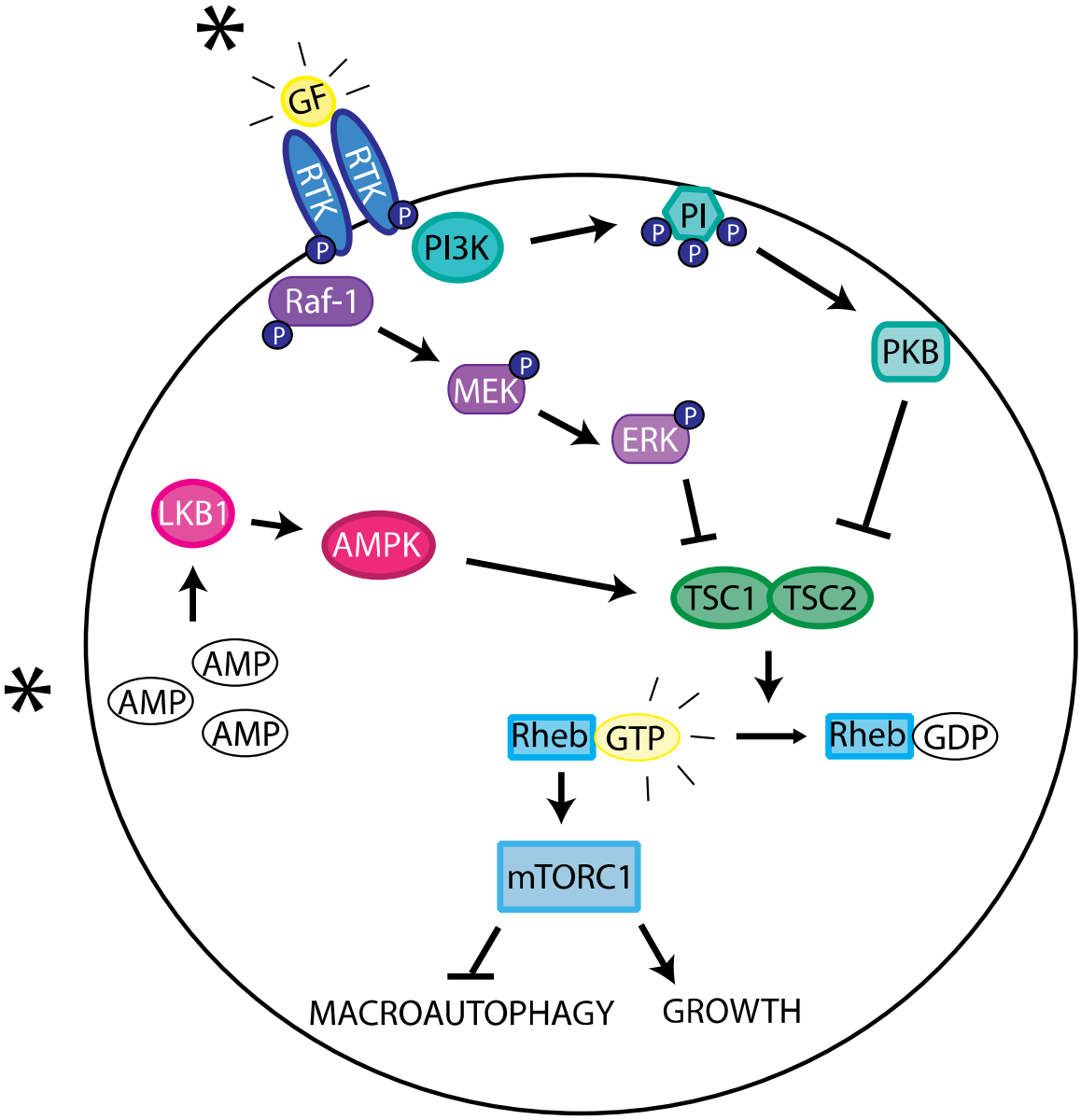

Figure 1: Select macroautophagy signaling pathways upstream of mTOR. mTOR complex 1 (mTORC1) promotes growth pathways while repressing macroautophagy. The activity of this complex is promoted by activated Rheb, and repressed by Rheb's GAP, the TSC1/2 complex. This complex can in turn be inhibited by growth factors, or promoted by energy depletion. * represents signaling initiation points. See text for further details.

One of the better-known stressors which upregulates autophagy is starvation-induced nutrient deficiency and reduction in energy levels. One pathway through which autophagy is upregulated in response to starvation is mediated by AMP kinase (AMPK). When the ratio of AMP to ATP increases as a result of energy depletion, the kinase LKB1 is activated, which phosphorylates and activates AMPK [117-119]. AMPK in turn phosphorylates and activates the TSC1/2 complex [120], leading to destabilization of Rheb-GTP, inactivation of mTOR, and upregulation of autophagy. Other pathways are also known to upregulate autophagy through AMPK; for example, an increasing free calcium ion concentration in the cytoplasm also activates AMPK and thus autophagy [121], as does the protein p53 in response to DNA damage [122].

In contrast, a signaling cascade which eventually inhibits macroautophagy is initiated by growth factors such as insulin. Receptor tyrosine-kinases, upon receiving the proper growth factor signal, auto-phosphorylate and activate two separate signaling pathways, mediated via class I PI3 kinases [30] or Ras GTPases [123], respectively. PI3 kinases activate protein kinase B (PKB, also called Akt), which in turn inhibits the tuberous sclerosis complexes (TSC1/TSC2) [31]. Separately, the Ras GTPases, once activated by the receptor tyrosine-kinases and in addition to promoting the activity of class I PI3 kinases [124], activate the Raf-1/MEK/ERK signaling cascade which also inhibits the TSC1/2 complex [125]. Inhibiting TSC1/2 by these two separate pathways then stabilizes Rheb-GTP and activates mTOR, thus inhibiting the autophagic process.

1.4.4 Core autophagic machinery

While the pathways which modulate levels of autophagy in the cell are numerous and varied, the core autophagic initiation, growth, and maturation machinery remains the same. Figure 2 diagrams the most important members of the basal autophagic machinery. Note that many of the core autophagy proteins have the stem name Atg, short for autophagy; former nomenclature referred to them as Apg proteins, though this is no longer in use.

The initiatory complex which is necessary to begin the process of autophagy in mammalian systems is called the unc-51-like kinase (ULK) complex. This complex consists of the scaffold FIP200 protein bound to both mAtg13 and one (or more) of the three mammalian ULKs [112,126-128]; a possible fourth member of the complex, Atg101, has also been described [129]. Interactions with the kinase complex mTORC1, the master repressor of autophagy, lead to a series of phosphorylations of various members of this complex, which represses its function; in the presence of signals promoting autophagy, however, mTORC1 dissociates from the ULK complex, and a separate series of phosphorylations promotes its function [112,127]. The overall role of this initatory complex is currently unclear, although its existence is necessary for initiation of autophagosome formation [126-129].

Once autophagosome formation has been initiated, a series of proteins assemble together at the phagophore assembly site, or PAS. The location of this site in mammals

appears to be near the endoplasmic reticulum [130,131]. The source of the membranes used to build the autophagosome is currently debated, but likely includes ER-derived membrane along with *de novo* membrane synthesis [130-133]. One complex of proteins recruited to the PAS is the class III PI3K complex. The core of this complex consists of the class III PI3 kinase hVps34, Beclin-1, and p150, which then associate competitively with either Atg14L/Barkor or UVRAG [134-138]. Atg14L is thought to direct localization of the complex to the PAS [134,135,137,138]. UVRAG, on the other hand, is thought to recruit Bif-1, a protein which has the ability to bend membranes and which may initiate the formation of the autophagosomal membrane [139,140]. Intriguingly, the UVRAG-bound complex also appears to be involved in autophagosome-lysosome fusion, both positively (when interacting with HOPS proteins [141]) and negatively (when interacting with Rubicon [137,138]), and thus may play a role in both initiation and maturation of autophagosomes.

A second protein complex targeted to the PAS involves a family of orthologues of the yeast protein Atg8, of which in mammalian cells there are eight members. This includes four proteins of the microtubule-associated protein 1A/1B-light chain 3 family, more commonly called LC3 proteins (A-C, including two splice forms of LC3A), and four GABARAP proteins (GABARAP and GABARAPL1-3). All of these proteins have been shown to decorate autophagosomal membranes [136,142]. While the exact roles of each member of the Atg8 family in mammals have yet to be elucidated, all of these

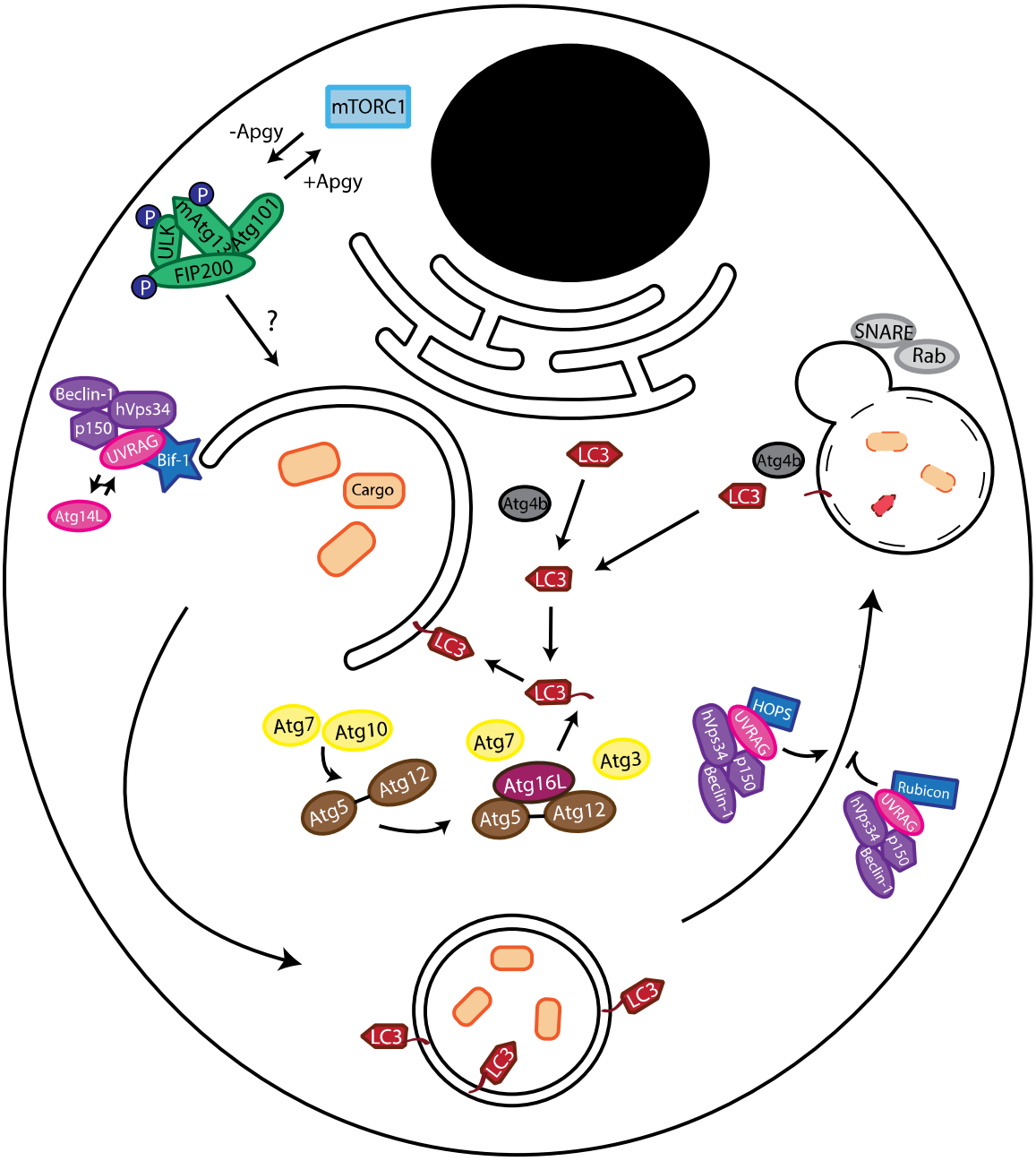

Figure 2: Core macroautophagic machinery. The ULK complex (green), class III PI3K complex (purple), Atg16L1 complex (yellow, brown, and fuschia), and LC3 (red) all play key roles in the process of macroautophagy. See text for further details.

members are necessary to autophagosome formation [142], and all have been found on pathogen-containing autophagosomes [143]. The LC3 proteins are the best studied Atg8 orthologues, and are often used as models of Atg8 orthologue functioning. LC3 proteins must first be proteolytically cleaved and lipidated before they can be incorporated into autophagosomes [144,145]; thus, a complex of LC3-processing proteins also assembles at the PAS [146,147]. To begin the progression of LC3-processing, the protease Atg4B cleaves the C-terminal residue of pro-LC3 to form LC3-I [148,149]. Next, a large complex called the Atg16L complex forms in order to lipidate the newly-exposed C-terminal glycine of LC3-I. To create the Atg16L complex, Atg7 (an E1-like enzyme [150]) and Atg10 (an E2-like enzyme [151]) facilitate conjugation of the proteins Atg5 and Atg12, which interact with Atg16L and then oligomerize [152,153]. This complex then conjugates LC3-I to phosphatidylethanolamine (PE), utilizing both Atg7 (the E1-like enzyme) and Atg3 (which acts as an E2-like enzyme) [154-156]. Intriguingly, this conjugated form of LC3, LC3-II, also appears necessary to the formation of the Atg5-12 complex, underlying the complexity of this dual-conjugation system [157]. LC3-II is integrated into both the outer and inner autophagosomal membranes, and is thought to effect closure of the autophagosomal membrane [157-159]. LC3-II is recycled off the outer membrane of the autophagosome via cleavage of the lipid bond by the protease Atg4B, forming LC3-I which can be reused in autophagosome synthesis [148]. Note that GABARAPs are also cleaved and lipidated using the same machinery [145,149,154,160-

162], but are believed to have a separate role from LC3 proteins in the genesis of autophagosomes [142].

Two other proteins, mAtg9 and vacuole membrane protein 1 (VMP1), are both integral to autophagic initiation in a manner which is poorly understood. Both are transmembrane proteins; mAtg9 may be involved in trafficking membrane to the PAS [163,164], while VMP1 may interact with Beclin-1 and/or other members of the class III PI3K complex [165,166].

Once the autophagosome has been fully formed, it is trafficked to late endosomes and/or lysosomes, with which it fuses to form a compartment often called the autophagolysosome [167,168]. This process, while not well studied, is known to involve Rab GTPases [169] and SNARE proteins [170,171], much like other types of vesicle fusion events. Upon fusion, the inner autophagosomal membrane is broken down by lysosomal lipases, including Atg15 in yeast [172,173] (the mammalian system has not been studied). The contents of the autophagosome are thus exposed to the degradative interior of the lysosome. Little is known about how the resultant macromolecules are released to the cytoplasm, although the lysosomal translocator LYAAT-1 has been identified as being responsible for some peptide translocation out of the lysosome [174].

1.4.5 Selective autophagy

Macroautophagy has often been thought of as a largely non-specific process; that is, the contents of the autophagosome are random, and the process is upregulated in

order to provide a stressed cell with abundant anabolic substrates from which to mount a response [175]. A more contemporary view has emerged in recent years to encompass the discovery that certain proteins and organelles can be specifically targeted to the autophagic machinery [176-178]. Certain patterns of ubiquitination, usually K48-linked ubiquitin chains, target proteins for proteasomal destruction [102]; however, a different set of ubiquitylation patterns are recognized by a category of adaptor proteins recently termed "sequestosome-like receptors," or SLRs [177]. These adaptor proteins also interact with the protein LC3 found in the membrane of the forming autophagosome, thus physically bringing specific targets to the forming autophagosome to be included in its cargo destined for degradation [176-178]. To effect binding of both LC3 and ubiquitin, the C-terminal region of SLR adaptor proteins contains two protein-protein interaction domains: an LC3-interacting region (LIR) and a ubiquitin-binding domain.

The four best-studied SLR adaptor proteins are p62/SQSTM1, NBR1, NDP52, and optineurin. Of these, p62, NBR1, and optineurin all contain a canonical LC3-interacting sequence [179-181]. These LIR domains are short, approximately twelve amino acids long, and possess several key structural features, including a series of acidic residues leading up to a key aromatic residue and a later hydrophobic residue (leucine, isoleucine, or valine); this structural sequence fits in a hydrophobic pocket of Atg8-family proteins [178,179]. The LIR domains of p62, NBR1, and optineurin bind to all eight members of the Atg8 orthologue family in mammals [179-182], indicating that

these SLRs undergo promiscuous binding to forming autophagosomes. It should be noted that a second non-canonical "LIR" region of NBR1 was determined to bind LC3 in *in vitro* studies, although it does not seem to play a role in LC3 interactions *in vivo* [179].

On the other hand, the LIR domain of NDP52 is non-canonical in both structure and function. This sequence does not contain an aromatic residue, but rather relies on a Leu-Val-Val sequence that binds only to LC3C, and not other Atg8 family members [143]. It remains to be seen whether or not this specific binding to only one Atg8 family member is an accident resulting from convergent evolution, or if a functional reason for this specificity exists. One possible explanation for the specificity of the NDP52-LC3C interation is that the two subfamilies of Atg8 proteins (LC3 proteins and GABARAP proteins) are thought to have differing roles in autophagosome biogenesis and thus may be present on autophagic membranes at distinct time points [142]. It is possible that NDP52's unique role in pathogen recognition and signaling requires recruitment at a specific step in autophagosome formation. More research is needed into the exact roles of each Atg8 family member before the reason for the NDP52-LC3C specific interaction can be deduced.

The second interaction region important to the autophagy adaptor function of SLRs is the ubiquitin-binding domain. This domain must be able to recognize only those ubiquitin chain signals which specifically target a protein to macroautophagic degradation. It is currently unclear, however, which types of ubiquitin signals are used

to signify that a target should be degraded by autophagy. Ubiquitin chains can be of any length, and linked through any of its five lysines, with each linkage conferring a unique chain conformation; for example, K48-linked ubiquitin chains form are tightly compact globules, whereas K63-linked chains adopt a looser, "beads-on-a-string" conformation [102]. Chains can be homogenous in linkage type, consist of several different linkages, or even include multiple branched chains, leading to millions of possible ubiquitin-derived signals, each conferring a different fate on its substrate [102]. Since it is well established that SLR adaptors target ubiquitinated targets to the autophagic pathway, determining what types of ubiquitin chains are recognized by various SLR proteins can give insight into which ubiquitin signals select a target for macroautophagic degradation.

There are two categories of ubiquitin-sensing domains found in the SLR adaptors dicussed here: the UBA domain and the UBAN + zinc-finger domain. p62 and NBR1 both share a UBA ubiquitin-binding domain. p62's UBA domain is specific for K63-linked ubiquitin chains [183], whereas the UBA domain of NBR1 seems to have its highest affinity for di-ubiquitin chains, and has only a slightly higher affinity for K63-linked di-ubiquitin than for K48-linked di-ubiquitin [184]. This disparity in recognized ubiquitin signals for two proteins with a similar function indicates that there is a great deal of complexity involved in the discernment of cellular fate through ubiquitin tagging, and there are likely many ubiquitin chain conformations that can lead to

autophagic degradation. It remains to be seen whether a specific ubiquitin tag, such as a K63-linked chain, is sufficient to target a substrate to the autophagy pathway, or if the context of the ubiquitin-substrate complex is necessary to properly recognize the ubiquitin tag.

Less work has been done on the ubiquitin-binding patterns of NDP52 and optineurin, which contain a zinc-finger domain (NDP52) or both a zinc-finger and UBAN domain (optineurin) to sense ubiquitin. NDP52's zinc-finger domain has been confirmed to bind to mono-ubiquitin, but has not yet been tested for ubiquitin chain binding [185]. Optineurin binds linear tetra ubiquitin, but not mono-ubiquitin or ubiquitin-related proteins [181]. These findings are further evidence of the complexity of the macroautophagic targeting system.

While not being specifically relevant to the work presented in this dissertation, it is worth mentioning that, in addition to their functions as adaptors of specific autophagy, SLRs play a role in upregulating innate immune signaling pathways. The N-termini of the four adaptor proteins discussed here all contain a series of protein-protein interaction domains associated either with upstream regulators of NF-kB (p62 and NBR1) or an unidentified TBK1-dependent antimicrobial pathway (NDP52 and optineurin) [181,185-189]. This dual-function nature of SLR adaptor proteins as specific autophagy mediators and innate immune signalers may imply that SLR adaptors bridge the gap between an immediate, cell-autonomous response to cytosolic bacteria

(autophagy) and upregulation of inflammatory responses to prevent further cellular invasion. More work is needed in this area to determine if this hypothesis is true.

1.4.6 The IRG family and the GBP family as mediators of macroautophagy

As outlined in the above sections, macroautophagy is a process of bulk degradation which is upregulated by stressors which require a catabolic response, such as nutrient deprivation, energy depletion, or DNA damage, and downregulated when conditions signal the need for anabolic processes, especially by growth factor signaling. Research on macroautophagy thus largely focused on its metabolic consequences, until a pivotal paper published in 2004 which introduced a major new function for macroautophagic processes. In this paper, the authors built upon the previous finding that *Mycobacterium tuberculosis* prevents fusion of its phagocytic compartment with lysosomes by specifically disrupting an hVPS34-dependent trafficking pathway and other PI3P-dependent signaling [190]. Noting that hVPS34 is a PI3K vital to the initiation of macroautophagy, as outlined previously in this dissertation, the researchers wondered whether this degradative process is responsible for the maturation of phagosomes. They treated mouse macrophage-like RAW 264.7 cells infected with *Mycobacterium tuberculosis* with rapamycin, a compound which upregulates autophagy by binding and inhibiting the mTORC1 complex; this treatment overcame the block on phagosomal maturation introduced by the bacteria, led the compartments to gain

macroautophagic markers such as LC3, and led to successful repression of bacterial growth [191]. This was the first paper demonstrating that macroautophagy has anti-microbial functions. Additionally, the authors demonstrated that treating these macrophage-like cells, which expressed an exogenous GFP-LC3 construct, with the cytokine interferon-γ led to the formation of GFP-LC3 puncta, implying that interferon-γ is able to upregulate macroautophagy as a defense mechanism to promote phagosome maturation and bacterial clearance [191]. And finally, the authors went on to claim that this macroautophagic response to interferon-γ is mediated by the protein Irgm1, an immunity-related GTPase of the M subfamily induced by interferons, by demonstrating that overexpression of a GFP-tagged version of Irgm1 led to the formation of large, acidic compartments which partially overlapped with LC3, and that this overexpression further increased maturation of *M. tuberculosis*-containing compartments [191]. This final observation, that Irgm1 may upregulate macroautophagy, was surprising given that no previous evidence had linked interferon-induced GTPases to macroautophagic processes, save the knowledge that wild-type Irgm1 localizes to endolysosomal compartments and mature lysosomes, a localization which requires a functional G domain [56].

The researchers soon followed up on these observations, and published a second study containing evidence that not only does GFP-tagged Irgm1 overexpression lead to the accumulation of acidic compartments, but that it also leads to an accumulation of

double-membraned compartments, which is a hallmark of autophagosomes, and to an increase in the amount of the lipidated form of LC3, LC3-II [41]. Furthermore, siRNAs against Irgm1 repressed the increase in GFP-LC3 puncta exhibited by interferon-treated cells, further supporting the notion that Irgm1 drives macroautophagy. Additional research by other groups linked the putative role that Irgm1 plays in driving autophagy to the previously observed interferon-γ-induced cell death of certain cell types, including demonstrating that Irgm1 protects CD4+ T-lymphocytes from cell death induced by IFN-γ in an autophagy-dependent manner [192], and that localization of Irgm1 to lysosomes promotes autophagy-related necrotic cell death of hepatocytes [58]. Other research has linked Irgm1 to driving autophagy in neurons [193].

Intriguingly, despite the truncated nature of human IRGM as compared to Irgm1, there is some evidence that human IRGM is also a modulator of autophagy. Two studies directly tested the ability of IRGM to affect macroautophagy, and found that IRGM siRNA blocked conversion of LC3-I to LC3-II, led to fewer GFP-LC3 puncta upon induction of autophagy, and led to defects in the maturation and clearance of *Mycobacteria*-containing [41] or *Salmonella typhimurium*-containing [194] compartments. Additionally, it has been shown that IRGM promotes macrophagic uptake of pathogenic adherent-invasive Escherichia coli in the intestines [195]. Other more circumstantial evidence involves the finding that certain IRGM SNPs lead to an increased susceptibility to Crohn's disease, an inflammatory disease of the digestive tract, and that

the main intestinal pathology associated with these SNPs is a defect in the granules of Paneth cells, immune cells of the intestinal crypt which secrete anti-microbial effectors into the intestinal lumen [194,196-198]. These same defects are also seen in patients with disease-associated SNPs in the core autophagy gene ATG16L1 [199,200], leading to the hypothesis that both ATG16L1 and IRGM are essential for the macroautophagic processing of Paneth cell granules. Intriguingly, similar Paneth cell abnormalities have been observed in Irgm1-deficient mice with induced intestinal inflammation, providing evidence of a role for murine Irgm1 in the same granule processing [201].

While there is much evidence in the literature that Irgm1 and IRGM are promoters of macroautophagy, some controversy does exist, as recent developments have called this putative function into question. First, it was recently demonstrated that GFP-tagging of Irgm1 (whether N- or C- terminal) leads to loss of Golgi localization in favor of endolysosomal localization, likely due to constitutive activation as loss of GTP-binding ability returned Irgm1 to the Golgi [56]. This finding casts doubt on the findings of previous experiments which utilized GFP-tagged Irgm1 to demonstrate increases in autophagic markers and colocalization with phagocytic compartments. The authors soon followed up with a paper demonstrating that endogenous Irgm1, in contrast to previous findings utilizing GFP-tagged Irgm1, does not colocalize directly with mycobacterial or listerial phagosomes [57]. Additionally, a second research group examined which of the interferon signaling cascade components were necessary to

mediate the induction of macroautophagy in response to interferon-γ [202]. They found that while JAK1/JAK2 kinases, the first step in the canonical interferon-γ signaling pathway, were necessary to this upregulation, the next step in the canonical pathway, activation of STAT-1, was dispensable [202]. Instead, autophagy upregulation in response to interferon-γ is mediated by a novel pathway that involves PI3K and p38 MAPK [202]. Characterization of this novel interferon-γ-induced signaling pathway was furthered by another group, which found that interferon-induced macroautophagy requires the C/EBP-β transcription factor binding to GATE elements, a pathway which does not involve STAT proteins [37]. Because the canonical STAT-1 signaling pathway is presumed necessary to Irgm1 expression (due to STAT-1's importance to innate immune responses to bacteria [203] and its necessity for other IRGs' innate immune functions [70]), the authors of the first paper then examined whether Irgm1 was necessary to the upregulation of autophagy in response to interferon-γ in macrophages, and found a normal macroautophagic response in Irgm1-deficient cells [202]. And to add further to the controversy, a recent study found that Crohn's disease patients displayed Paneth cells which constitutively upregulate autophagy, regardless of the presence of disease-associated SNPs in ATG16L1 or IRGM, and that this upregulation is what leads to Paneth granule defects, rather than an autophagic defect caused by loss of ATG16L1 or IRGM [204]. Thus, evidence exists both for and against the notion that

Irgm1 and IRGM are mediators of cytokine-induced autophagy, and more research is needed in this area to fully examine this hypothesis.

In addition to a possible role for immunity-related GTPases in regulating macroautophagy, studies have examined the role of the guanylate-binding proteins in modulating this process. In one study, it was found that murine Gbp1 interacts directly with the specific autophagy adaptor protein p62 outside of its ubiquitin-binding domain; additionally, Gbp1 colocalized with LC3 puncta, and its absence led to defects in p62 degradation, indicating a block in autophagic maturation [85]. Additionally, murine Gbp7 was found to bind to Atg4b, the protease responsible for cleaving pro-LC3 to its lipidatable state and for LC3 recycling; in the absence of Gbp7, defects in autophagosome membrane closure were observed, consistent with an inability of LC3 to incorporate into autophagosomal membranes [85]. The authors propose that, since Gbp7 was found to bind equally well to both active and inactive Atg4b, Gbp7 is a membrane-trafficking protein which delivers antimicrobial effectors, including autophagic machinery, to the appropriate intracellular sites [85]. Thus, two of the guanylate-binding proteins have been linked to the autophagic system. More work is needed to determine if other GBPs play a role in this degradative process.

1.5 Motivation for this work

In this chapter, we have outlined research which establishes interferon-induced GTPases, including the immunity-related GTPases (IRGs) and the guanylate-binding

proteins (GBPs), as major effectors of the interferon-induced innate immune response. These proteins have been demonstrated to control the growth of intracellular membrane-bound pathogens through processes which involve membrane modulation. These processes can include direct effects on pathogen-containing membranes, as well as regulatory roles of membrane-trafficking processes which ultimately deliver anti-microbial effectors.

Yet while much research has been done to elucidate the mechanisms of interferon-induced GTPase action, several important questions remain to be definitively answered. The first, and most important, question arises from the knowledge that the GMS subfamily of IRGs exerts a regulatory function over other subfamilies of IRGs, affecting their expression and localization; yet, in the absence of GMS IRGs, there exists an almost complete deficiency of interferon-γ-induced host resistance to certain pathogens, a deficiency which is not found in the absence of GKS IRGs. These data strongly imply an additional role(s) for GMS IRGs in innate immunity outside of the regulation of GKS IRGs. Additionally, certain species (such as primates) encode GMS IRGs but no innate-immune related GKS IRGs, which is further indication that GMS IRGs do more than regulate other IRGs. This additional role played by GMS IRGs in innate immunity may include their possible involvement in macroautophagy, as outlined previously. However, contradictory data both supporting and disputing this putative function exist, and more work is needed to fully elucidate whether or not GMS

IRGs play a direct role in the regulation of macroautophagy. If GMS IRGs do not affect macroautophagy, it is possible that they exert regulatory effects over other effector families induced by interferons; one possible candidate for regulation is the guanylate-binding protein family, which is induced by the same cytokines, belongs to the same superfamily of dynamin-related membrane modulators, and displays anti-microbial activity toward many of the same micro-organisms. There are currently no known interactions between these two protein families, leaving this possibility to be explored. On a related note, several of the guanylate-binding proteins have also been implicated in macroautophagic processes, but the roles of many members of this family have yet to be investigated.

In this work, we have further studied the varied roles of two interferon-induced GTPase families, the IRGs and the GBPs, in the innate immune response. We have focused particularly on the regulatory roles of GMS IRGs on overall interferon-induced immunity. These findings will provide further insight into the mechanisms of cell-autonomous innate immunity, with the ultimate goal of discovering novel therapeutic interventions which will promote public health.

2. The GMS IRG subfamily influences the localization of Gbp2 by modulating macroautophagy

[Note: this chapter contains research and excerpted text which was originally published in the Journal of Biological Chemistry : Traver MK, Henry SC, Cantillana V, Oliver T, Hunn JP, Howard JC, Beer S, Pfeffer K, Coers J, Taylor GA. Immunity-related GTPase M (IRGM) proteins influence the localization of guanylate-binding protein 2 (GBP2) by modulating macroautophagy. *J Biol Chem*. 2011; 286(35):30471-80. © the American Society for Biochemistry and Molecular Biology.]

2.1 Introduction

The innate immune system is comprised of multiple effector pathways that are induced in host cells by pro-inflammatory cytokines such as interferon-γ. Such effectors confer on the host cells the ability to more easily eradicate invading pathogens through diverse mechanisms. A prominent family of IFN-γ-induced proteins that are required for resistance to intracellular bacteria and protozoa are the immunity-related GTPases, or IRGs.

IRG proteins can be separated into subfamilies based on homology across the GTP-binding domain. Proteins in the M subfamily (often called the GMS IRGs) are distinguished from the other proteins by possessing a non-canonical GMS sequence in the first GTP-binding motif (G1), while the remaining subfamilies all possess the canonical GKS sequence. Previous work from our lab and others has demonstrated that

GMS IRGs play a particularly important role in innate immune resistance to intracellular bacteria and protozoa in mice, as described further in chapter 1 of this dissertation. This importance is thought to stem from the ability of GMS IRGs to regulate the localization, expression, and function of the GKS IRGs. And yet, this limited regulatory function does not explain the apparent complete absence of IFN-γ-induced host resistance that has been noted against several different pathogens as a result of GMS IRG deficiency, nor does it explain why certain species, including chimpanzees and humans, express GMS IRGs but do not encode innate-immune related GKS IRGs. An open question, therefore, is whether GMS IRGs possess broader regulatory functions over other interferon-induced innate immune effector families.

In this chapter, we address the possibility of broader regulatory functions of GMS IRGs by examining whether these proteins can affect the localization and functioning of another important family of IFN-γ-induced effectors, the guanylate-binding proteins (GBPs). Like the IRG proteins, GBPs can be functionally classified within the dynamin protein superfamily and have been implicated in vacuolar processing and resistance to pathogens such as *Toxoplasma gondii*, *Listeria monocytogenes*, and *Chlamydia trachomatis*. Despite no previous evidence of interactions between these two protein families, we find that the absence of GMS IRGs has striking effects on the localization of GBPs. Our findings suggest that GMS IRG proteins may have activities

that extend beyond the IRG protein family to influence other IFN-γ-induced effectors by modulating macroautophagy.

2.2 Results

2.2.1 Altered localization of Gbp2 in the absence of GMS IRGs

We and others have previously demonstrated that the GMS IRG proteins Irgm1 and Irgm3 regulate the localization of GKS IRG proteins; absence of either leads to the relocalization of Irga6 and Irgb6 from the ER and cytosol [51] into aggregate-like complexes [60,62]. We chose to address whether absence of the GMS IRGs has similar effects on other interferon-regulated innate immune effectors. We found that absence of Irgm1 or Irgm3 in interferon-treated mouse fibroblasts or macrophages grossly altered distribution of the interferon-induced protein Gbp2. Gbp2 is a member of the guanylate-binding protein family, a little-studied interferon-induced family of proteins with some similarities to the immunity-related GTPases, as outlined further in chapter 1 of this dissertation. In the absence of GMS IRGs, we found that the localization of Gbp2 changed from punctate cytoplasmic structures – presumably small vesicles to which Gbp2 has been purported to localize in previous studies [89] – to much larger, aggregate-like structures (Figure 3). A hollow core was apparent in most of the Gbp2-positive structures, (Figure 3, arrows), particularly in deconvolved images, suggesting that they might be membranous/vesicular, although this structural feature might also be a result of an artifact introduced by deconvolution. These structures strongly resemble

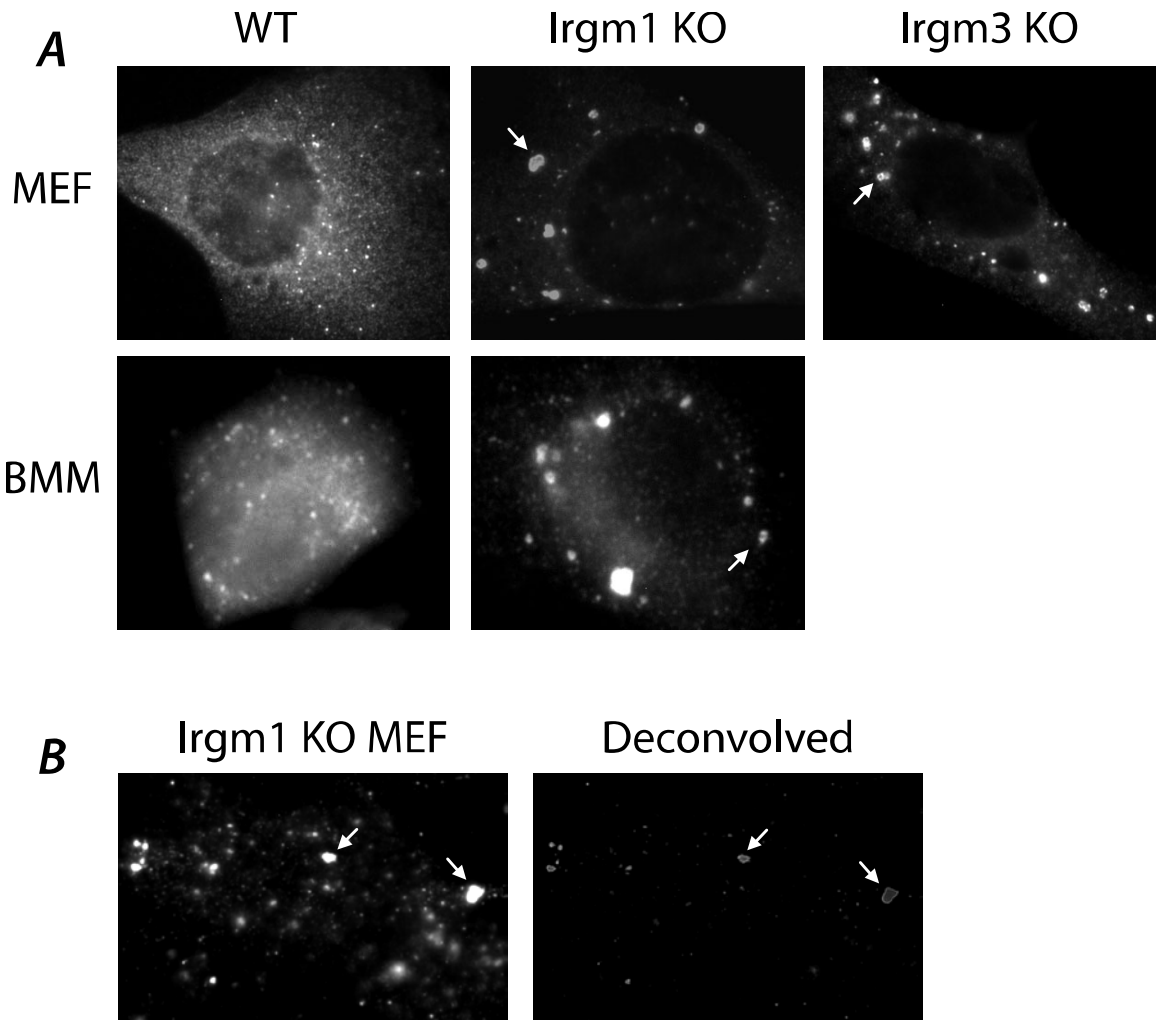

Figure 3: Altered localization of Gbp2 in the absence of GMS IRGs. *A*) 3T3 MEFs or primary BMM of the indicated genotypes were treated with 100 U/mL IFNγ for 24h. Cells were then processed for immunofluorescence with αGbp2 antibody. Representative of three trials. Arrows denote puncta displaying a ring-like structure. *B*) 3T3 Irgm1-deficient MEFs were treated with 100 U/mL IFNγ for 24h, then processed for immunofluorescence with αGbp2 antibody. Z-stack images were obtained (left panel, one plane), then deconvolved (right panel, one plane). Representative of three trials. Arrows denote puncta displaying a ring-like structure.

those formed by Irga6 and Irgb6 in the absence of GMS IRGs, implying a similar regulatory mechanism of GMS IRGs over guanylate binding proteins.

2.2.2 Gbp2 colocalizes with GKS IRGs in the absence of GMS IRGs

Because of the strong resemblance between aggregate-like structures formed by GKS IRGs and Gbp2 in the absence of GMS IRGs, we next chose to determine whether GKS IRG proteins were concurrently present in the Gbp2-positive compartments. Co-staining studies demonstrated that nearly all of the Gbp2-positive structures in Irgm1- and Irgm3-deficient cells also contained Irga6 (94±2% and 77±9%, respectively) (Figure 4). In contrast, Irga6 and Irgb6 colocalized in only a fraction of these structures (38±4% in Irgm1-deficient cells and 46±11% in Irgm3-deficient cells), indicating that while these structures contained both GBPs and IRG proteins, there was some heterogeneity in composition among them. Collectively, these data suggest that Irgm1 and Irgm3 regulate processes that control the transfer of GBP and IRG proteins from diverse initial locations within the cells to an overlapping set of large, aggregate-like compartments.

2.2.3 GMS IRG deficiency leads to an accumulation of Gbp2-containing autophagosomes

Because of the ring-like nature of the structures containing Gbp2 and GMS IRGs, along with the preference of dynamin-like proteins for binding intracellular membranes [43,44], we postulated that these structures were membranous compartments within the cell; thus, we attempted to identify the specific compartment with a variety of co-

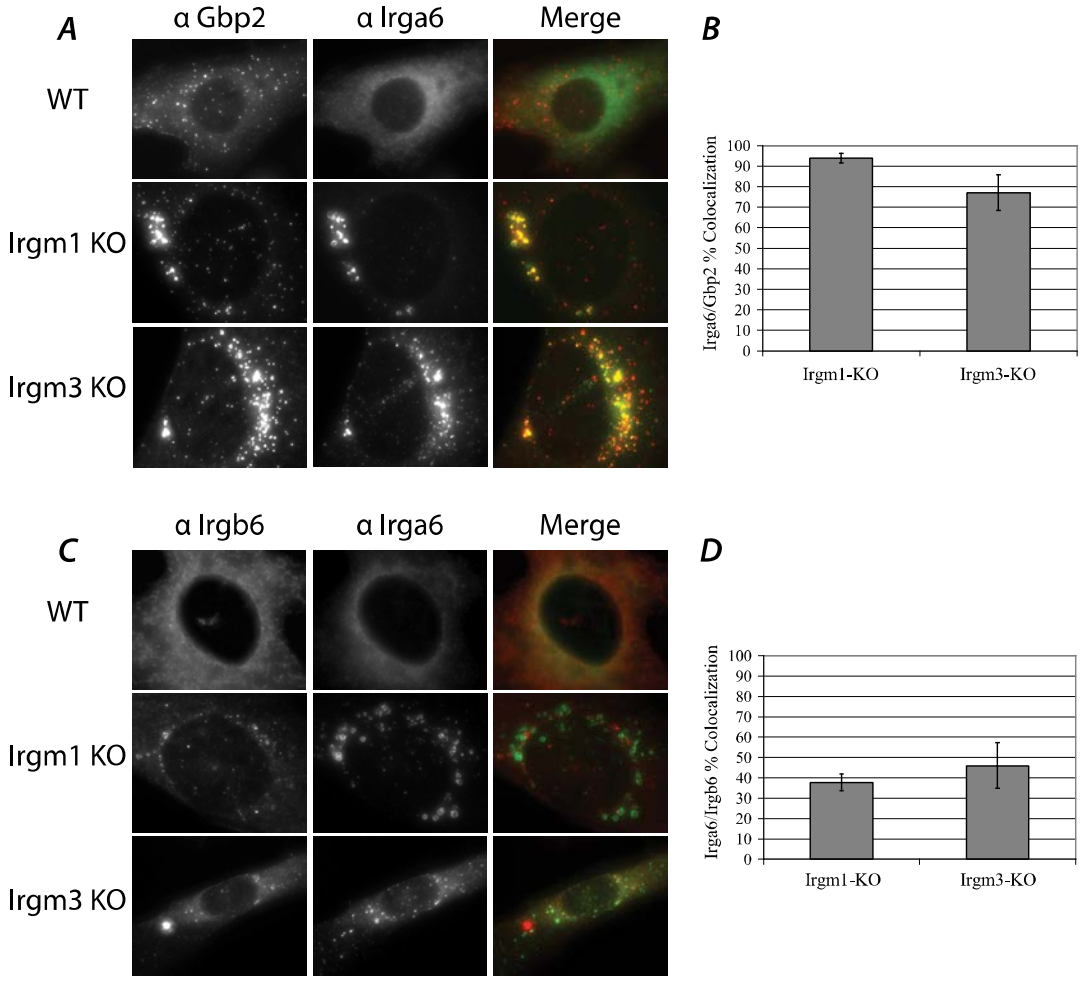

Figure 4: Gbp2 colocalizes with GKS IRGs in the absence of GMS IRGs. *A*) 3T3 MEFs of the indicated genotypes were treated with 100 U/mL IFNγ for 24h. Cells were then processed for immunofluorescence with the indicated antibodies. Images are two-dimensional projections of z-stacks of the entire volume of the cell. Representative of three trials. *B)* The percentage of Irga6 puncta which colocalized with Gbp2 was scored in a treatment-blinded fashion in 10 cells per treatment. Cells with no Irga6 puncta were not scored. Differences between populations were not statistically significant by Student's t-test. *C*) 3T3 MEFs of the indicated genotypes were treated with 100 U/mL IFNγ for 24h. Cells were then processed for immunofluorescence with the indicated antibodies. Images are two-dimensional projections of z-stacks of the entire volume of the cell. Representative of three trials. *D)* The percentage of Irga6 puncta which colocalized with Irgb6 was scored in a treatment-blinded fashion in 10 cells per treatment. Cells with no Irga6 puncta were not scored. Differences between populations were not statistically significant by Student's t-test.

staining studies utilizing markers for intracellular lipid compartments and the cytoskeleton. The Gbp2-positive structures did not colocalize with a number of these markers, including TRAP-α (ER), GM130 (Golgi), EEA1 (early endosomes), LAMP1 (late endosomes / lysosomes), mitotracker red (mitochondria), bodipy (lipid droplets), actin, tubulin, or vimentin (data not shown). We did find, however, that some (32-42%) of the Gbp2-positive structures were positive for LC3, a marker of autophagosomes (Figure 5). Macroautophagy (described in detail in chapter 1 of this dissertation) is a system of bulk degradation in which a double membrane forms around a portion of the cytoplasm, creating an autophagosome that fuses with late endosomes/lysosomes and becomes

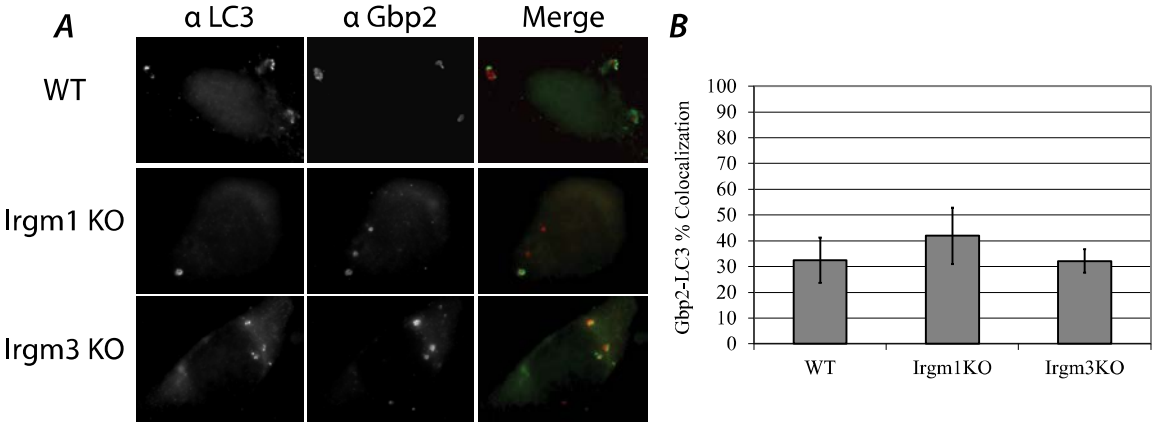

Figure 5: Gbp2 colocalizes with autophagosomes. *A)* Primary MEFs of the indicated genotypes were treated with 100 U/mL IFNγ for 24h. Cells were then processed for immunofluorescence with the indicated antibodies. Images are two-dimensional projections of z-stacks of the entire volume of the cell. Representative of three trials. *B)* The percentage of Gbp2 puncta which colocalized with LC3 was scored in 2-7 cells per treatment per trial over three trials. ANOVA did not indicate a significant treatment effect.

acidified, leading to the degradation of its contents. In our co-staining studies, it was clear that certain Gbp2 aggregate-like structures colocalized with LC3 in GMS IRG-deficient cells (Figure 5). Additionally, a similar percentage of the very few Gbp2 aggregate-like structures found in wild-type cells also colocalized with LC3 (Figure 5). While the Gbp2-positive structures found in all genotypes were LC3-positive, they were not LAMP1-positive (data not shown), which suggests that these are likely immature or abortive autophagosomal structures. Finally, partial rings that were Gbp2 positive were commonly noted in Irgm1-deficient cells, indicating that Gbp2 may be acquired early during the process of autophagosome formation (data not shown).

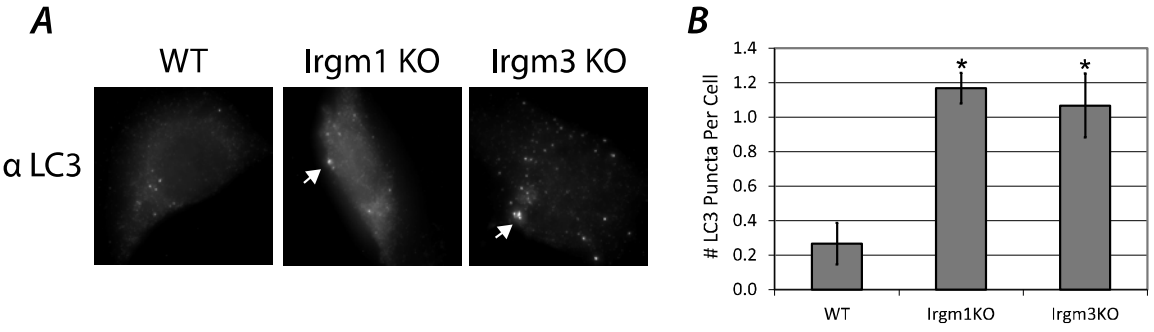

Figure 6: GMS IRG deficiency leads to an increased number of autophagosomes. *A*) Primary MEFs of the indicated genotypes were treated with 100 U/mL IFNγ for 24h. Cells were then processed for immunofluorescence with αLC3 antibody. Images are two-dimensional projections of z-stacks of the entire volume of the cell. White arrows denote autophagosomes, defined as puncta which are larger and more intense than background puncta. Representative of three trials. *B)* The number of autophagosomes per cell was scored in a treatment-blinded fashion in 10 cells per treatment per trial over three trials. ANOVA indicated a significant treatment effect, $p < 0.01$; * significant difference from wild-type, $p < 0.05$ via Tukey's HSD test.

Together, the data we have just presented imply that in the absence of GMS IRGs, Gbp2 and GKS IRGs localize to aggregate-like structures which are cleared by macroautophagy. Thus, it would be expected that in the absence of GMS IRGs, macroautophagy would be upregulated to facilitate the clearance of the increased number of protein aggregates, leading to an overall increase in the number of autophagosomes in GMS IRG-deficient cells. To test this, we identified autophagosomes in wild-type and GMS IRG-deficient MEFs via LC3 immunostaining. In IFN-γ-activated Irgm1- and Irgm3-deficient cells, there was an increase in the number of large, intense LC3 puncta per cell relative to activated WT cells (Figure 6), suggesting that GMS IRG deficiency does lead to an increase in autophagosome levels.

Much of the literature concerned with determining the effects of various conditions on autophagosome number utilizes a GFP-LC3 expression construct to fluorescently mark autophagosomes and make them amenable to counting. This use of an exogenously expressed construct, however, can introduce artifacts into the results; for example, GFP-LC3 has been shown to be attracted to protein aggregates (of which we have demonstrated there are many in GMS IRG deficient cells), leading to fluorescent puncta which are indistinguishable from true autophagosomes [205,206]. Thus, we felt that our use of endogenous LC3 staining to determine autophagosome number in Figure 6 was a better choice; however, few articles in the literature utilize this method of autophagosome counting, and so we decided to compare endogenous LC3 staining and

GFP-LC3 expression in determining autophagosome number in GMS IRG-deficient cells. First, we compared the overall number of GFP puncta in GFP-LC3 expressing cells to the number of large, endogenous LC3 puncta in untransfected cells (Figure 7, *A*+*C*). As we found in our first experiment, the number of large, endogenous LC3 puncta significantly increased in Irgm1-deficient cells in an interferon-dependent manner. [It should be noted that it is unfeasible to count all endogenous LC3 puncta because of the technical difficulty in distinguishing small puncta from background, thus the reason for counting only large, intense puncta (for example endogenous LC3 staining, see Figure 6)]. In comparison, the number of GFP puncta in GFP-LC3-transfected cells exceeded the number of endogenous puncta by a factor of 50-100, which was expected given the increased ability to distinguish GFP puncta from background. However, while the absence of Irgm1 did increase the number of LC3 puncta in these cells, this effect was not interferon-dependent, and thus was not due to the increase in aggregation of interferon-induced proteins found in Irgm1-deficient cells. The most likely cause for this increase, then, is that GFP puncta were counted which were not true autophagosomes, thus artificially inflating the number of autophagosomes and masking real effects on autophagy; this reasoning is supported by previous data from the literature indicating 1-2 autophagosomes per cell in GFP-LC3-transfected wild-type cells [41], a number more closely resembling the findings of our endogenous LC3 experiments. Thus, we decided to recount the autophagosome number in our GFP-LC3 transfected cells, only counting

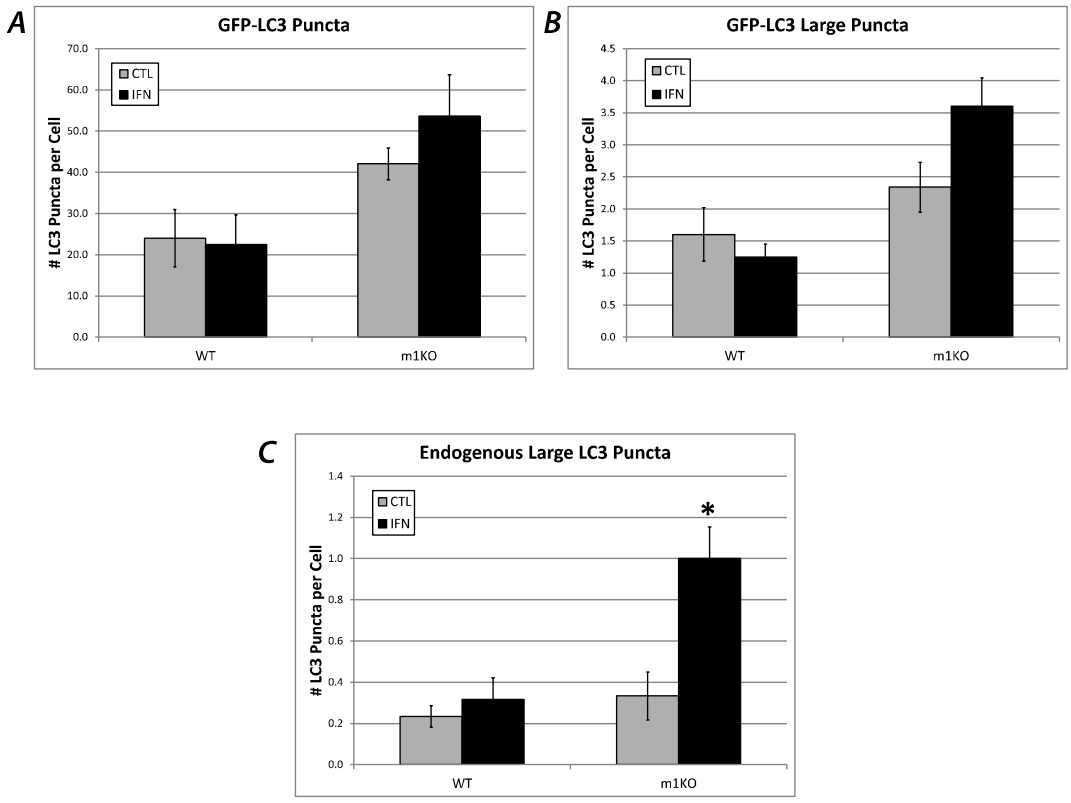

Figure 7: A comparison of endogenous vs exogenous LC3 puncta in determining autophagosome number in GMS IRG deficient MEFs. *A)* 3T3 MEFs of the indicated genotypes were nucleofected with a GFP-LC3 expression construct, then treated with 100 U/mL IFNγ for 24h. Cells were then processed for fluorescent microscopy. The number of LC3 puncta per cell was scored in a treatment-blinded fashion in 10-20 cells per treatment per trial over three trials. 2x2 ANOVA indicated a main effect of genotype, $p < 0.02$. *B)* 3T3 MEFs of the indicated genotypes were nucleofected with a GFP-LC3 expression construct, then treated with 100 U/mL IFNγ for 24h. Cells were then processed for fluorescent microscopy. The number of large LC3 puncta (defined as puncta which are larger and more intense than background puncta) per cell was scored in a treatment-blinded fashion in 10-20 cells per treatment per trial over three trials. 2x2 ANOVA indicated a main effect of genotype, $p < 0.005$. *C)* 3T3 MEFs of the indicated genotypes were treated with 100 U/mL IFNγ for 24h. Cells were then processed for immunofluorescence with αLC3 antibody. The number of large LC3 puncta (defined as puncta which are larger and more intense than background puncta) per cell was scored in a treatment-blinded fashion in 20 cells per treatment per trial over three trials. 2x2 ANOVA indicated a significant interaction term, $p < 0.05$; * $p < 0.05$ via Tukey's HSD test.

the larger, more intense puncta as we did for the endogenous LC3 (Figure 7, *B*). This time, we found a similar number of autophagosomes per cell as in endogenous cells, along with a similar pattern of interferon-dependent autophagosome increase in Irgm1-deficient cells; this increase was just short of significance, $p < 0.07$. In summary, we conclude that the number of autophagosomes in Irgm1-deficient cells, when properly counted, increases in an interferon-dependent manner, consistent with the hypothesis that autophagy is upregulated to degrade the protein aggregates caused by GMS IRG deficiency.

Importantly, previous studies have shown that Irgm1 may drive autophagosome initiation; for example, overexpression of Irgm1 in RAW 264.7 cells led to an increased number of autophagosomes, while knock-down of Irgm1 expression led to a decrease in IFN-γ-induced autophagosome number [41]. However, the data we have just presented indicate that autophagy is also induced in the *absence* of GMS IRG proteins. This seeming contradiction could be explained by a hypothetical twofold function of GMS IRGs: firstly, to upregulate autophagy as a mechanism to remove intracellular pathogens, and secondly, to prevent premature activation and aggregation of GKS IRGs and GBPs. Thus, the presence of Irgm1 may drive autophagy, but in its absence, autophagy may additionally be upregulated to degrade the resultant GKS IRG/GBP aggregates. It should additionally be noted that considerable controversy over whether Irgm1 is a driver of autophagy exists in the literature, as described further in chapter 1 of

this dissertation, casting doubt on whether this contradiction does exist. Further research into the role of Irgm1 in macroautophagy is needed, and will be addressed in chapter 3 of this dissertation.

2.2.4 Gbp2 colocalizes with ubiquitin and p62 in the absence of GMS IRGs

There are several mechanisms through which proteins may enter the autophagic pathway for degradation. One of these involves ubiquitination of targeted proteins, followed by their transfer to the autophagic system by an adapter protein called p62/Sqstm1. This protein binds both ubiquitin and the autophagosome outer membrane component LC3, physically bringing polyubiquitinated molecules to the forming autophagosome, with p62 eventually being degraded along with the other contents of the autophagosome [180,182]. Additionally, p62 has been determined to be important not only for the clearance of aggregates, but for the initial formation of aggregate inclusions [207]. To determine whether p62 plays a role in the clearance of the Gbp2- and GKS IRG- containing aggregate structures through autophagy, we first performed costaining with anti-ubiquitin and anti-p62 antibodies, revealing that the Gbp2-positive structures (Figure 8) and Irga6-positive structures (data not shown) seen in the absence of Irgm1 or Irgm3 are also positive for ubiquitin and p62, providing further evidence that these aggregate structures are targeted to the macroautophagic pathway.

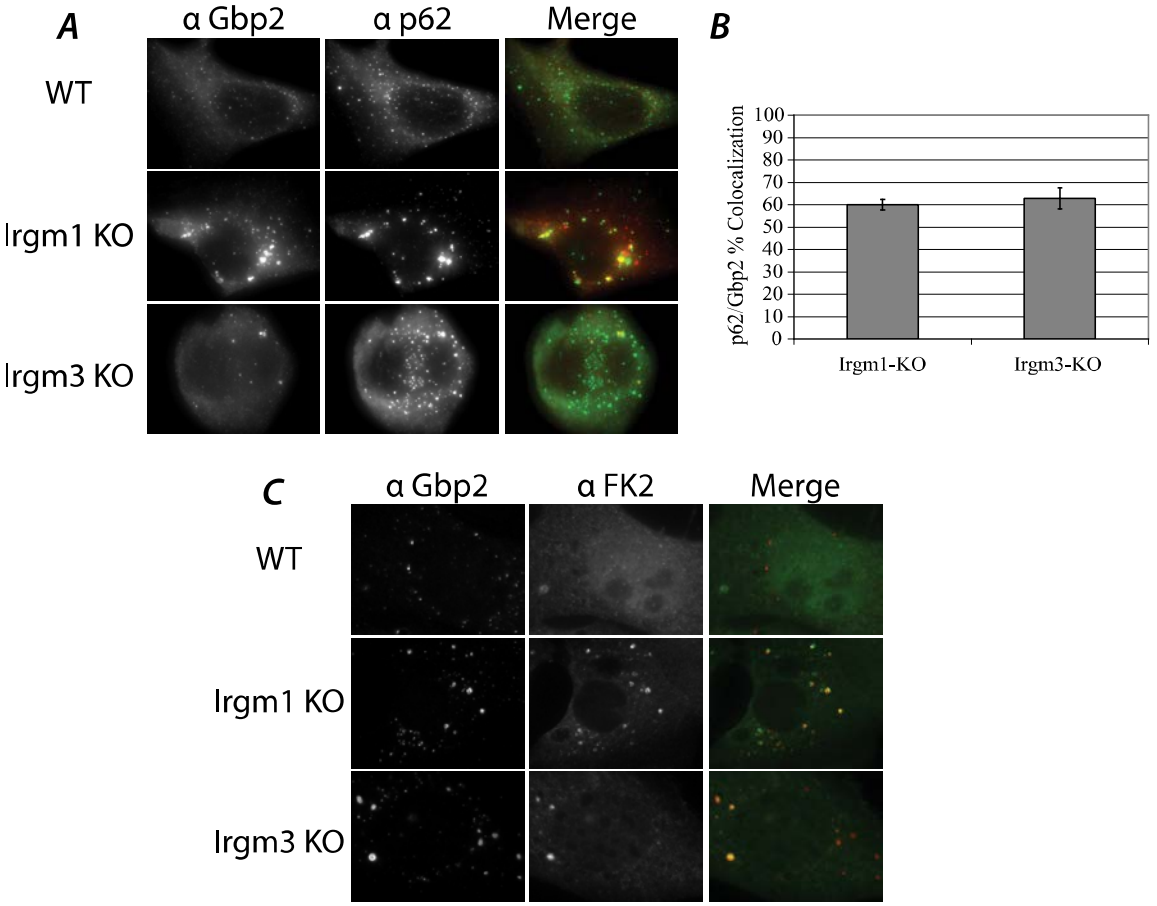

Figure 8: Gbp2 colocalizes with p62 and ubiquitin in the absence of GMS IRGs. *A)* Primary MEFs of the indicated genotypes were treated with 100 U/mL IFNγ for 24h. Cells were then processed for immunofluorescence with the indicated antibodies. Images are two-dimensional projections of z-stacks of the entire volume of the cell. Representative of three trials. *B)* The percentage of Gbp2 puncta which colocalized with p62 was scored in a treatment-blinded fashion in 10 cells per treatment. Cells with no Gbp2 puncta were not scored. Differences between populations were not statistically significant by Student's t-test. *C)* Primary MEFs of the indicated genotypes were treated with 100 U/mL IFNγ for 24h. Cells were then processed for immunofluorescence with the indicated antibodies. Images are two-dimensional projections of z-stacks of the entire volume of the cell. Representative of three trials.

2.2.5 GMS IRG deficiency leads to increased levels of K63-linked-ubiquitinated proteins

Polyubiquitin chains can be linked through any of seven lysines in the ubiquitin sequence, leading to chains with unique three-dimensional structures and characteristics [208]. It has recently been shown that unlike the commonly studied K48-linked polyubiquitin chains, K63-linked polyubiquitinated proteins are largely insensitive to degradation by the proteasome [209]. Furthermore, depolarized mitochondria are decorated with K63- and K27-linked polyubiquitin chains, leading to selective autophagy of these organelles [210]. Additionally, the ubiquitin-binding domain of the selective autophagy adaptor protein p62 is specific to K63-linked ubiquitin chains [183]. Together, these results imply that K63- and K27-linked polyubiquitin tags may be signals for selective quality control autophagy. In the current studies, we utilized TUBE 1, a peptide designed to stabilize and identify polyubiquitinated proteins and which has approximately a ten-fold higher affinity for K63-linked polyubiquitin chains over K48-linked chains, to examine levels of polyubiquitinated protein in GMS IRG deficient cells. Total levels of TUBE1-precipitated proteins, which may be enriched for K63-linked polyubiquitinated proteins, were increased in Irgm1- and Irgm3-deficient cells (Figure 9), indicating that there was an increase in formation and/or a block in removal of at least some ubiquitinated proteins in these cells, consistent with the idea that GMS IRG proteins could be required for normal autophagic clearance of GKS IRG proteins.

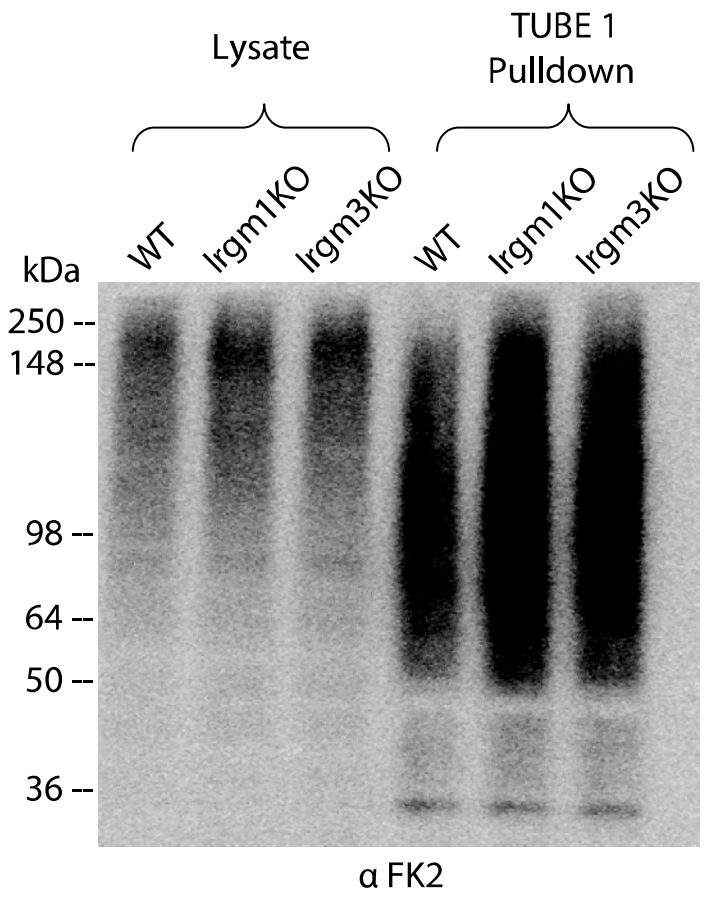

Figure 9: GMS IRG deficiency leads to increased levels of K63-linked-ubiquitinated proteins. Primary MEFs of the indicated genotypes were treated with 100 U/mL IFNγ for 24h, then lysed. Poly-Lys-63-ubiquitinated proteins were precipitated from these lysates using TUBE1-conjugated resin. Resultant proteins were examined via western analysis using αFK2 (conjugated ubiquitin) antibody. This study was done by Stanley Henry.

2.2.6 IRGM deficiency leads to an increase in K63-linked ubiquitination of Irga6, but not Gbp2

We next studied whether TUBE1 could specifically precipitate certain proteins found in the aggregates formed in the absence of Irgm1, which would indicate that these

proteins are polyubiquitinated, likely through K63 linkages, and thus might be targeted to macroautophagic degradation. TUBE 1 was able to precipitate protein species recognized by anti-Irga6 antiserum that were of higher molecular weight than Irga6, and likely represent ubiquitinated Irga6 (Figure 10). Apparent in the samples derived from Irgm1- and Irgm3-deficient cells was a ladder/smear that is typical of proteins in ubiquitin-positive inclusions [211], suggesting an increase in K63-linked polyubiqutinated Irga6 in those cells. This finding thus implies that GKS IRG proteins form polyubiquitinated aggregates that are transferred via p62/Sqstm1 to the autophagic system for degradation.

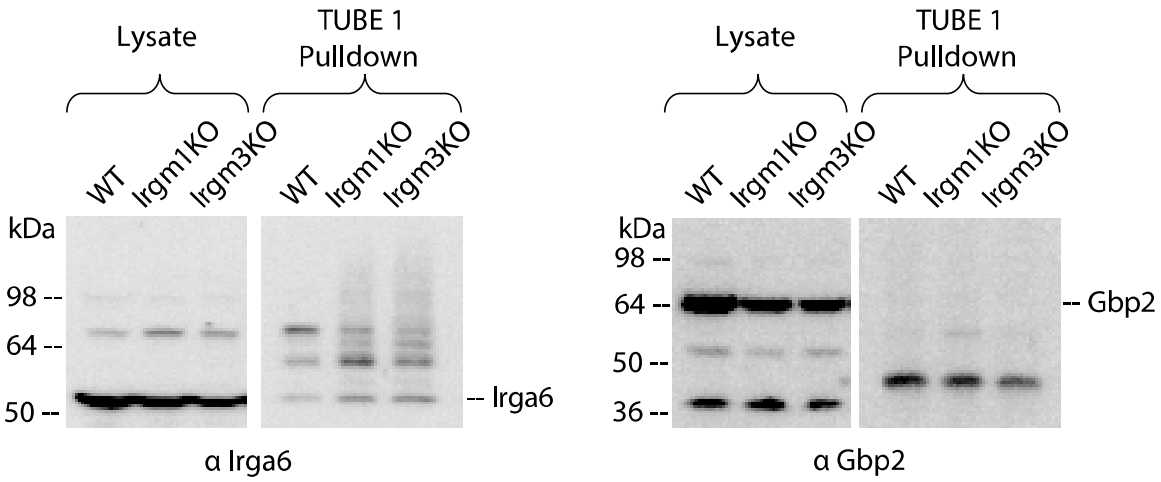

Figure 10: GMS IRG deficiency leads to an increase in K63-linked-ubiquitination of Irga6, but not Gbp2. Primary MEFs of the indicated genotypes were treated with 100 U/mL IFNγ for 24h, then lysed. Poly-Lys-63-ubiquitinated proteins were precipitated from these lysates using TUBE1-conjugated resin. Resultant proteins were examined via western analysis using αIrga6 (left) or αGbp2 (right) antibodies. Representative of three trials. This study was done by Stanley Henry.

We also addressed whether Gbp2 was ubiquitinated using the TUBE 1 pulldown assay (Figure 10). In contrast to the results examining Irga6, no high molecular weight species identified by Gbp2 antibodies were found in the TUBE 1 pulldowns, suggesting that Gbp2 is not substantially K63-ubiquitinated in wild-type, Irgm1-deficient, or Irgm3-deficient cells, although an additional treatment with the autophagy inhibitor wortmannin would confirm that ubiquitinated Gbp2 is not simply degraded at an accelerated rate. Furthermore, this finding suggests that Gbp2 is not itself a degradative target of autophagy, and thus might be found in autophagosomal structures because it is a part of the autophagic machinery. This hypothesis will be examined further in chapter 4 of this dissertation.

2.3 Discussion

In this chapter, we have presented evidence that in the absence of GMS IRG proteins, Gbp2 and the GKS IRGs Irga6 and Irgb6 form aggregate-like structures of a heterogeneous composition. It should be noted that these structures are not classic aggresomes, as they lack several important features: classic aggresomes are typically surrounded by a vimentin cage [212], whereas this cage is lacking in the Irgm1/3-regulated structures; classic aggresomes are localized near the microtubule organizing center of the cells [212], whereas the Irgm1/3-regulated structures do not demonstrate this restricted localization; and classic aggresomes occur at one per cell [212], whereas several of the Irgm1/m3-regulated structures were often found in a single cell. Next, we

demonstrated that these structures colocalize with LC3, ubiquitin, and p62, which together are markers of specific autophagy. We established that the formation of these aggregates is accompanied by an overall increase in autophagosome number. And finally, we showed that GMS IRG deficiency alters K63-linked polyubiquitination of Irga6, but not Gbp2. From these data, we propose the following model for autophagic maintenance of GKS IRG protein levels in wild-type cells. GKS IRG proteins are held in an inactive state by direct interactions with GMS IRGs, as proposed previously [62]. Excess GKS IRGs aggregate, a process that likely occurs continuously at a low level, as we found that approximately 10% of wild-type MEFs contain at least one Irga6- and Gbp2-positive aggregate-like structure (data not shown). These aggregates are recognized by unknown factors, and are then polyubiquitinated through K63 linkages. Polyubiquitinated aggregates are recognized and consolidated into aggregate inclusions by p62/Sqstm1, colocalize with Gbp2, and are brought to autophagosomes, where they are degraded.

While the model we have proposed explains many of the observations we have made, there is an alternative model through which these data could be interpreted. We have proposed that the increase in autophagosome number found in the absence of GMS IRGs is due to an increase in autophagosome formation to degrade an increased number of protein aggregate inclusions. A second possible explanation for this increase in autophagosome number, however, is that GMS IRGs are directly involved in increasing

the maturation of autophagosomes, such that in their absence an accumulation of immature autophagosomes would occur. In fact, several lines of data we and others have produced support this hypothesis. First, while the aggregate-like structures we have characterized are both LC3 and p62 positive, indicating that they are autophagosomal compartments, they are LAMP-1-negative, demonstrating that they have not yet fused with lysosomes. Second, many of the LC3-positive structures we found appeared abnormally large, a feature which may indicate autophagosome-autophagosome fusion which can occur when autophagic maturation is blocked [213]. And third, a previous study indicated that Irgm1 is able to directly interact with Snapin, a part of the SNARE complex whose primary function is to enable vesicle docking, including autophagosome-lysosome fusion [170,171,214]. Together, these data suggest that GMS IRGs may play a role in regulating autophagosome maturation, a hypothesis we will explore further in chapter 3 of this dissertation.

One question raised by the data presented in this chapter concerns the clear distinction between the way in which GMS IRG proteins affect Gbp2 and GKS IRG proteins. The latter, represented by Irga6 in our studies, are likely ubiquitinated through K63 linkages, as suggested by the TUBE 1 pull down studies. In absence of Irgm1 or Irgm3, the amount of ubiquitinated Irga6 that accumulates in cells increases substantially, possibly due to lack of efficient removal through Irgm1/3-driven autophagy. In contrast, our studies suggest that there is little K63-linked-ubiquitinated

Gbp2 in IFN-γ-activated cells, whether wild-type or lacking Irgm1 or Irgm3. These findings raise the question of whether GMS IRGs are directly regulating the localization of Gbp2, leading to it being targeted for degradation by autophagy in the absence of GMS IRGs, or whether instead Gbp2 is recruited to autophagosomes in GMS-IRG-deficient cells as a protein that is involved in the autophagic process itself. This latter hypothesis is supported by previous studies indicating a role for certain guanylate-binding proteins in macroautophagy, including direct interactions between Gbp1 and p62, and evidence that Gbp7 colocalizes with LC3 and affects the rate of p62 degradation [85]. We will examine the relationship between the guanylate-binding proteins and autophagy further in chapter 4 of this dissertation.

We have described here data which indicate a role for the GMS IRGs in regulating the formation of protein aggregate structures which are cleared by macroautophagy. The work presented in the next chapters will provide additional descriptive details about the nature of these aggregates, and clarify the mechanisms whereby GMS IRGs and GBPs affect macroautophagy. Our ultimate goal remains to determine the importance of this pathway in cell autonomous immune responses to intracellular infection.

2.4 Materials and methods

2.4.1 Cell culture

Irgm1 (LRG-47)-deficient and Irgm3 (IGTP)-deficient mice were generated as described previously [215]. The mice were maintained according to Institutional Animal Care and Use Committee-approved protocols at the Durham VA and Duke University Medical Centers (Durham, NC). Mouse embryonic fibroblasts were derived from these mouse lines and immortalized by the standard 3T3 procedure [216]. Atg5-deficient fibroblasts were a gift from Herbert Virgin, Washington University, St. Louis, MO. 3T3 fibroblasts were cultured in DMEM (Invitrogen) supplemented with 10% (v/v) FBS (Hyclone, Logan, UT); 10 ug/mL ciprofloxacin was occasionally added to control infection. 18-24 hours prior to many experiments (as indicated in the text), 100 units/ml IFN-γ (#407320, Calbiochem, EMD Biosciences, San Diego, CA or #IF005, Millipore, Billerica, MA) was added to the culture medium.

Primary BMM were isolated from the tibia and femurs of 2- to 4-month-old mice. Bone marrow was flushed from the bones using a 27-gauge needle fitted to a syringe filled with DMEM, and the marrow was dispersed by drawing through the needle three to four times. Red cells were lysed with ACK lysing buffer (Invitrogen). Adherent cells were cultured for 6 days in bone marrow macrophage medium (culture medium supplemented with 30% (v/v) L929 cell-conditioned culture medium). The cells were cultured on Petri dishes, resulting in cultures that were loosely adherent and easily

removed from the plates with cell dissociation buffer (#13150–016, Invitrogen). After day 6, procedures diverged depending on the experiment.

2.4.2 Transfection and Nucleofection

DNA transfections were performed using X-tremeGENE 9 or HP transfection reagent (#06365779001, Roche, Pleasanton, CA) according to manufacturer's instructions. Nucleofections were performed using the Amaxa Biosystems Nucleofector II (Lonza, Basel, Switzerland), along with nucleofector kit R (#VCA-1001, Lonza), according to manufacturer's instructions. MEF were nucleofected using program number U-30, and BMM were nucleofected using program number Y-1.

2.4.3 Immunocytochemistry

Cells were plated on poly-D-lysine-coated (#P7280, Sigma) coverslips and subjected to treatment conditions as described in the text. Cells were then fixed with 4% paraformaldehyde (w/v) in PBS for 15 min, rinsed in 100 mM glycine/ PBS for 5 min, and permeabilized with 0.2% (w/v) saponin/PBS for 10 min. Cells were blocked with 10% (v/v) FCS/PBS for 60 min. As indicated in the text, the cells were then stained with various primary antibodies for 60 min, followed by AlexaFluor-conjugated secondary antibodies (Molecular Probes/Invitrogen) for 60 min. Primary antibodies used include anti-Irga6 mouse monoclonal clone 10E7 antibody [51] at 1:10, anti-Irgb6 rabbit polyclonal antiserum [60] at 1:1000, anti-GM130 mouse antibody (#612009, BD Transduction Laboratories) at 1:250, anti-TRAPα rabbit polyclonal antiserum (a gift of

Chris Nicchitta, Duke University) at 1:125, anti-EEA1 mouse antibody (#610456, BD Transduction Laboratories) at 1:25, anti-proteasome 20S C2 rabbit polyclonal antiserum (#ab3325, Abcam, Inc.) at 1:500, anti-p62/Sqstm1 rabbit polyclonal antiserum (#ab91526, Abcam, Inc.) at 1:500, anti-LC3B mouse monoclonal antibody (#M152–3, MBL International, Woburn, MA) at 1:50, phalloidin-conjugated AlexaFluor 488 (Molecular Probes/Invitrogen) at 1:40 (no secondary antibody used), anti-Gbp2 rabbit polyclonal antiserum [77] at 1:500, or anti-Gbp2 rabbit polyclonal antiserum (Jörn Coers, Duke University) at 1:1500 (these two Gbp2 antisera were used interchangeably with essentially identical results in all contexts), and anti-mono- and poly- ubiquitin mouse monoclonal clone FK2 (#BML-PW8810, Enzo Life Sciences, Farmingdale, NY) at 1:750. Images were collected on an Olympus IX70 microscope equipped with a Hamamatsu C8484–03G01 digital camera. Cells were magnified x1000. Wide-field fluorescence images and z-stacks were collected using Metamorph 6.2.3.5. As mentioned in the text, images were, when appropriate, deconvolved using Auto Quant 9.3 software.

2.4.4 Western blotting

Western blot analyses were performed according to standard protocols. In brief, lysates were boiled in SDS and separated on 8–16% gradient Tris-glycine gels (#EC60485, Invitrogen). Proteins were transferred overnight to Immobilon synthetic membranes (Millipore). Membranes were blocked in 5% (w/v) milk in TBS-Tween 20 for 60 min, then incubated in primary antibody for 60 min, washed, and incubated in secondary antibody

for 60 min. Primary antibodies utilized include anti-Gbp2 rabbit polyclonal antiserum (Jörn Coers, Duke University) at 1:1000, anti-Irga6 rabbit polyclonal antiserum 165/3 [51] at 1:10000, and anti-mono- and poly- ubiquitin mouse monoclonal clone FK2 (#BML-PW8810, Enzo Life Sciences, Farmingdale, NY) at 1:500. Secondary antibodies used were goat anti-rabbit (H+L) HRP-conjugated IgG and goat anti-mouse (H+L) HRP-conjugated IgG (#AP307P and #AP308P, Millipore) at 1:1000. Blots were developed in SuperSignal west pico chemiluminescent substrate (#34708, Thermo Scientific, Rockford, IL) and imaged on a Kodak Image Station 4000R using Carestream Molecular Imaging software.

Carestream software was used to quantify band intensities. The "find lanes" feature was used, and lanes were adjusted manually as necessary. The "find bands" feature was then used, and extraneous bands were deleted. The band intensity was measured as the sum intensity of the resultant band peak.

2.4.5 TUBE 1 pull-down of polyubiquitinated protein

Wild-type, Irgm1-/-, and Irgm3-/- 3T3 cells were grown in 15-cm tissue culture dishes and exposed to 100 units/ml IFN-γ for 24 h prior to lysis. Cells were washed in PBS and lysed in 0.6 ml of lysis buffer (50mM Tris-HCL (pH 7.4), 0.15 M NaCl, 1mM EDTA, 1% Nonidet P-40, 10% glycerol). Input control samples were obtained by removing 0.2-ml aliquots and centrifuging at 16,000 x g at 4 °C for 5 min. Supernatants were mixed 3:1 with 4x sample buffer containing 0.4 M DTT (Invitrogen). To assay for

detergent-insoluble protein aggregates that might sediment during centrifugation, pellets were suspended in 0.2 ml of 1x sample buffer containing 0.1 M DTT. Viscosity of the pellet suspension was reduced by 10–15 passages through a 23-gauge needle attached to a 1-ml syringe. To keep aggregated proteins in the suspension, the lysates were not cleared by centrifugation. Agarose beads coupled to tandem ubiquitin binding entity 1 (TUBE 1, LifeSensors, Malvern, PA) or uncoupled beads were equilibrated in TBS-T (10mM Tris-HCl (pH 8.0), 0.15 M NaCl, 0.05% Tween 20) according to the supplier's recommendations. A sedimented bead volume of 30 ul was used per pull-down sample. Lysates were incubated with uncoupled agarose beads for 30 min at 4 °C. Beads were sedimented at low speed (700 x g), and the supernates were transferred to tubes containing TUBE 1-coupled beads. Incubation at 4 °C was continued for 1 h. Beads were sedimented and washed in TBS-T a total of four times. Beads destined for proteomic analysis were stored at 4ºC in 100 uL of storage buffer [PBS, 1:50 Protease Inhibitor Cocktail Set III (#539134, Calbiochem), 50 uM DUb inhibitor PR-619 (#SI9619, LifeSensors)] until further analysis.

2.4.6 Data Analysis

Results are presented as mean ± SE unless otherwise indicated. Treatment effects and/or variable interactions were determined by analysis of variance (ANOVA). Where such effects were found, post-hoc analysis for specific mean comparisons was completed

using Tukey's HSD test. Significance levels were set at $p < 0.05$ (95% confidence, two-tailed) for all analyses.

3. The regulation of Irga6 and Irgb6 aggregate formation and clearance by Irgm1

3.1 Introduction

In chapter 2 of this dissertation, we established that loss of Irgm1 and/or Irgm3 leads to the formation of protein aggregates containing the GKS IRG proteins Irga6 and/or Irgb6, as well as the related interferon-induced GTPase Gbp2. Furthermore, we identified markers of specific autophagy in these aggregates, indicating a role for macroautophagy in their clearance. We showed that loss of Irgm1 may have global effects on clearance levels of aggregated proteins marked for specific autophagy. And finally, we demonstrated that while Irga6 is marked for specific autophagic clearance, Gbp2 is not. Together, these findings imply that GKS IRG proteins form aggregate inclusions which are removed by a macroautophagic process which may be GMS-IRG mediated. In this chapter, we will further explore the regulation of the formation and/or clearance of GKS IRG protein aggregate inclusions by GMS IRG proteins.

Several important questions about this regulation of GKS IRGs by GMS IRGs are raised by the findings presented in chapter 2 of this dissertation. First, while we demonstrated that GKS IRG protein aggregates are marked for specific autophagic clearance by the p62 adaptor protein, we presented no direct evidence that p62 is necessary for this clearance; thus it remains to be answered what role p62 plays in this process. A second unaddressed question is which other of the many GKS IRG proteins

form aggregates in the absence of GMS IRG proteins, and whether or not other proteins or protein families similarly aggregate in the absence of GMS IRGs. And finally, the exact role of GMS IRG proteins in regulating macroautophagy, if any such exists, has yet to be fully determined. As we mentioned in the previous chapter, our and other labs' data indicate that GMS IRGs may affect autophagy in several ways: they may drive autophagy initiation, as seen in certain experiments indicating an increase in autophagosomes when Irgm1 is expressed in cells [41,191]; they may drive autophagosome maturation, which would explain the build up of possibly immature autophagosomes we found in their absence; and/or they may indirectly affect autophagy by preventing the formation of the GKS IRG aggregates that drive autophagy upregulation in their absence. The answers to these questions will further elucidate the associations of GMS and GKS IRG proteins with the process of macroautophagy, and may provide further insight into their roles in innate immunity.

In this chapter, we will present evidence to resolve these remaining questions surrounding the regulation of aggregate formation and clearance by GMS IRG proteins. We will demonstrate that, while absence of the autophagy adaptor protein p62 affects Irga6 protein levels, it is surprisingly not necessary for the formation of Irga6 aggregate inclusions, nor for their colocalization with LC3. Next, we will present the findings of an unbiased proteomic approach to determine proteins that are destined for specific autophagy in the absence of GMS IRG proteins, which indicates that Irga6 and Irgb6 are

the only GKS IRG proteins which are tagged in this fashion. And finally, we will examine the role of Irgm1 in the process of macroautophagy, demonstrating mixed results that may imply cell-type specific effects of Irgm1 on macroautophagy in macrophages, but reveal no effect of Irgm1 on autophagic initiation or maturation in fibroblasts. Together, these findings clarify the uniqueness of the connection between Irgm1, Irga6, and Irgb6, and add further evidence of the complex relationship between GMS IRGs and macroautophagy.

3.2 Results

3.2.1 p62 is not necessary for the formation or clearance of Irga6 aggregate inclusions

Given our previous data indicating p62 colocalization with Irga6 protein aggregates, we set out to determine whether or not p62 is necessary for Irga6 aggregate localization to autophagosomes. In order to study this, we depleted MEFs of both Irgm1 (to induce high numbers of GKS IRG protein aggregates) and p62, and then examined colocalization of Irga6 with the autophagosomal marker LC3. We first accomplished this double depletion via siRNA temporary knockdown of p62 in Irgm1 knockout MEFs to, on average, 12% of wild-type protein levels via western analysis (Figure 11, A-B). Surprisingly, Irga6 aggregates in these cells were found to colocalize with LC3 (Figure 11, C), indicating autophagic clearance of these aggregates even when p62 has been largely depleted. It is possible, however, that the level of p62 knockdown we achieved

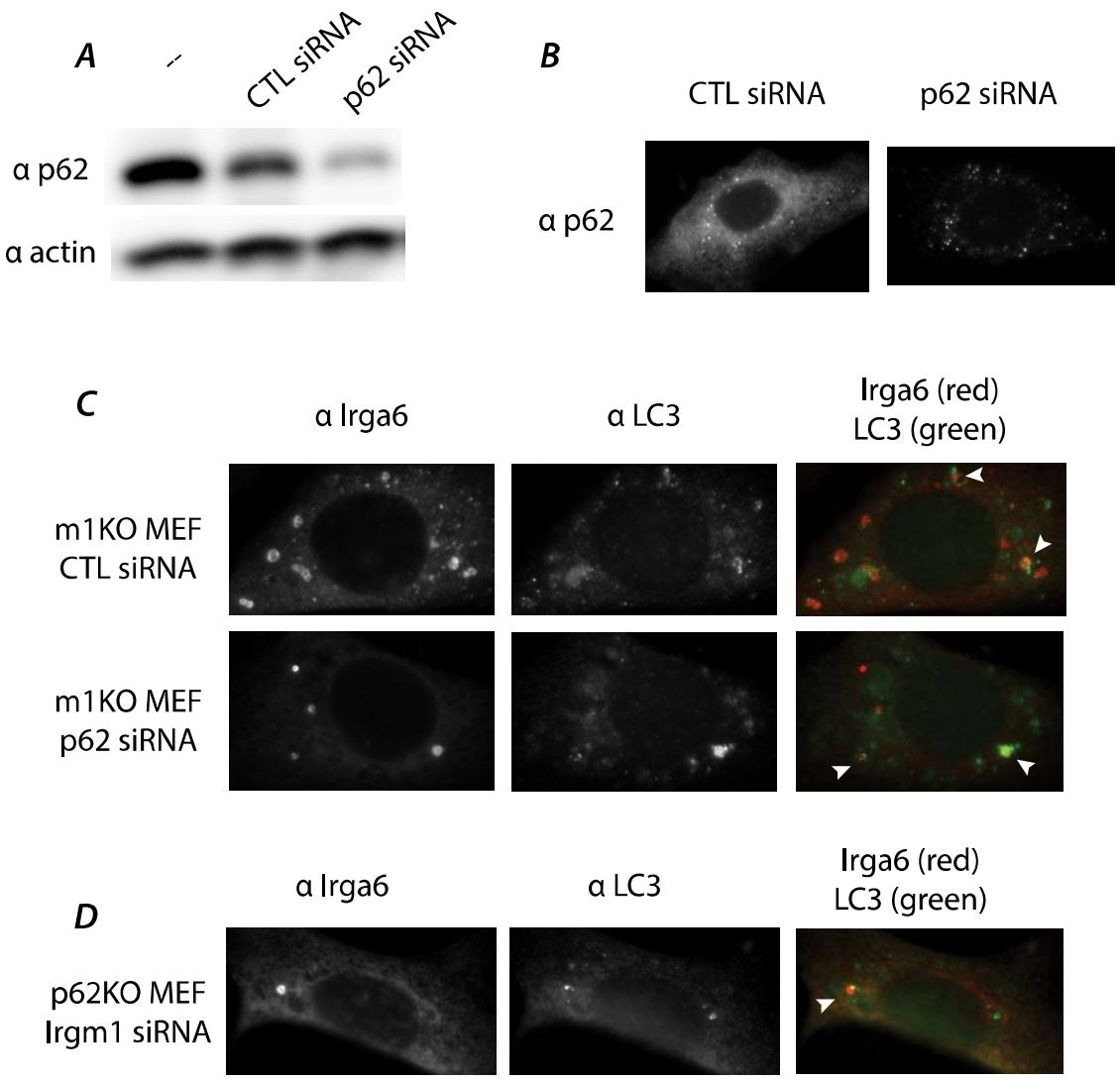

Figure 11: p62 deficiency does not affect LC3-Irga6 colocalization. *A)* p62 knock-down (western). Wild-type 3T3 MEFs were or were not treated with the indicated siRNAs for 24h, then were processed for western analysis. *B)* p62 knock-down (immunofluorescence). Wild-type 3T3 MEFs were or were not treated with the indicated siRNAs overnight, then were treated with 100 U/mL IFNγ for 18h. Cells were then processed for immunofluorescence. *C)* Irgm1-deficient MEFs were treated with the indicated siRNAs overnight, then were treated with 100 U/mL IFNγ for 18h. Cells were then processed for immunofluorescence. Arrowheads indicate colocalization between Irga6 and LC3. *D)* p62-deficient MEFs were treated with Irgm1 siRNA overnight, then were treated with 100 U/mL IFNγ for 20h. Cells were then processed for immunofluorescence. Arrowheads indicate colocalization between Irga6 and LC3.

was insufficient to completely negate p62 function; thus, we repeated the experiment utilizing Cre-adenovirus infected floxed p62 MEFs ($p62^{fl/fl}$) [217] treated with Irgm1 siRNA to induce GKS IRG protein aggregation (Figure 11, D). These cells also exhibited colocalization of Irga6 and LC3, indicating that p62 is not necessary to thedegradation of GKS IRG protein aggregates. It is likely, therefore, that while p62 can be involved in GKS IRG protein aggregate clearance, a redundant autophagic SLR adaptor protein such as NBR1 is also able to aid in the clearance of Irga6 aggregates formed in the absence of Irgm1.

3.2.2 Proteomic analysis of K63-linked ubiquitinated proteins that accumulate in Irgm1 knockout cells

Now that we have further examined the mechanism of clearance of GKS IRG protein aggregates by macroautophagy, we turn to another question, that of which (if any) other interferon-induced proteins aggregate in a similar fashion to Irga6 and Irgb6 in the absence of Irgm1. We chose to base our assessment on which proteins are marked for specific autophagy in the same fashion as Irga6 in the absence of Irgm1 – that is, which proteins display an increase in lysine-63-linked ubiquitination in Irgm1-deficient cells. We thus performed TUBE1 pull-downs on wild-type and Irgm1-deficient primary MEFs to isolate polyubiquitinated proteins, then subjected the resultant supernatant to GeLC-MS/MS analysis to identify component proteins (Figure 12). Proteins which were identified in a control resin sample were excluded from further analysis. The semi-

quantitative spectral counting method was then applied, which assigns proteins their abundance in the sample based on the number of spectra found for each of their

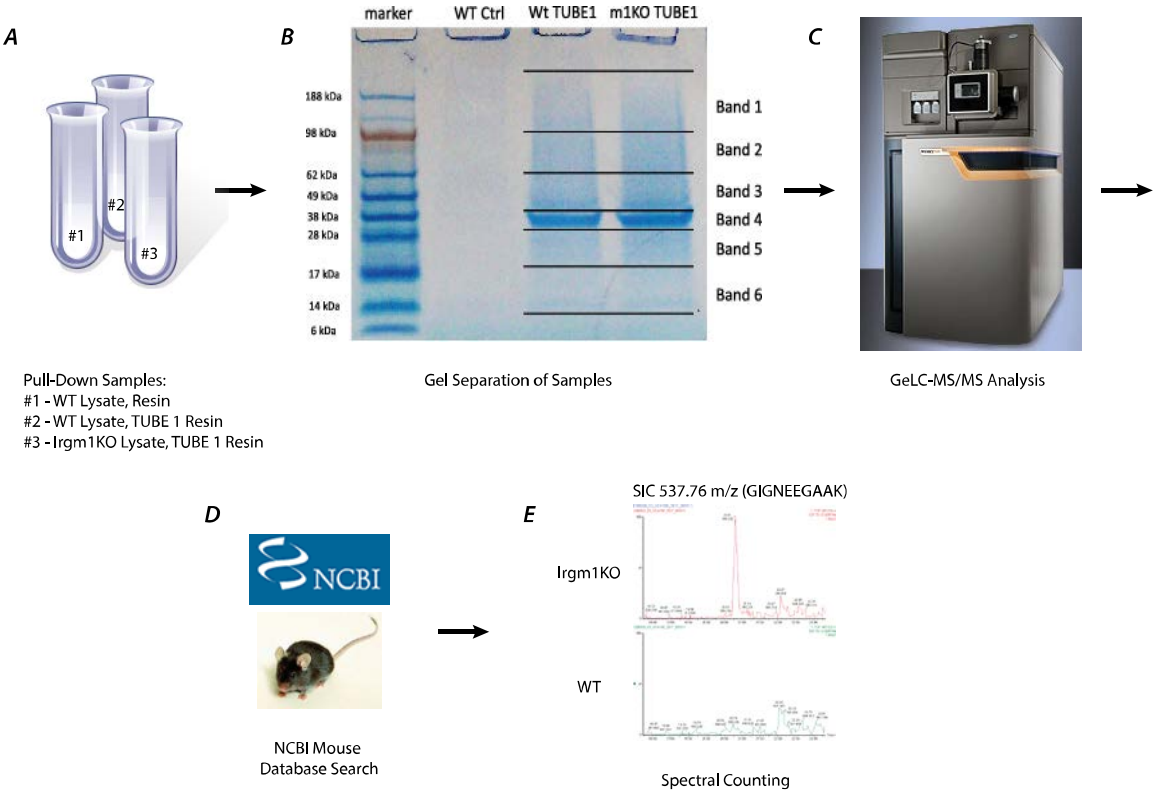

Figure 12: Schematic of Proteomic Analysis of TUBE 1 Pull-Down Experimental Design. *A)* Three samples were analysed: one control sample, one WT MEF lysate pull-down, and one Irgm1KO MEF lysate pull-down. *B)* Samples were separated on a polyacrylamide gel and visualized via coomassie staining. Pull-down samples were divided into six gel bands to minimize masking effects. The thick protein band in slice 4 corresponds to eluted TUBE 1 protein. *C)* Each gel slice was analysed separately via GeLC-MS/MS. *D)* Resultant spectra were identified by searching against the NCBI mouse protein database. Note that proteins found in the control resin sample were excluded from further analysis. *E)* Pull-down samples were compared via the semi-quantitative spectral counting method.

identified component peptides. A table of all 137 proteins identified in this proteomic screen, along with their estimated fold changes between wild-type and Irgm1 knockout samples based on the spectral counting method, can be found in Appendix A of this dissertation. Select proteins of interest identified in the study are summarized in Table 2.

A few interesting findings can be reported from the results of this proteomic assay. First, the only GKS IRG proteins pulled down in any sample by TUBE1 are Irga6, Irgb6, and Irgb10. (Note that many murine IRGs, including members of the A,B,C,D, and M subfamilies, are found in the NCBI mouse database; however, of the A subfamily, only Irga6 is contained in the database, and of the B subfamily, only Irgb5, Irgb6, and Irgb10 are represented.) Of these three proteins pulled down by TUBE1, only Irga6 and Irgb6 increased in abundance in the Irgm1 knockout pull-down sample, which correlates with the increased number of GKS IRG protein aggregates in Irgm1 knockout cells. This finding implies that Irga6 and Irgb6 may have a special relationship with Irgm1 among GKS IRG proteins. Additionally, Irga6 had one of the highest fold changes of any protein in the sample, with an approximately 3.6 fold increase in the Irgm1 knockout pull-down sample, indicating a further special relationship between the presence of Irgm1 and Irga6 aggregation.

Interestingly, although all murine GBPs are found in the NCBI mouse database, the only guanylate-binding proteins identified in the pull-down samples were Gbp2 and

Table 2: Select Proteins Differentially Found in TUBE 1 Pull-Down Samples. Fold change is reported with respect to Irgm1KO; positive fold changes are higher in Irgm1KO, while negative fold changes are lower in Irgm1KO. Fold changes ≥1.5 are considered biologically significant and are reported in green (positive) or red (negative).

Name	Reference Number	Peptide Count	Fold Change
Irga6	NP_068564.4	4	3.6
Irgb6	NP_001138636.1	2	1.5
Irgb10	NP_001128587.1	1	-1.0
Gbp2	NP_034390.1	3	1.2
Gbp6	NP_919317.2	3	-1.5
p62	NP_035148.1	3	-1.1
Stat1	NP_001192243.1	1	-2.8

Gbp6. Gbp6 (but not Gbp2) was identified previously in a screen to determine which GBPs were important to cell-autonomous immunity to *Mycobacterium bovis* (BCG) and/or *Listeria monocytogenes* [85]. This previous screen also identified Gbp1 and Gbp7 as being both important to immunity and involved in macroautophagy, Gbp1 as an interactor with p62, and Gbp7 as an interactor with the protease Atg4b [85]. The proteomic screen reported here did not identify Gbp1 or Gbp7 as being highly ubiquitinated, which supports the finding of the previous screen that Gbp1 associates with p62 outside of its ubiquitin-binding domain, and that neither of these two proteins are macroautophagic cargo proteins [85]. The identification of Gbp6 as being ubiquitinated highlights a possible involvement of this protein with macroautophagy which warrants further

investigation. Furthermore, Gbp6 displayed slightly decreased ubiquitination (1.5-fold) in the absence of Irgm1, a relationship which should be further explored. In contrast, the abundance of ubiquitinated Gbp2 remained relatively equal between wild-type and Irgm1-deficient samples. This finding that Gbp2 is ubiquitinated differs slightly from the TUBE1 pull-down western analysis reported in chapter 2 of this dissertation, in which full-length Gbp2 was not identified in TUBE1 pull-down of wild-type or Irgm1 deficient lysates. This lack of identification indicates that levels of ubiquitinated Gbp2 protein are quite low in abundance; alternatively, the identification of Gbp2 in the proteomic screen might imply that Gbp2 briefly associates with ubiquitinated proteins captured in the pull-down studies. Importantly, though, Gbp2 abundance does not significantly change between wild-type and Irgm1-deficient samples, which indicates that the presence of Irgm1 does not affect the relationship between Gbp2 and macroautophagy, a finding we will explore further in chapter 4 of this dissertation.

Finally, the abundance of ubiquitinated Stat1, a member of the interferon family signal cascade, decreased significantly in the Irgm1 deficient pull-down sample. This finding may imply that Stat1 is upregulated (ie, not degraded) in the absence of Irgm1. It seems more likely, however, that Stat1 is ubiquitinated as a function of its signaling capacity, instead of because of a link with specific autophagy [102]; this would imply that Stat1 signaling is decreased when the interferon response is confounded by the absence of Irgm1, possibly as a mechanism of down-regulating the interferon response

to limit toxic effects on the cell. These hypotheses are worthy of further consideration, but such studies must rely on further research into the ubiquitin signaling code.

It should be noted that this proteomic analysis is a good first step to answer the question of which interferon-induced proteins are ubiquitinated in the absence of Irgm1; however, due to time and money constraints, only one trial of this assay was able to be completed, and thus the results should be examined in that light. It is very important that further experimentation be done to confirm the results reported here, including western analysis of TUBE1 pulldown samples utilizing antisera for additional IRG and GBP proteins. These confirmatory studies are currently planned, but were unable to be completed before the publication of this dissertation.

In summary, the results of the proteomic analysis of TUBE1 pull-downs indicates that a special relationship may exist between Irgm1 and the GKS IRG proteins Irga6 and Irgb6, leading these two specific proteins to aggregate in Irgm1's absence. Furthermore, the presence of Irgm1 seems to have little or no effect on ubiquitination of Gbp2, which will be explored further in chapter 4 of this dissertation.

3.2.3 Effects of Irgm1 deficiency on autophagosome maturation

We have now discussed specific characteristics of the Irga6 and Irgb6 aggregates that form in the absence of Irgm1, but we have yet to address the mechanism whereby loss of Irgm1 leads to an accumulation of these aggregates. As we have demonstrated that these GKS IRG aggregates colocalize with autophagic markers, we have

hypothesized that the formation of these aggregates is related to the process of macroautophagy. GMS IRGs may affect autophagy directly or indirectly. Direct effects may include driving autophagosome initiation, supported by the demonstrated increase in autophagosomes when Irgm1 is expressed in cells [41,191], or driving autophagosome-lysosome fusion, evidenced by an accumulation of LC3-positive but not LAMP-1 positive structures in GMS IRG-deficient cells; indirect effects may include preventing the formation of GKS IRG aggregates which themselves increase autophagy. It should be noted that none of these hypotheses are mutually exclusive, and some combination of these may be true. The third of these hypotheses, that GMS IRGs directly interact with and thus prevent the premature activation and aggregation of GKS IRGs, has been described previously [62]; thus we will focus on the possible direct effects of Irgm1 on macroautophagic processes.

To begin, we will examine whether or not GMS IRGs promote the maturation of autophagosomes.

3.2.3.1 p62 degradation assay

The first of three assays which we utilized to examine autophagosome maturation as a function of Irgm1 is the p62 degradation assay. As an SLR adaptor protein, p62 is reliably degraded by the process of macroautophagy; thus, if autophagosome maturation is blocked, p62 will no longer be degraded and will accumulate within the cell. We examined levels of p62 both before and after induction

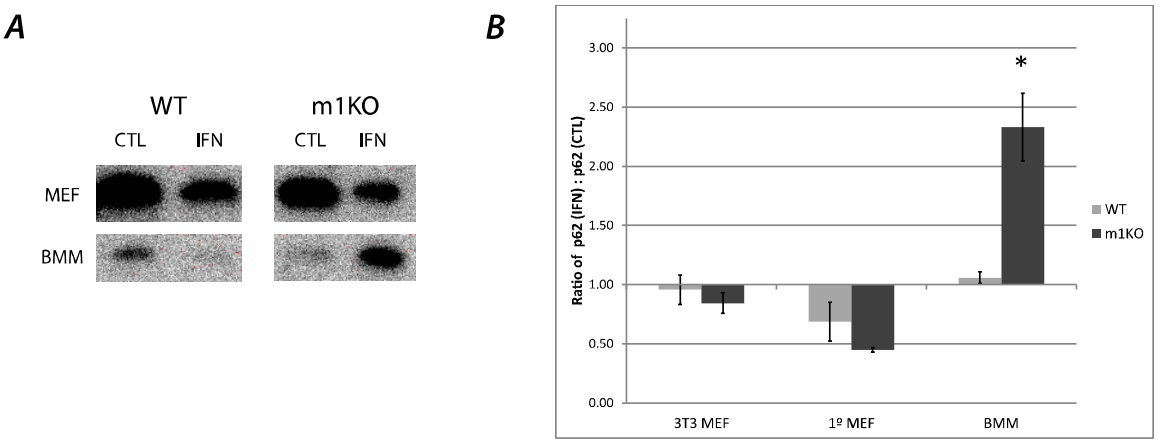

Figure 13: Irgm1 deficiency does not affect autophagosome maturation (p62 degradation assay). *A)* Sample blot. Primary MEFs or BMM of the indicated genotypes were incubated with or without 100 U/mL IFNγ for 24 hours, then were processed for western analysis. Representative of n = 3 trials. This experiment was done by Stanley Henry. *B)* Quantitative analysis of western results. 3T3 transformed MEFs, primary MEFs, or BMM of the indicated genotypes were incubated with or without 100 U/mL IFNγ for 24 hours, then were processed for western analysis. Band intensities were quantified and normalized to actin levels. Values are reported as ratios of normalized p62 in IFN-treated sample to normalized p62 in untreated sample. 2x3 ANOVA results indicated a significant interaction term, $p < 0.02$; this analysis was followed by 1 way ANOVA, indicating a significant treatment effect, $p < 0.0002$. * $p < 0.01$ via Tukey's HSD test. Data represent n = 2-4 trials with 1-2 replicates per trial.

of autophagy by interferon-γ treatment in MEFs, immortalized MEFs, and bone-marrow macrophages. In wild-type cells of both kinds of MEFs, p62 levels decreased as expected upon interferon-γ treatment, indicating typical autophagic induction in these cell types in response to interferon-γ (Figure 13). Wild-type BMM, however, exhibited a more varied response to interferon, showing either a decrease in p62 (Figure 13, *A*) or a relatively equivalent amount of p62 (Figure 13, *B*). The reason for this varied response is unclear, as previous studies found that macrophage-like RAW 264.7 cells exhibited an

induction of autophagy upon interferon treatment [41,191]. This finding may suggest that p62 levels are a poor readout for autophagic activity in bone-marrow-derived macrophages, as discussed further at the end of this section.

Next, we examined changes in p62 levels in Irgm1-deficient cells of all three cell types. In both primary and immortalized MEFs with Irgm1 deficiency, p62 levels similarly decreased in response to autophagic induction, indicating normal autophagy in these cell types even in the absence of Irgm1 (Figure 13). In contrast, p62 levels increased over 2-fold upon induction of autophagy in Irgm1-deficient BMM; this finding could indicate a cell-specific role for Irgm1 in autophagic maturation in macrophages.

The results of this assay suggest that interferon-γ may have differential effects on autophagy as a consequence of cell type, and that Irgm1 may function differently based on cellular context. Past studies have often focused on macrophages and macrophage-like cells to determine the effects of Irgm1 on autophagy [41,191]; the results of the assay presented here, which indicate varied induction of autophagy in macrophages in response to interferon-γ, do somewhat contradict the results of those previous studies. However, assays utilizing p62 as a marker of autophagic flux have the major caveat that p62 has functions outside of macroautophagy. As described further in chapter 1 of this dissertation, p62 also interacts with upstream regulators of NF-kB and has been demonstrated to affect levels of inflammatory cytokines such as IL-1β and TNF-α, in addition to playing a role in the stress response to reactive oxygen species [187,188,218-

220]. Thus, other functions of p62 may play a more important role in macrophages than in fibroblasts and could account for the differences observed between these two cell types. We therefore conducted studies of autophagic maturation utilizing two other assays in both cell types.

3.2.3.2 GFP-LC3 degradation assay

The second assay we used to examine autophagosome maturation is the GFP-LC3 degradation assay. When exogenously expressed in cells, GFP-LC3 is incorporated into autophagosomes; upon acidification of the autophagosomal lumen, the fluorescent tag is cleaved from LC3 prior to degradation of both proteins. Thus, levels of free GFP fluctuate in response to changes in the maturation of autophagosomes. We demonstrated that levels of free GFP decrease in cells treated with bafilomycin A1, a pharmacological inhibitor of autophagosome-lysosome fusion, in a treatment-time dependent manner (Figure 14, *A*). We then examined levels of free GFP in wild-type and Irgm1-deficient MEFs (Figure 14, *B*) and BMM (Figure 14, *C*). In direct contrast to the results we obtained from the p62 degradation assay, we found in both MEFs and BMM that levels of free GFP increase in response to Irgm1 deficiency. This finding implies that loss of Irgm1 in either of these cell types does not affect autophagic maturation, and in fact leads to an *increase* in autophagic activity. An increase in autophagy in response to Irgm1 deficiency is consistent with the hypothesis that Irgm1

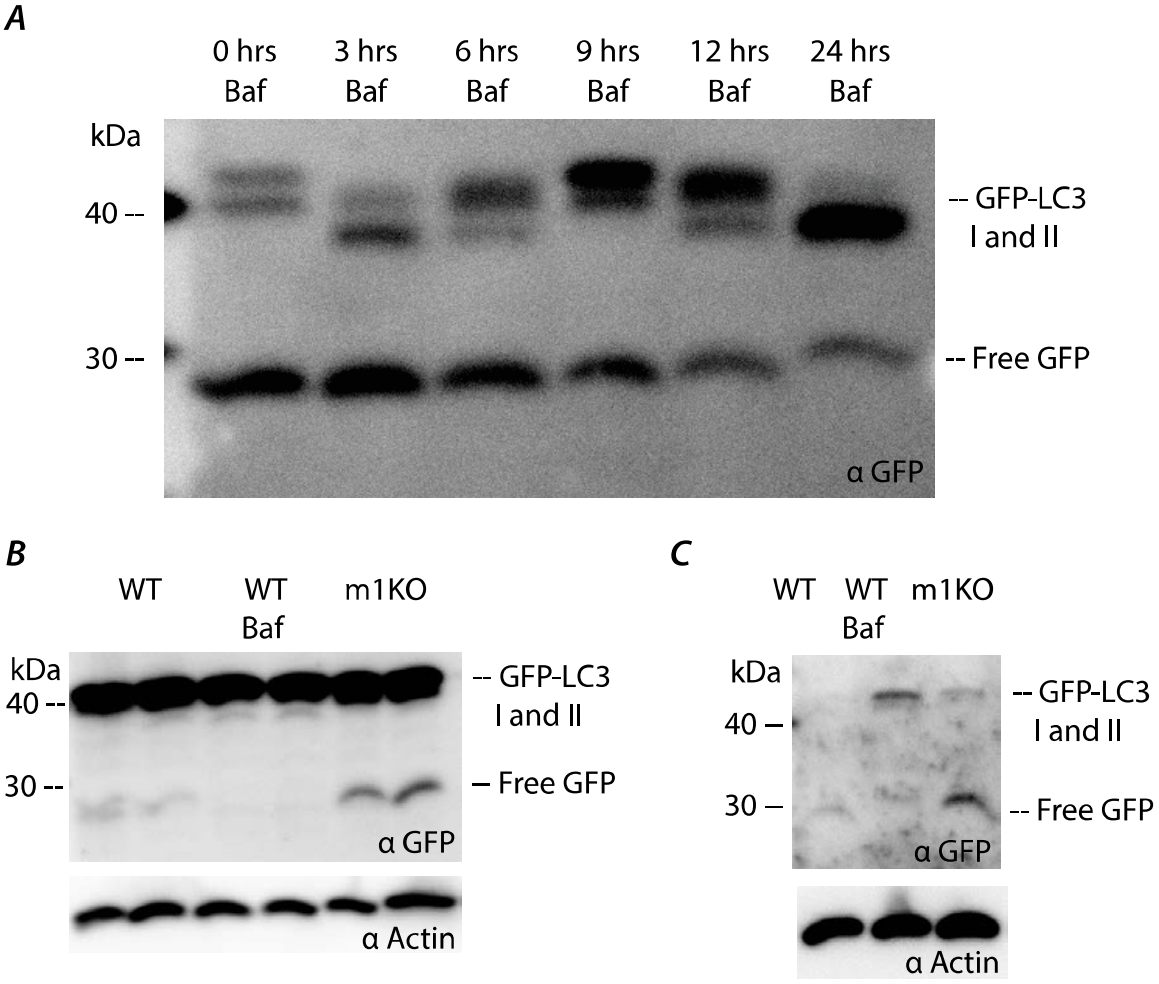

Figure 14: Irgm1 deficiency does not affect autophagosome maturation (free GFP assay). *A)* Proof of concept assay. Wild-type MEFs were nucleofected with GFP-LC3 and treated with 100 U/mL interferon-γ for 24 hours. Cells were concurrently treated with 100 nM bafilomycin A1 for the indicated lengths of time. After treatment, cells were processed for western analysis. *B)* MEFs of the indicated genotypes were nucleofected with GFP-LC3 and treated with 100 U/mL interferon-γ and 100 nM bafilomycin A1 (where indicated) for 24 hours. Following treatment, cells were processed for western analysis. Blot is representative of 3 trials. *C)* BMM of the indicated genotypes were nucleofected with GFP-LC3 and treated with 100 U/mL interferon-γ and 100 nM bafilomycin A1 (where indicated) for 24 hours. Following treatment, cells were processed for western analysis. Blot is representative of 2 trials.

affects autophagy indirectly, by preventing the formation of GKS IRG aggregates which themselves upregulate autophagy. However, a cautionary note should be applied to the interpretation of these findings, as possible differences in transfection efficiencies between genotypes not fully evident in the western blots may have affected the results.

3.2.3.3 Tandem-fluorescent LC3 assay

The third and final assay we utilized to examine autophagosome maturation in Irgm1-deficient cells is the tandem-fluorescent LC3 assay. This assay directly measures immature autophagosome number by taking advantage of the different sensitivities to acidic environments of the fluorescent tags GFP and mCherry. An LC3 construct that is tagged with both GFP and mCherry is expressed in cells and incorporated into forming autophagosomes. Both tags fluoresce in the non-acidic environment of an immature autophagosome, causing those structures to fluoresce yellow; upon maturation of the autophagosome by lysosome fusion, however, the lumen is acidified, which quenches the fluorescence of GFP but not mCherry, and leads mature autophagosomes to fluoresce red (Figure 15, *A*). Thus, the number of mature and immature autophagosomes can be counted separately in individual cells (Figure 15, *B*). We subjected both primary MEFs and BMM to this analysis, using cells treated with the pharmacological maturation blocker bafilomycin A1 as positive controls (Figure 15, *C*). The average percentage of immature autophagosomes in MEFs did not change between wild-type and Irgm1-deficient cells, which supports the results of the previous two

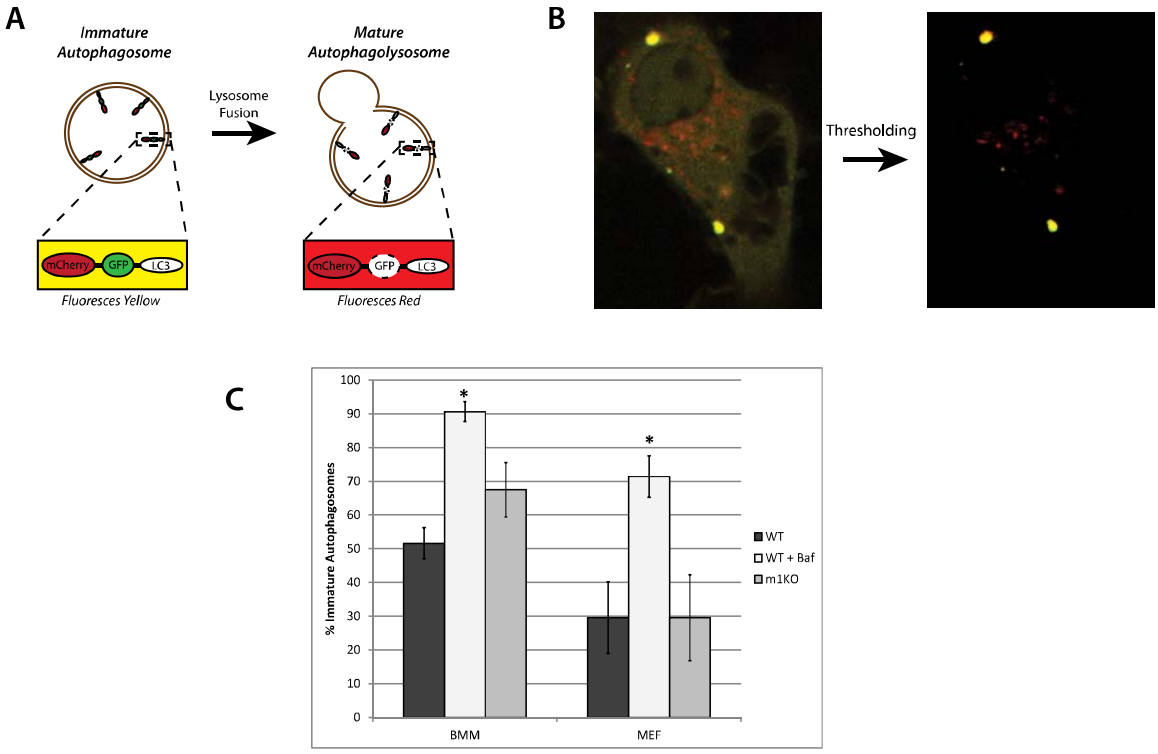

Figure 15: Irgm1 deficiency does not affect autophagosome maturation (tandem fluorescence assay). *A*) Schematic representation of tandem fluorescence assay. Doubly-fluorescent-tagged LC3 is expressed in cells and incorporated into forming autophagosomes. Both tags fluoresce in the non-acidic environment of immature autophagosomes, leading to yellow fluorescence. Once the autophagosome matures and is acidified, GFP fluorescence is quenched, leading to red fluorescence. *B)* Representative image obtained from assay. After the image is thresholded to remove background fluorescence, red and yellow puncta are clearly distinguishable. *C)* Assay results. MEFs were nucleofected with tandem fluorescent LC3 construct and examined live with resonant scanning confocal microscopy. n=3 experiments with 5-10 cells imaged per treatment group. ANOVA indicates a significant treatment effect, $p < 0.05$; * $p < 0.05$ via Tukey's HSD post-hoc analysis. BMM were nucleofected with tandem fluorescent LC3 construct after five days of treatment with CSF. Cells expressing the construct at high levels (1-5% of the population) were sorted by FACS analysis and examined live with resonant scanning confocal microscopy. n=4 trials with 5-10 cells imaged per treatment group per trial. ANOVA indicates a significant treatment effect, $p < 0.05$; * $p < 0.05$ via Tukey's HSD post-hoc analysis.

assays indicating no block in autophagic flux in MEFs in the absence of Irgm1. In bone-marrow macrophages, a ~15% increase in immature autophagosomes was seen in the absence of Irgm1, but this increase was not statistically significant, and additionally was far less than the increase seen upon bafilomycin treatment. We thus conclude that the absence of Irgm1 may cause a small, cell-type specific negative effect on autophagic maturation, but further study is needed.

The major caveat to this assay is the technical challenge of ensuring nearly equal intensities of the green and red channels in image collection and analysis. Due to technical considerations, the red channel was often less intense, and occasionally autophagosomes which fluoresced green (not yellow) were observed, which should not be possible given the nature of the experiment. The presence of these green puncta indicates that the red channel was slightly under-collected and that mature (red-fluorescent) autophagosomes may occasionally have been missed, leading to the likely over-estimation of the percentage of immature autophagosomes that we report. However, excitation and collection parameters were kept constant for all treatment conditions, and thus each condition was affected by this technical issue to the same extent, making comparisons between these conditions valid.

In summary, the results of these three flux assays, taken together, strongly indicate that in MEFs, Irgm1 deficiency does not affect the maturation of autophagosomes. However, a small, cell-type dependent effect on autophagosome

maturation may exist in bone-marrow macrophages, coupled with a possible increase in autophagic initiation (observed in the free GFP assay), likely due to an increased number of protein aggregates. The cell-type dependent nature and small magnitude of the observed effect on autophagic flux strongly implies that any effects of Irgm1 on autophagosome maturation are indirect, as a result of other consequences of Irgm1 on cellular function.

3.2.4 Effects of Irgm1 overexpression on autophagosome initiation

Finally, we turn to the question of whether or not Irgm1 may directly promote autophagic initiation. Previous studies demonstrated that overexpression of GFP-tagged Irgm1 promoted the formation of acidic, double-membraned structures in macrophage-like RAW 264.7 cells [41,191]. Given the cell-type dependent effect of Irgm1 on autophagosome maturation that we found, we decided to expand the results of these previous studies to include MEFs. We chose to overexpress wild-type Irgm1 in MEFs, as opposed to the GFP-Irgm1 construct used in previous studies, because of concerns raised previously that the GFP tag may constitutively activate Irgm1 [56]. We compared the number of endogenous LC3 puncta in cells expressing Irgm1 to the number found in untreated wild-type cells and interferon-treated Irgm1-deficient MEFs (Figure 16). Our results in MEFs did not confirm those of previous experiments in RAW 264.7 cells; expression of Irgm1 in wild-type cells did not significantly increase the

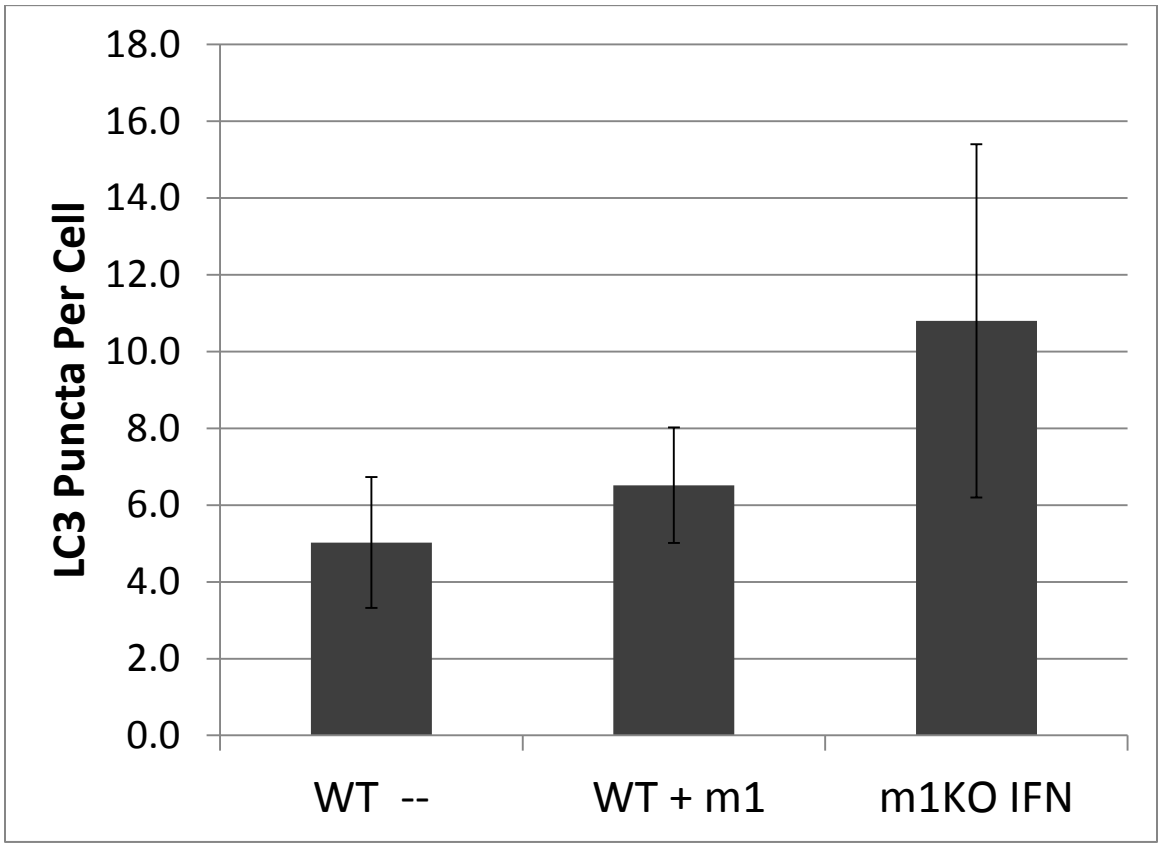

Figure 16: Overexpression of Irgm1 does not increase autophagosome number. 3T3 MEFs of the indicated genotypes were or were not nucleofected with an Irgm1 expression construct, and were or were not treated with IFNγ for 24 hours, then were processed for immunofluorescence using αIrgm1 and αLC3 antibodies. The number of LC3 puncta per cell was quantified in a blinded fashion. ANOVA indicated no significant treatment effects. Data represent n = 2-3 trials with 8-12 cells quantified per treatment group per trial.

number of LC3 puncta above that found in untreated wild-type cells. These conflicting results may be due to different methodologies (GFP-tagged vs. wild-type Irgm1, and double-membraned structure observance vs endogenous LC3 puncta counting). However, given that the results of many assays we have outlined in this chapter are cell-

type dependent, it seems likely that if Irgm1 has direct effects on autophagy, they are cell-type specific, and assays should be interpreted based on their cellular context.

3.3 Discussion

In this chapter, we have further characterized the GKS IRG protein aggregates that form in the absence of Irgm1. We have presented evidence that p62 is not necessary to the degradation of Irga6 aggregate inclusions, but does have an effect on overall levels of Irga6. We demonstrated via proteomic analysis of K63-linked ubiquitinated proteins that Irga6 and Irgb6 may have a special relationship with Irgm1 and may be the only GKS IRG proteins to form aggregates in its absence. We then examined the mechanism by which absence of Irgm1 leads to an accumulation of protein aggregates, focusing on the effects of Irgm1 on macroautophagy. We demonstrated that Irgm1 overexpression in fibroblasts does not affect autophagic initiation, nor does its absence in fibroblasts affect autophagosome maturation; however, a small negative effect on autophagosome maturation may occur in macrophages in the absence of Irgm1.

Our finding that p62 was unnecessary to both the formation of Irga6 aggregate inclusions and their colocalization with LC3 was very surprising, given the well-established role of p62 as a promoter of aggregate inclusion formation and an autophagic adaptor. However, we have proposed that a redundant SLR adaptor protein is able in the absence of p62 to mediate the transfer of Irga6 aggregates to autophagic compartments. We were unable to determine if the SLR adaptor NBR1, which has many

structural similarities to p62, also localized to Irga6 aggregates due to technical issues with antibody visualization by immunofluorescence (data not shown); we hope that future advances in SLR research will provide the tools to definitively answer whether other SLR adaptors provide a redundant function to p62 in this context.

The results of the proteomic analysis of TUBE1 pulldown samples, implying that Irga6 and Irgb6 are the only GKS IRGs which are K63-linked ubiquitinated, suggest that these two GKS IRGs are the only ones with a relationship to the macroautophagic system. A previous study indicated a role for macroautophagy in targeting Irga6 to pathogen-containing vacuoles [221], but no evidence has previously linked Irgb6 to macroautophagy. Additionally, our results imply that Irga6 and Irgb6 have a different relationship with Irgm1 than other GKS IRGs. Previous models of GMS IRG function proposed that this subfamily interacts with all GKS IRGs to prevent their premature activation [62]. However, our data indicate that Irga6 and Irgb6 behave differently than other IRGs in the absence of Irgm1; it remains to be seen whether this difference is a result of characteristics inherent to Irga6 and Irgb6, or inherent to the relationship between Irgm1 and these IRGs.

Finally, our experimental results describing the effects of Irgm1 on macroautophagy lend further complexity to the already thorny debate over whether GMS IRGs mediate interferon-induced macroautophagy. Our data indicate that effects of Irgm1 on macroautophagy vary based on cell type, and argue against a direct role of

Irgm1 in autophagosome initiation or maturation in MEFs, while reaching somewhat inconclusive results in BMM. Furthermore, the results of the GFP-LC3 degradation assay indicating an increase in autophagosome activity in the absence of Irgm1 support the hypothesis proposed previously that Irgm1 indirectly affects autophagy by preventing the premature activation (and aggregation) of its effector proteins Irga6 and Irgb6 [62]. Further research is still needed to ascertain any direct effects Irgm1 may have on macroautophagy in macrophages, and the discovery of a mechanism for this effect is imperative.

In summary, the results presented in this chapter further clarify the mechanism of Irga6 and Irgb6 aggregate formation and clearance in the absence of Irgm1. Our ultimate goal for this research remains to determine how the IRG protein system promotes cell autonomous immune responses to intracellular infection, and to expand this understanding to include how human IRGM functions in innate immunity.

3.4 Materials and methods

3.4.1 Cell culture

Irgm1 (LRG-47)-deficient and Irgm3 (IGTP)-deficient mice were generated as described previously [215]. The mice were maintained according to Institutional Animal Care and Use Committee-approved protocols at the Durham VA and Duke University Medical Centers (Durham, NC). Mouse embryonic fibroblasts were derived from these mouse lines and immortalized by the standard 3T3 procedure [216]. Atg5-deficient

fibroblasts were a gift from Herbert Virgin, Washington University, St. Louis, MO. 3T3 fibroblasts were cultured in DMEM (Invitrogen) supplemented with 10% (v/v) FBS (Hyclone, Logan, UT); 10 ug/mL ciprofloxacin was occasionally added to control infection. 18-24 hours prior to many experiments (as indicated in the text), 100 units/ml IFN-γ (#407320, Calbiochem, EMD Biosciences, San Diego, CA or #IF005, Millipore, Billerica, MA) and 100 nM bafilomycin A1 (#B1793, Sigma, St. Louis, MO), were added to the culture medium.

Primary BMM were isolated from the tibia and femurs of 2- to 4-month-old mice. Bone marrow was flushed from the bones using a 27-gauge needle fitted to a syringe filled with DMEM, and the marrow was dispersed by drawing through the needle three to four times. Red cells were lysed with ACK lysing buffer (Invitrogen). Adherent cells were cultured for 6 days in bone marrow macrophage medium (culture medium supplemented with 30% (v/v) L929 cell-conditioned culture medium). The cells were cultured on Petri dishes, resulting in cultures that were loosely adherent and easily removed from the plates with cell dissociation buffer (#13150–016, Invitrogen). After day 6, procedures diverged depending on the experiment.

3.4.2 Transfection and nucleofection

DNA transfections were performed using X-tremeGENE 9 or HP transfection reagent (#06365779001, Roche, Pleasanton, CA) according to manufacturer's instructions. Nucleofections were performed using the Amaxa Biosystems Nucleofector II (Lonza,

Basel, Switzerland), along with nucleofector kit R (#VCA-1001, Lonza), according to manufacturer's instructions. MEF were nucleofected using program number U-30, and BMM were nucleofected using program number Y-1.

3.4.3 Knock-downs

siRNA transfections were performed using Lipofectamine RNAiMAX (#13778, Invitrogen) according to manufacturer's instructions. siRNAs were transfected overnight, and assays were performed either immediately or 24 hours later, as indicated in the text. siRNAs utilized include Stealth® siRNA Sqstm1 #MSS207329 (#1320001, Invitrogen), Stealth® RNAi Negative Control High GC duplex (#12935-400, Invitrogen), Silencer® Select siRNA Irgm1 #s68045 (#4390771, Invitrogen), and Silencer® Select Negative Control No. 1 siRNA (#4390843, Invitrogen).

3.4.4 Immunocytochemistry

Cells were plated on poly-D-lysine-coated (#P7280, Sigma) coverslips and subjected to treatment conditions as described in the text. Cells were then fixed with 4% paraformaldehyde (w/v) in PBS for 15 min, rinsed in 100 mM glycine/ PBS for 5 min, and permeabilized with 0.2% (w/v) saponin/PBS for 10 min. Cells were blocked with 10% (v/v) FCS/PBS for 60 min. As indicated in the text, the cells were then stained with various primary antibodies for 60 min, followed by AlexaFluor-conjugated secondary antibodies (Molecular Probes/Invitrogen) for 60 min. Primary antibodies used include anti-p62/Sqstm1 rabbit polyclonal antiserum (#ab91526, Abcam, Inc.) at 1:500, anti-Irga6

rabbit polyclonal antiserum 165/3 [51] at 1:4000, and anti-LC3B mouse monoclonal antibody (#M152–3, MBL International, Woburn, MA) at 1:50. Images were collected on an Olympus IX70 microscope equipped with a Hamamatsu C8484–03G01 digital camera. Cells were magnified x1000. Wide-field fluorescence images were collected using Metamorph 6.2.3.5.

3.4.5 Western blotting

Western blot analyses were performed according to standard protocols. In brief, lysates were boiled in SDS and separated on 8–16% gradient Tris-glycine gels (#EC60485, Invitrogen). Proteins were transferred overnight to Immobilon synthetic membranes (Millipore). Membranes were blocked in 5% (w/v) milk in TBS-Tween 20 for 60 min, then incubated in primary antibody for 60 min, washed, and incubated in secondary antibody for 60 min. Primary antibodies utilized include anti-p62/Sqstm1 rabbit polyclonal antiserum (#ab91526, Abcam, Inc.) at 1:500, anti-Irga6 rabbit polyclonal antiserum 165/3 [51] at 1:2000, anti-actin clone C4 mouse monoclonal antibody (#MAB1501, Millipore) at 1:1500, and anti-GFP rabbit polyclonal antiserum (#A6455, Invitrogen) at 1:500. Secondary antibodies used were goat anti-rabbit (H+L) HRP-conjugated IgG and goat anti-mouse (H+L) HRP-conjugated IgG (#AP307P and #AP308P, Millipore) at 1:1000. Blots were developed in SuperSignal west pico chemiluminescent substrate (#34708, Thermo Scientific, Rockford, IL) and imaged on a Kodak Image Station 4000R using Carestream Molecular Imaging software.

Carestream software was also used to quantify band intensities. The "find lanes" feature was used, and lanes were adjusted manually as necessary. The "find bands" feature was then used, and extraneous bands were deleted. The band intensity was measured as the sum intensity of the resultant band peak.

3.4.6 TUBE 1 pull-down of polyubiquitinated protein

Wild-type, Irgm1-/-, and Irgm3-/- 3T3 cells were grown in 15-cm tissue culture dishes and exposed to 100 units/ml IFN-γ for 24 h prior to lysis. Cells were washed in PBS and lysed in 0.6 ml of lysis buffer (50mM Tris-HCL (pH 7.4), 0.15 M NaCl, 1mM EDTA, 1% Nonidet P-40, 10% glycerol). Input control samples were obtained by removing 0.2-ml aliquots and centrifuging at 16,000 x g at 4 °C for 5 min. Supernatants were mixed 3:1 with 4x sample buffer containing 0.4 M DTT (Invitrogen). To assay for detergent-insoluble protein aggregates that might sediment during centrifugation, pellets were suspended in 0.2 ml of 1x sample buffer containing 0.1 M DTT. Viscosity of the pellet suspension was reduced by 10–15 passages through a 23-gauge needle attached to a 1-ml syringe. To keep aggregated proteins in the suspension, the lysates were not cleared by centrifugation. Agarose beads coupled to tandem ubiquitin binding entity 1 (TUBE 1, LifeSensors, Malvern, PA) or uncoupled beads were equilibrated in TBS-T (10mM Tris-HCl (pH 8.0), 0.15 M NaCl, 0.05% Tween 20) according to the supplier's recommendations. A sedimented bead volume of 30 ul was used per pull-down sample. Lysates were incubated with uncoupled agarose beads for 30 min at 4 °C.

Beads were sedimented at low speed (700 x g), and the supernates were transferred to tubes containing TUBE 1-coupled beads. Incubation at 4 °C was continued for 1 h. Beads were sedimented and washed in TBS-T a total of four times. Beads destined for proteomic analysis were stored at 4ºC in 100 uL of storage buffer [PBS, 1:50 Protease Inhibitor Cocktail Set III (#539134, Calbiochem), 50 uM DUb inhibitor PR-619 (#SI9619, LifeSensors)] until further analysis.

3.4.7 Proteomic analysis of TUBE-1 pull-down protein

After TUBE-1 pull-down (see above), proteins were eluted from beads by boiling in NuPAGE MES SDS running buffer (#NP002, Invitrogen) and separated on a 4–12% gradient Bis-Tris gel (#NP0321, Invitrogen). Proteins were visualized via coomassie staining (#LC6025, Invitrogen); the control lane was divided into two gel slices and the sample lanes were divided into six slices each to minimize masking effects from high concentrations of protein. In-gel tryptic digestion was performed on each gel slice via standard protocol as previously described [222]. Samples were then analysed via GeLC-MS/MS utilizing a SYNAPT G2 ToF mass spectrometer (Waters, Milford, MA). Resulting spectra were identified using the NCBI mouse protein database. Semi-quantitative comparisons were made between samples via the spectral-counting method.

3.4.8 Tandem fluorescence studies

Primary MEFs were cultured as described above, nucleofected with pDest-tfLC3 as described above, then plated in 35mm poly-D-lysine coated glass-bottom culture dishes (#P35GC-1.0-14-C, MatTek, Ashland, MA). Plates were incubated at 37ºC overnight, then rinsed with PBS to remove dead cells. 100 U/mL interferon-γ and, when appropriate, 100 nM bafilomycin A1, was added, and cells were incubated at 37ºC for 18-24 h prior to imaging.

BMM were cultured as described above; on day 6 of culture in BMM medium, cells were nucleofected with pDest-tfLC3 as described above, replated in fresh petri dishes, and incubated at 37ºC overnight. Cells expressing high levels of both mCherry and GFP fluorescence (approximately 1-5% of input) were then isolated via FACS analysis utilizing a Becton Dickinson DiVa cell sorter run at 30 psi. Live cells were determined in conventional fashion by using the FSC and SSC light scatter histogram. GFP was excited with a 488 nm laser running at 100mW power. The GFP emission was collected behind a 530/30 bandpass filter. mCherry was excited with a dye laser at 600 nm and 200mW of power. The mCherry fluorescence was collected behind a 620/22 bandpass filter. Resultant cells were then plated in 35mm poly-D-lysine coated glass-bottom culture dishes (#P35GC-1.0-14-C, MatTek) in a minimal amount of media. 2-4 hours after plating, 2 mL of culture medium containing 100 U/mL interferon-γ and,

when appropriate, 100 nM bafilomycin A1, was added to each plate. Plates were incubated at 37ºC for 18-24 h prior to imaging.

Images were collected on an inverted Leica DMI6000CS confocal microscope run with Leica LAS AF v2.6 software, utilizing an Argon laser emitting at 488 nm, a 561 nm diode laser, and an 8000 Hz resonant scanner to enable rapid multi-channel scanning and limit photo-damage. Resultant images were analysed further using Metamorph 6.2.3.5 software. Images were separated into two channels, one red and one green, then thresholded to remove background fluorescence. Thresholded channels were then overlaid to generate one image. Images were randomized and quantified in a treatment-blinded fashion.

3.4.9 Data Analysis

Results are presented as mean ± SE unless otherwise indicated. Treatment effects and/or variable interactions were determined by analysis of variance (ANOVA). Where such effects were found, post-hoc analysis for specific mean comparisons was completed using Tukey's HSD test. Significance levels were set at $p < 0.05$ (95% confidence, two-tailed) for all analyses.

4. The regulation of Irga6 and Irgb6 aggregate formation and clearance by guanylate-binding proteins

4.1 Introduction

In chapter 2 of this dissertation, we established that in the absence of Irgm1, the GKS IRG proteins Irga6 and Irgb6 form aggregates which colocalize with macroautophagic markers. These aggregates further colocalize with Gbp2, a member of the guanylate-binding protein family which is closely related to the IRG family and is also involved in innate immune functions, as outlined further in chapter 1. The colocalization of Gbp2 with GKS IRG protein aggregates implies a functional relationship between these two protein families which has been previously undescribed. We further demonstrated in chapter 2 that, while Irga6 was precipitated by a K63-linked ubiquitination binding construct, no detectable Gbp2 was similarly precipitated. We clarified this finding in chapter 3, showing that Gbp2 was actually precipitated by this same construct at levels too insignificant to be picked up by western, but that unlike Irga6, levels of K63-linked ubiquitination did not change in the absence of Irgm1.

These data imply that Gbp2 is *not* specifically targeted to macroautophagic degradation in the absence of Irgm1, unlike Irga6. The small amount of Gbp2 picked up by the K63-linked ubiquitination binding construct may be precipitated because it associates with K63-linked ubiquitinated proteins, and not because it is itself tagged. Furthermore, the lack of change in the abundance of Gbp2 precipitated from wild-type

and Irgm1 deficient lysates suggests that Gbp2 is not regulated by GMS IRGs in the same fashion as is Irga6.

From these findings, we have developed the following hypothesis: Gbp2 colocalizes with GKS IRG protein aggregates in the absence of Irgm1 because it is a part of the macroautophagic machinery utilized to degrade protein aggregates. This hypothesis is further supported by previous data indicating roles for other guanylate-binding proteins in the process of macroautophagy, including direct interactions between Gbp1 and p62 (outside of the ubiquitin-binding domain) and a decreased degradation rate of p62 in its absence, as well as direct interactions between Gbp7 and Atg4b, the LC3 protease, along with defects in autophagosomal closure in Gbp7-deficient cells [85].

In this chapter, we will further explore this hypothesis. We will demonstrate that Irga6 protein aggregates do not form in Gbp-deficient (but Irgm1 expressing) cells, indicating that Gbps are not involved in the prevention of Irga6 aggregate formation. We will further establish that, unlike Irga6, Gbp2 protein levels are unaffected by Irgm1 deficiency, which implies that Gbp2 expression is not downregulated in the absence of Irgm1 and is therefore not toxic to the cell. In addition, we will show the lack of a direct interaction between Gbp2 and Irgm3, suggesting that GMS IRGs do not directly regulate GBPs. We will reveal that the number of Gbp2 puncta in Irgm1-deficient cells decreases when autophagy is upregulated by starvation, demonstrating a role for macroautophagy

in the clearance of these puncta. We will show that Gbp2, but not Irga6, forms large punctate structures in the presence of protein aggregates in wild-type cells. And finally, we will demonstrate that a greater number of Irga6 aggregates are found in Gbp- and Irgm1- doubly deficient MEFs than in Irgm1-deficient MEFs, indicating a role for guanylate binding proteins in the clearance of Irga6 aggregate inclusions. Taken together, these data indicate a role for chromosome 3 guanylate-binding proteins in the macroautophagic clearance of protein aggregates, including those formed by GKS IRGs in the absence of GMS IRG proteins.

4.2 Results

4.2.1 Absence of chromosome 3 Gbp locus does not lead to the presence of Irga6 aggregates

In order to address whether guanylate-binding proteins are part of the protein aggregate clearance machinery, we first must address competing hypotheses describing roles for guanylate-binding proteins. A previous study into the relationship between GBPs and IRGs demonstrated that the five GBP genes and one GBP pseudogene found on murine chromosome 3 were necessary to the proper localization of Irgb6 to the *Toxoplasma gondii*-containing vacuole; the authors thus proposed that guanylate-binding proteins actively regulate the localization of GKS IRGs [95]. Thus, we asked whether

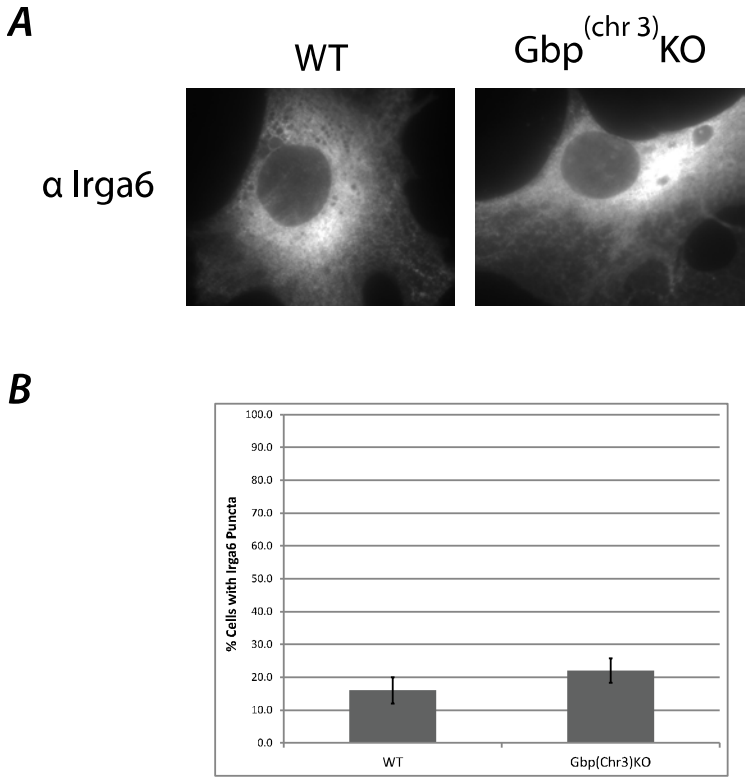

Figure 17: Loss of chromosome 3 Gbp proteins does not cause Irga6 aggregation. *A)* Sample Images. MEFs of the indicated genotypes were incubated with 100 U/mL IFN-γ for 24h, then processed for immunofluorescence. *B)* The percentage of cells containing Irga6 aggregates was quantified in a treatment-blinded fashion. Data represent n=5 trials with 10 cells quantified per treatment per trial. Differences in populations are not statistically significant by Student's T-test.

GBP proteins might also prevent the premature activation and aggregation of GKS IRGs such as Irga6.

To determine this, we utilized the MEFs from the previous study in which a 173 kb portion of murine chromosome 3 containing a large GBP gene locus has been deleted [95]. The specific GBPs deleted include Gbp1-3, Gbp5, Gbp7, and Gbp2ps; we will use

the notation Gbp$^{(chr\ 3)}$KO to denote this genotype for the rest of this dissertation. We compared the localization of Irga6 in WT and Gbp$^{(chr\ 3)}$KO primary MEFs, and found no statistically significant differences in the average number of aggregates per cell; in each cell type, Irga6 largely maintained its normal localization, appearing to be concentrated in the endoplasmic reticulum (Figure 17, *A*). Approximately 20% of cells of each genotype displayed one or more large Irga6 puncta (Figure 17, *B*), consistent with our results in chapter 2 of this dissertation; no statistical difference was found in the percentage of cells containing Irga6 aggregates between the two populations. This result indicates that none of the GBP genes found on murine chromosome 3, including Gbp2, functions to downregulate the formation of GKS IRG protein aggregates, and thus these guanylate-binding proteins maintain a different functional relationship with GKS IRGs than do the GMS IRGs.

4.2.2 Levels of Gbp2 protein are unaffected by Irgm1 deficiency

A second alternative hypothesis to the idea that GBPs regulate macroautophagic clearance of protein aggregates is that GBPs are regulated by GMS IRGs, and similarly to GKS IRGs, aggregate in their absence. Our previous data indicating that Irga6 is targeted to specific macroautophagy via K63-linked ubiquitin, while Gbp2 is not, argues against this hypothesis. However, this is only one line of evidence, and there are other aspects of the GMS-GKS IRG relationship which we can explore to ascertain if GMS IRGs regulate GBPs. For example, we and others have established that in the absence of

Irgm1, protein levels of the GKS IRGs Irga6 and Irgb6 decrease [60]. We initially proposed that this decrease is due to a negative feedback loop which downregulates expression of the toxically aggregated GKS IRGs to prevent further detrimental effects on cellular function. Given our results presented in chapter 3, however, showing that Irgm1 has little effect on macroautophagy, we here propose a different theory, that

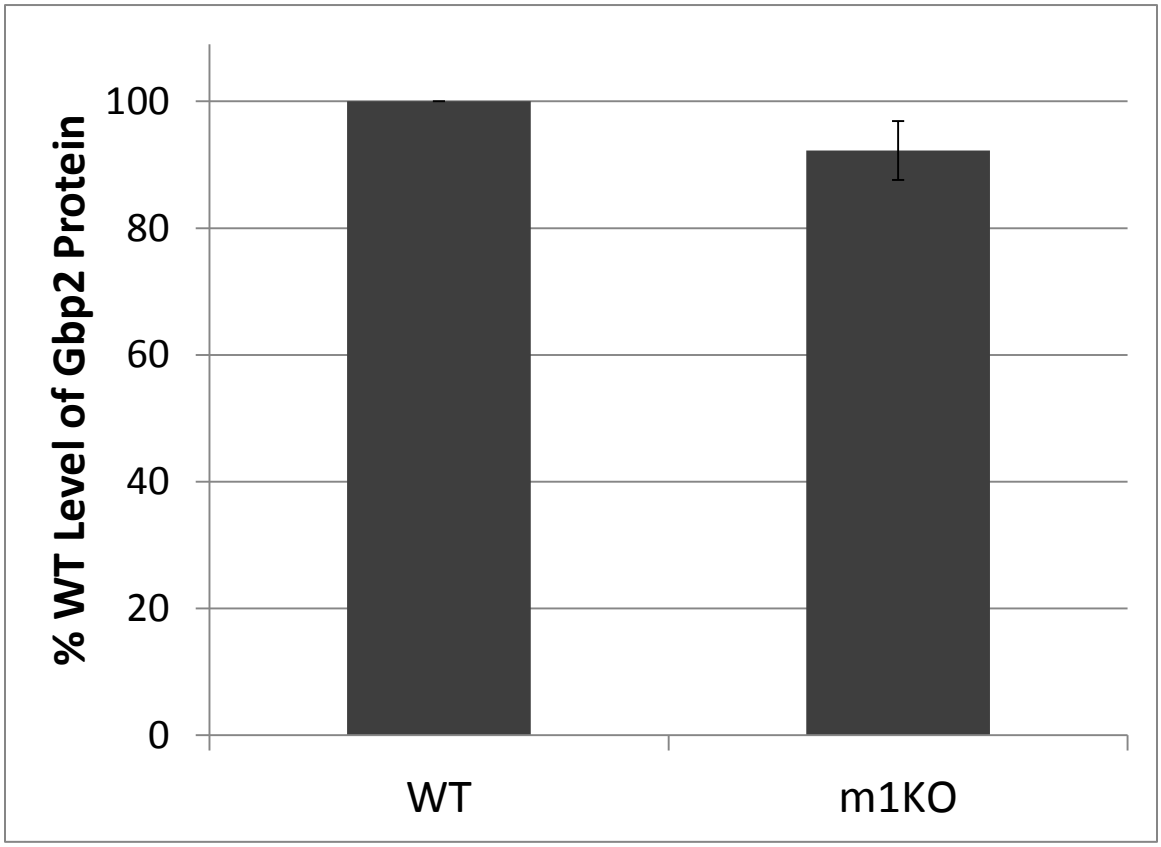

Figure 18: Irgm1 deficiency does not lead to a decrease in Gbp2 protein levels. 3T3 MEFs of the indicated genotypes were treated with 100 U/mL IFNγ for 24h, then were processed for western analysis. Raw band intensities were adjusted for actin levels and normalized to wild-type levels. No statistical difference in the populations was detected by Student's T-test. Data represent n=3 trials, with 1-3 replicates per trial.

overall levels of these GKS IRG proteins decrease because they are being degraded through macroautophagy. Thus, if Gbp2 aggregates in a similar fashion to GKS IRGs in the absence of Irgm1, its protein levels should similarly decrease. We decided to ascertain whether Irgm1 deficiency has a similar effect on Gbp2 protein levels to provide further evidence that GMS IRGs do not directly regulate GKS IRGs. We measured p62 protein levels (normalized to actin) via western analysis in wild-type and Irgm1-deficient cells; as expected, we found that Irgm1 deficiency had no statistically significant effect on Gbp2 protein levels (Figure 18). These data demonstrate that Gbp2 expression does not fluctuate in the absence of Irgm1, thus suggesting that large Gbp2 puncta seen in the absence of Irgm1 are not aggregates to be degraded. Furthermore, this suggests that Gbp2 is not regulated by GMS IRGs.

4.2.3 Gbp2 does not directly interact with Irgm3

Another facet of the GMS-GKS IRG relationship is direct interactions between these two subfamilies. A previous study demonstrated several of these direct interactions, including between Irgm1-Irgm3, Irgm1-Irga6, Irgm3-Irga6, and Irga6-Irgb6, via yeast two-hybrid assays and/or GST pulldowns [62]. Importantly, our lab has spent a significant amount of time attempting to confirm these direct interactions via co-immunoprecipitation assays, GST-pulldowns, and/or FRET assays. We have been unable to provide clear evidence of interactions between Irgm1-Irgm3, Irga6-Irgb6, or Irgm1-Irgb6 (data not shown). We were able to demonstrate, however, that Irgm3 is

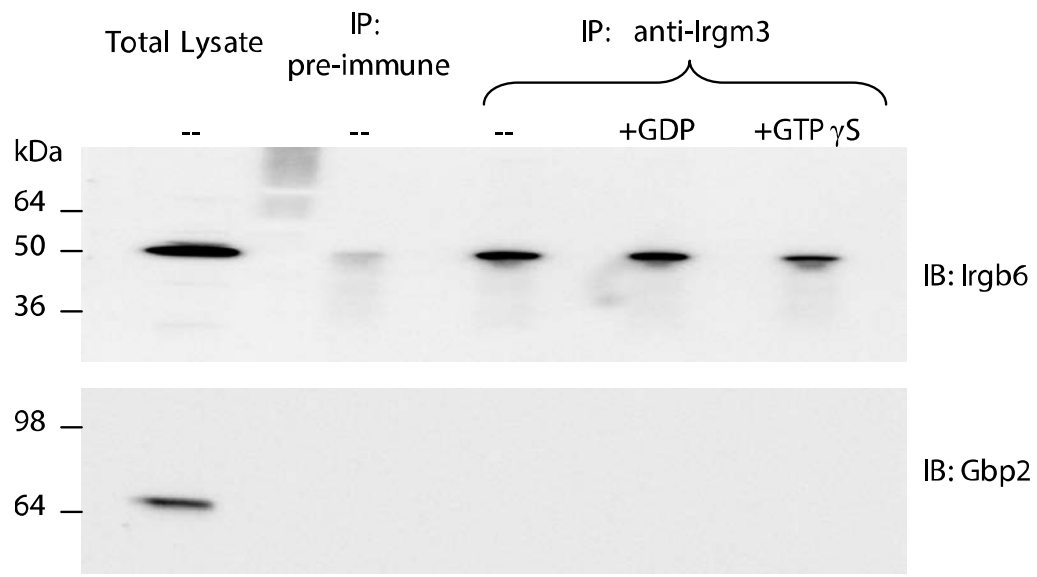

Figure 19: Gbp2 does not directly interact with Irgm3. Wild-type 3T3 MEFs were incubated with 100 U/mL IFN-γ for 24h, then were or were not loaded with 0.5 mM of the indicated guanine nucleotides, as indicated. Lysates were then used for immunoprecipitation with anti-Irgm3 antibodies. Resultant proteins were subjected to western analysis. Data are representative of three trials. This experiment was done by Stanley Henry.

able to precipitate Irgb6 in a nucleotide-independent manner (Figure 20). We thus decided to determine whether Gbp2 also interacts with Irgm3, as evidence of a direct regulatory effect of this GMS IRG on guanylate binding proteins. We were unable to co-precipitate Gbp2 using an Irgm3 antibody, from which we infer that Gbp2 and Irgm3 do not directly interact (Figure 19). This result is further evidence that GMS IRGs do not regulate the guanylate-binding proteins.

4.2.4 Gbp2 is affected by macroautophagic processes

Based on the evidence we have now shown, it seems that GBPs do not regulate GKS IRGs, and GMS IRGs do not regulate GBPs. Thus we turn our attention to our original hypothesis: that Gbp2 colocalizes with GKS IRG protein aggregates in the absence of Irgm1 because it is a part of the macroautophagic machinery utilized to

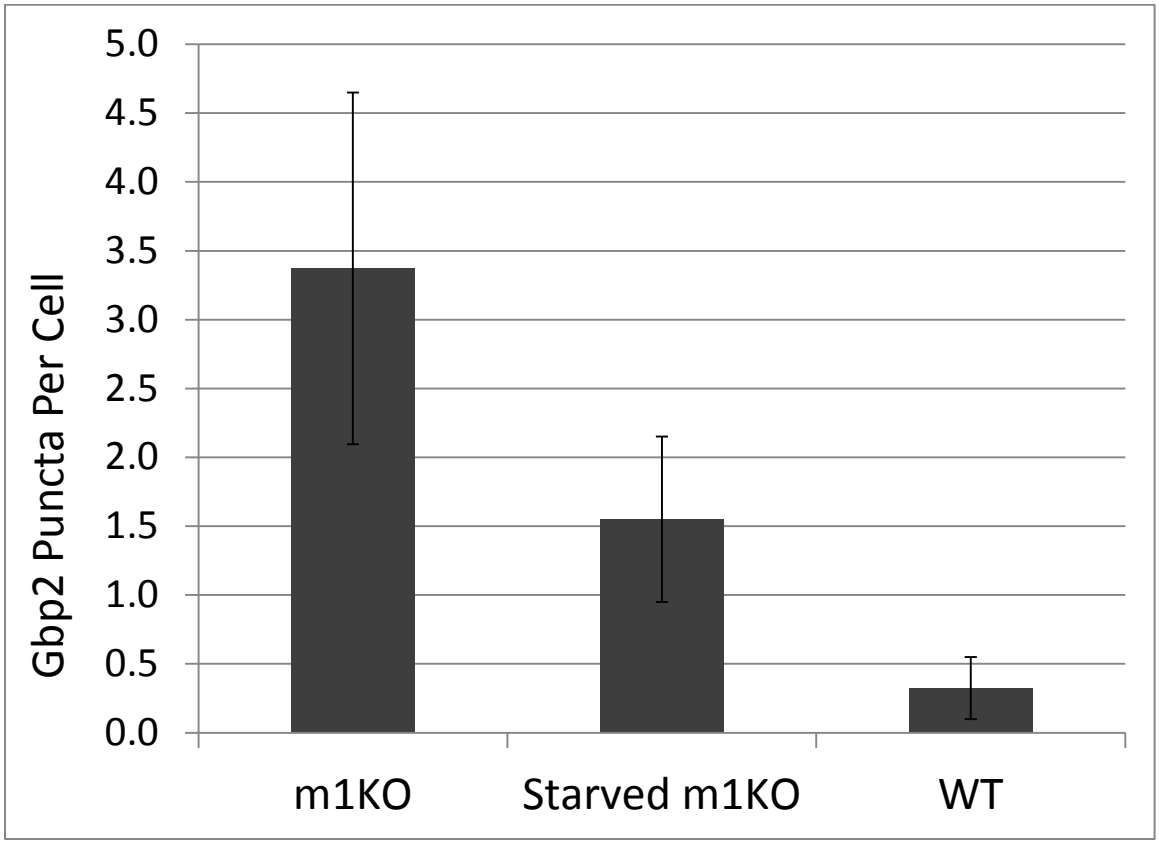

Figure 20: Induction of autophagy by starvation leads to fewer Gbp2 puncta in the absence of Irgm1. MEFs of the indicated genotypes were incubated with 100 U/mL IFN-γ for 24h, and concurrently were or were not starved in Hank's balanced salt solution for the final 4h. Cells were then processed for immunofluorescence with αGbp2 antibodies. Data represent n = 2 trials, with 20-21 cells quantified per treatment per trial.

degrade protein aggregates.

To study this hypothesis, we first wanted to establish a clearer link between Gbp2 and the process of macroautophagy; thus, we examined whether the number of Gbp2 puncta was affected by upregulation of autophagy. We compared the number of Gbp2 puncta found in Irgm1-deficient MEFs to the number found in the same cells in which autophagic flux was additionally induced via starvation in Hank's balanced salt solution (Figure 20). The starved cells displayed fewer Gbp2 puncta per cell than the unstarved cells, indicating that upregulating macroautophagy leads to clearance of these puncta. Given our previous findings that Gbp2 is not targeted to specific autophagy and that its expression level is unaffected by Irgm1 deficiency, these data further suggest that Gbp2 puncta are not aggregates, but are instead autophagosomal compartments.

4.2.5 Gbp2, but not Irga6, localizes to protein aggregates

If Gbp2 is a part of the general autophagic protein aggregate clearance machinery, as we have hypothesized, it should additionally colocalize with protein aggregates other than those formed by Irgm1 deficiency; that is, Gbp2 should colocalize with protein aggregates in wild-type cells. We induced protein aggregation in wild-type cells utilizing both MG132 treatment (which blocks proteasomal function, leading to an accumulation of proteins unable to be degraded except through macroautophagy [107,223]), and puromycin treatment (which serves as a tRNA imitator, leading to the accumulation of prematurely terminated peptides called defective ribosomal products

or DRiPs, which form aggregate inclusions in the cell [224-226]). The percentage of wild-type cells displaying large Gbp2 puncta increased dramatically upon treatment with either of these two compounds; however, an equivalent increase in Irga6 puncta was not observed (Figure 21). These findings can be interpreted in one of two ways. First, it is

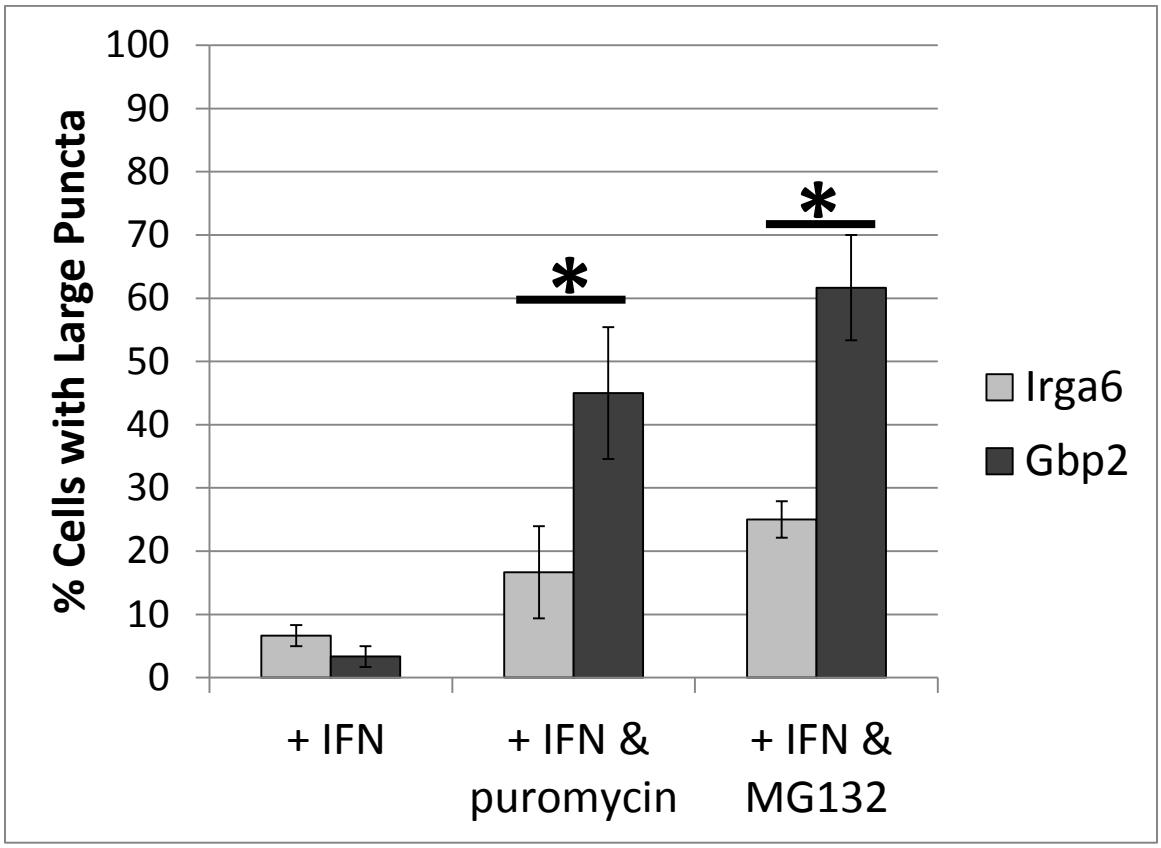

Figure 21: Gbp2, but not Irga6, displays a punctate localization in the presence of protein aggregates. WT 3T3 MEFs of the indicated genotypes were incubated with 100 U/mL IFN-γ for 24h, and concurrently were or were not treated with 5 ug/mL puromycin or 10 uM MG132 for the final 6h, as indicated. Cells were then processed for immunofluorescence with αGbp2 or αIrga6 antibodies. 2x3 ANOVA indicates a significant interaction term, $p < 0.05$. * $p < 0.05$ via Fisher's PLSD test. Data represent n = 3 trials, with 20 cells quantified per treatment per trial.

possible that Gbp2 is for some reason sensitive to aggregation in response to these two treatments, while Irga6 is not. A second interpretation, however, is that Gbp2 forms puncta in the presence of generic protein aggregates, rather than due to Irgm1 deficiency, which would suggest once more that Gbp2 puncta are not themselves aggregates, but rather autophagosomes.

4.2.6 Absence of chromosome 3 Gbp locus leads to an increase in the number of Irga6 aggregates

Now that we have shown that Gbp2 forms puncta in the presence of protein aggregates which colocalize with autophagosomal markers, we next asked whether guanylate-binding proteins are involved in the clearance of protein aggregates, and more specifically, the Irga6 aggregates formed in the absence of Irgm1. We stimulated Irga6 aggregate formation in wild-type and $Gbp^{(chr\ 3)}$KO MEFs by treatment with Irgm1 siRNA and compared the average number of Irga6 puncta found in these two genotypes. On average, there were three times as many Irga6 puncta in cells lacking the GBP locus than in wild-type cells (Figure 22, *A* + *C*). However, while every trial demonstrated an increase in aggregate number in GBP-deficient cells, the absolute number of aggregates per cell varied significantly by trial, likely due to variations in Irgm1 knockdown levels, which lead to no statistical difference between the two populations detected by Student's T-test (Figure 22, *B*). In order to compensate for the

effects of each trial on aggregate number, we took the log-transformed aggregate number ratios of Gbp$^{(chr\ 3)}$KO to WT and compared them to the null hypothesis of no

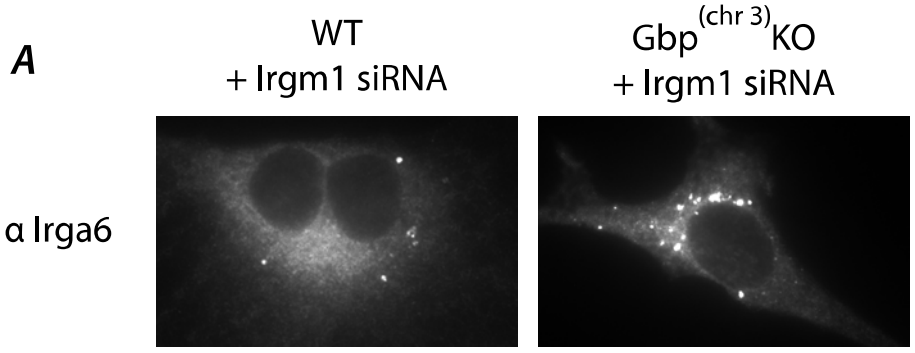

B

	WT + m1KD	Gbp (chr 3) KO + m1KD
Trial #1	1.3	2.8
Trial #2	1.7	4.4
Trial #3	4.1	8.4
Trial #4	0.4	1.9

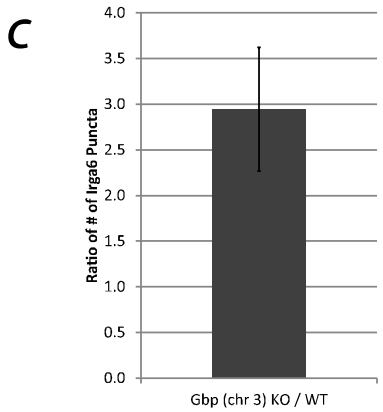

Figure 22: Loss of chromosome 3 Gbp proteins leads to an increased number of Irga6 aggregates in Irgm1-deficient cells. *A)* Sample images. Primary MEFs of the indicated genotypes were transfected with Irgm1 siRNAs overnight, then were treated with 100 U/mL IFNγ for 24h. Cells were then processed for immunofluorescence. *B)* Data table. The number of large Irga6 puncta per cell was calculated in a treatment-blinded fashion. n=4 trials, with 4-10 cells per treatment per trial, were quantified. *C*) Data from part *B* presented as the average ratio of the number of Irga6 aggregates in Gbp$^{(chr\ 3)}$KO cells to the number of Irga6 aggregates in WT cells. The observed log-transformed ratios were compared to the null hypothesis of no differences in the number of Irga6 aggregates between genotypes (Irga6^{GbpKO} / Irga6^{WT} = 1) via one-group T-test; genotype was found to have a significant effect on the number of Irga6 aggregates, $p < 0.02$.

difference in the number of Irga6 aggregates between genotypes ($Irga6^{GbpKO}$ / $Irga6^{WT}$ = 1) via one-group T-test. This test indicated a significant effect of genotype on the number of Irga6 aggregates. We therefore conclude that the chromosome 3 GBP locus is involved in the clearance of Irga6 aggregates. It should be noted, however, that we did not examine the effects of the absence of the chromosome 3 GBP locus on overall levels of Irgm1. We know of no evidence to suggest that this locus would affect Irgm1 expression, but we cannot rule out the possibility. It is therefore possible, although unlikely, that the increase in Irga6 aggregates in $Gbp^{chr\ 3}KO$ cells is due to a decrease of Irgm1 protein in these cells, and this contingency should be investigated.

4.3 Discussion

In this chapter, we have discussed the role of the guanylate-binding proteins in the formation and clearance of GKS IRG aggregates formed in the absence of GMS IRGs. In response to the hypothesis presented by others that GBPs are able to control the localization of IRGs, we presented evidence that GBPs do not regulate GKS IRG aggregate formation by demonstrating that loss of the guanylate-binding protein locus on the murine chromosome 3 does not lead to the formation of GKS IRG aggregates. We showed that Gbp2 expression levels are unaffected by Irgm1 deficiency, implying that Gbp2 does not form aggregates in GMS IRG-deficient cells and thus is not regulated by GMS IRGs. This conclusion was further supported by our inability to demonstrate direct interactions between GMS IRGs and GBPs. We demonstrated that the number of

Gbp2 puncta found in Irgm1-deficient cells decreased when autophagy was upregulated by starvation, linking the fate of these structures to macroautophagy. We revealed that Gbp2 puncta formation is linked not to GMS IRG deficiency, but to the presence of protein aggregates, and demonstrated that the chromosome 3 GBP locus is involved in clearance of the Irga6 aggregates formed in the absence of GMS IRGs.

Together, these data support the hypothesis we proposed in chapter 2 of this dissertation: that Gbp2 colocalizes with GMS-IRG-deficiency-induced Irga6 aggregates not because it is aggregating, but because it is part of the autophagic machinery used to degrade protein aggregates. This hypothesis is further supported by a previous study indicating a role for guanylate-binding proteins in macroautophagic processes [85]. This study did not find that Gbp2 was necessary for cell-autonomous immunity to *Listeria monocytogenes* or *Mycobacterium bovis*, which is consistent with our supposition that Gbp2 is involved in aggregate clearance, a function not normally required for bacterial or protozoan resistance. We speculate that Gbp2 may have evolved as an antiviral effector to combat toxic defective ribosomal products caused by viral interference with host translation. However, it should be noted that a recent study found that Gbp2 localizes to the *Toxoplasma gondii*—containing vacuole and is necessary for control of *T. gondii* replication, implying that Gbp2 has roles in bacterial resistance outside of aggregate clearance [227]. The exact roles of Gbp2 in cell-autonomous innate immunity thus remain to be fully elucidated.

While the data presented here collectively support our hypothesis that Gbp2 is involved in the autophagy of protein aggregates, there is additional work that could be done which would significantly strengthen the conclusions we have drawn. We suggested by the results of our co-immunoprecipitation that guanylate-binding proteins do not directly interact with immunity-related GTPases; however, this inference should be supported by more comprehensive yeast two-hybrid or pulldown studies exploring interactions between a larger set of GMS IRGs and guanylate-binding proteins. Second, while we demonstrated that Gbp2 forms puncta in the presence of protein aggregates, a quantification of the colocalization between Gbp2 and ubiquitinated aggregates in these cells would significantly strengthen our position that Gbp2 is associated with generic protein aggregation. Additionally, it would be instructive to separate Irgm1-deficient cell lysates on a native gel and examine whether Gbp2 and/or Irga6 multimeric complexes are found; we would predict that abundant Irga6 complexes would be found, but no Gbp2 complexes. And finally, while we demonstrated that the chromosome 3 GBP locus is involved in clearance of Irga6 aggregates, we did not discover which specific GBPs on this locus are responsible for this clearance. Targeted knockdowns of specific GBPs and/or reconstitution of specific GBPs into the $Gbp^{(chr\ 3)}$KO MEFs would elucidate the individual IRGs which contribute to aggregate degradation.

In summary, the results presented in this chapter further clarify the mechanism of action of guanylate-binding proteins with respect to immunity-related GTPases.

These results further support previous research indicating a role for GBPs in macroautophagy, and provide impetus for studies into how the participation of guanylate-binding proteins in macroautophagy aids in cell-autonomous innate immunity to intracellular pathogens.

4.4 Materials and methods

4.4.1 Cell culture

Irgm1 (LRG-47)-deficient and Irgm3 (IGTP)-deficient mice were generated as described previously [215]. The mice were maintained according to Institutional Animal Care and Use Committee-approved protocols at the Durham VA and Duke University Medical Centers (Durham, NC). Mouse embryonic fibroblasts were derived from these mouse lines and immortalized by the standard 3T3 procedure [216]. Atg5-deficient fibroblasts were a gift from Herbert Virgin, Washington University, St. Louis, MO. 3T3 fibroblasts were cultured in DMEM (Invitrogen) supplemented with 10% (v/v) FBS (Hyclone, Logan, UT); 10 ug/mL ciprofloxacin was occasionally added to control infection. 18-24 hours prior to many experiments (as indicated in the text), 100 units/ml IFN-γ (#407320, Calbiochem, EMD Biosciences, San Diego, CA or #IF005, Millipore, Billerica, MA) and 100 nM bafilomycin A1 (#B1793, Sigma, St. Louis, MO), were added to the culture medium.

Primary BMM were isolated from the tibia and femurs of 2- to 4-month-old mice. Bone marrow was flushed from the bones using a 27-gauge needle fitted to a syringe

filled with DMEM, and the marrow was dispersed by drawing through the needle three to four times. Red cells were lysed with ACK lysing buffer (Invitrogen). Adherent cells were cultured for 6 days in bone marrow macrophage medium (culture medium supplemented with 30% (v/v) L929 cell-conditioned culture medium). The cells were cultured on Petri dishes, resulting in cultures that were loosely adherent and easily removed from the plates with cell dissociation buffer (#13150–016, Invitrogen). After day 6, procedures diverged depending on the experiment.

4.4.2 Transfection and nucleofection

DNA transfections were performed using X-tremeGENE 9 or HP transfection reagent (#06365779001, Roche, Pleasanton, CA) according to manufacturer's instructions. Nucleofections were performed using the Amaxa Biosystems Nucleofector II (Lonza, Basel, Switzerland), along with nucleofector kit R (#VCA-1001, Lonza), according to manufacturer's instructions. MEF were nucleofected using program number U-30, and BMM were nucleofected using program number Y-1.

4.4.3 Knock-downs

siRNA transfections were performed using Lipofectamine RNAiMAX (#13778, Invitrogen) according to manufacturer's instructions. siRNAs were transfected overnight, and assays were performed either immediately or 24 hours later, as indicated in the text. siRNAs utilized include Stealth® siRNA Sqstm1 #MSS207329 (#1320001, Invitrogen), Stealth® RNAi Negative Control High GC duplex (#12935-400, Invitrogen),

Silencer® Select siRNA Irgm1 #s68045 (#4390771, Invitrogen), and Silencer® Select Negative Control No. 1 siRNA (#4390843, Invitrogen).

4.4.4 Immunocytochemistry

Cells were plated on poly-D-lysine-coated (#P7280, Sigma) coverslips and subjected to treatment conditions as described in the text. Cells were then fixed with 4% paraformaldehyde (w/v) in PBS for 15 min, rinsed in 100 mM glycine/ PBS for 5 min, and permeabilized with 0.2% (w/v) saponin/PBS for 10 min. Cells were blocked with 10% (v/v) FCS/PBS for 60 min. As indicated in the text, the cells were then stained with various primary antibodies for 60 min, followed by AlexaFluor-conjugated secondary antibodies (Molecular Probes/Invitrogen) for 60 min. Primary antibodies used include anti-Irga6 rabbit polyclonal antiserum 165/3 [51] at 1:4000 and anti-Gbp2 rabbit polyclonal antiserum (Jörn Coers, Duke University) at 1:500. Images were collected on an Olympus IX70 microscope equipped with a Hamamatsu C8484–03G01 digital camera. Cells were magnified x1000. Wide-field fluorescence images and z-stacks were collected using Metamorph 6.2.3.5.

4.4.5 Western blotting

Western blot analyses were performed according to standard protocols. In brief, lysates were boiled in SDS and separated on 8–16% gradient Tris-glycine gels (#EC60485, Invitrogen). Proteins were transferred overnight to Immobilon synthetic membranes (Millipore). Membranes were blocked in 5% (w/v) milk in TBS-Tween 20 for 60 min, then

incubated in primary antibody for 60 min, washed, and incubated in secondary antibody for 60 min. Primary antibodies utilized include anti-Irgb6 rabbit polyclonal antiserum [60] at 1:1000, anti-Gbp2 rabbit polyclonal antiserum (Jörn Coers, Duke University) at 1:500, and anti-actin clone C4 mouse monoclonal antibody (#MAB1501, Millipore) at 1:1500. Secondary antibodies used were goat anti-rabbit (H+L) HRP-conjugated IgG and goat anti-mouse (H+L) HRP-conjugated IgG (#AP307P and #AP308P, Millipore) at 1:1000. Blots were developed in SuperSignal west pico chemiluminescent substrate (#34708, Thermo Scientific, Rockford, IL) and imaged on a Kodak Image Station 4000R using Carestream Molecular Imaging software.

Carestream software was also used to quantify band intensities. The "find lanes" feature was used, and lanes were adjusted manually as necessary. The "find bands" feature was then used, and extraneous bands were deleted. The band intensity was measured as the sum intensity of the resultant band peak.

4.4.6 Immunoprecipitation

For the immunoprecipitation assay reported in Figure 20, 50 ul of protein A-coupled paramagnetic beads (Dynabeads, Invitrogen) were isolated on a magnetic stand (Promega, Madison, WI) and suspended in 0.2 ml of PBS containing 0.02% (v/v) Tween 20 (PBS-T). One microliter of either preimmune serum or anti-Irgm3 polyclonal antiserum [228] was added, and bead suspensions were incubated with rotation at room temperature for 20 min. Antibody-bound beads were washed once in PBS-T prior to

addition of cell lysates. Wild-type, Irgm1-/-, or Irgm3-/- 3T3 cells in 10-cm tissue culture dishes were given 100 units/ml IFN-γ for 24 h and lysed in PBS containing 1% (v/v) Nonidet P-40 and proteinase inhibitors (Calbiochem). 0.35 ml cell lysate with or without 0.5 mM GDP or GTPγS was added to the antibody-bound beads and incubated at room temperature for 20 min with rotation. Beads were magnetically separated and washed three times. Washed beads were removed to a fresh tube and suspended in 1x sample buffer (0.09 M DTT, 1.2% SDS, 0.012 M EDTA, 0.0025% bromphenol blue, 6% sucrose). Samples were heated to 100 °C to elute proteins and used for western blotting. To minimize cross-reaction of the secondary antibody with eluted IgG, a secondary antibody that does not recognize denatured IgG (Clean Blot, Thermo Scientific) was used.

4.4.7 Data Analysis

Results are presented as mean ± SE unless otherwise indicated. Treatment effects and/or variable interactions were determined by analysis of variance (ANOVA), Student's T-test, or one-group T-test, where appropriate. Where such effects were found via ANOVA, post-hoc analysis for specific mean comparisons was completed using Fisher's PLSD. Significance levels were set at $p < 0.05$ (95% confidence, two-tailed) for all analyses.

5. Conclusions

The immunity-related GTPases, or IRGs, are a family of interferon-induced, dynamin-like proteins with roles in cell-autonomous innate immunity. The family can be divided into two subcategories: the GKS IRGs, which comprise the majority of the family and contain the canonical P-loop GTP-binding motif (GxxxxGKS), and the GMS IRGs, which contain a methionine substitution (GxxxxGMS) in this motif [38]. The differences in GTP-binding caused by this alteration likely impart distinct functions to these two classes of IRGs. While members of the larger GKS IRG subfamily are thought to utilize their putative dynamin-like membrane modulation ability to effect membrane stripping from pathogen-containing compartments [229], the roles of the GMS IRG subfamily in innate immunity remain poorly characterized.

Previous studies reported in the literature have developed a working model of IRG function which describes a role for GMS IRGs in preventing the premature activation of GKS IRGs. In this model, the GMS IRGs, which are localized to the Golgi apparatus, the endoplasmic reticulum, and other intracellular membrane compartments, directly interact with GKS IRGs and prevent their activation at those membranes [62]. Upon direct infection of the cell by an invasive pathogen, the GKS IRGs are trafficked to the pathogen-containing compartment, which lacks robust GMS IRG association [73], where they effect membrane stripping and exposure of the invading organism to the cytoplasmic environment [229]. In the event of premature activation of GKS IRGs,

perhaps due to the disabling of GMS IRG function or a mismatch in levels of these two protein subfamilies, GKS IRGs are incorrectly trafficked to compartments which resemble aggregate inclusions, where they must be degraded to prevent toxic effects on cellular functions [60].

While this model incorporates much of the current literature surrounding IRG function, it does not account for several experimental results. For example, it has been demonstrated that more profound deficiencies in innate immunity exist in mice lacking GMS IRGs than in mice lacking GKS IRGs, which is unexpected if GMS and GKS IRGs function in the same innate immune pathway [55,61,63]. This finding could be explained by redundancies in the functions of the extensive group of mouse GKS IRGs that could compensate for loss of one member, or alternatively by pathological consequences of GKS IRG aggregate formation occurring in the absence of GMS IRGs. However, certain species, including primates, encode only GMS IRGs within their genomes [38,39], suggesting an additional explanation: that GMS IRGs encompass a broader range of activities than mere control of GKS IRG function.

The goals of the research undertaken for this dissertation were to extend this working model of IRG function to include a role or roles for GMS IRGs outside of GKS IRG control. We initially proposed that GMS IRGs might exhibit regulatory control over a related family of interferon-induced GTPases, the guanylate-binding proteins, by demonstrating the mislocalization of Gbp2 in the absence of GMS IRGs to the same

structures as the similarly mislocalized GKS IRGs. This finding suggests that GMS IRGs may control Gbp2 in a similar manner to their control of GKS IRGs. This discovery of a broader utility for GMS IRGs would help explain the discrepancy in innate immune responses between GMS- and GKS- lacking mice, since GMS-IRG lacking mice would be deficient for both the GKS IRG and Gbp2 response pathways; additionally, since primates encode a variety of guanylate-binding proteins, this finding could also explain why certain species do not encode GKS IRGs. However, in subsequent studies, we found evidence that GMS IRGs may not exert a direct control over Gbp2 localization; rather, it is likely that Gbp2 localizes to GKS IRG aggregates because it is directly involved in their macroautophagic clearance. Thus, the localization of Gbp2 in the absence of GMS IRGs, while providing tantalizing hints to the poorly understood function of guanylate-binding proteins in innate immunity, does not provide evidence of a role for GMS IRGs outside of GKS IRG regulation.

A second possible broader regulatory role of GMS IRGs that could explain their increased importance to innate immunity is a previously proposed role in controlling macroautophagy. While this is supported by previous studies indicating that overexpression of GFP-tagged Irgm1 in macrophage-like cells induced autophagosome formation [41,191], other studies do not support this role, including those showing that GFP-tagged Irgm1 may be constitutively activated [56], and that interferon-gamma-induced autophagy does not require Irgm1 [202]. We proposed that Irgm1 might play a

role in autophagosome maturation, as its absence led to a buildup of LC3-positive but LAMP-1-negative compartments; thus, we examined whether faulty autophagic flux in the absence of Irgm1 might be responsible for the observed GKS IRG aggregates. However, we were unable to detect an effect of the absence of Irgm1 on the maturation of autophagosomes in MEFs, and only a very small and statistically insignificant decrease in bone-marrow macrophages. Additionally, given the cell-specific differences in assay results we found, we attempted to confirm that Irgm1 expression in fibroblasts induces autophagosome initiation, but found no difference in LC3-tagged compartment formation in these cells. Our results thus do not suggest a role for Irgm1 in the modulation of macroautophagy. Nevertheless, it remains surprising that GMS IRGs do not play a direct role in modulating autophagy, as Crohn's disease related intestinal pathologies of human patients with SNPs in the core autophagy gene Atg16L1 closely resemble those of patients with SNPs in the IRGM locus, implying that these two genes function in the same autophagic pathway [199,200]. Future studies are needed to investigate a role for human IRGM in macroautophagy modulation.

As we have found no evidence that GMS IRGs either directly regulate the guanylate-binding proteins, nor that they directly affect macroautophagy, the initial goal of our research study, which aimed to uncover the role(s) of GMS IRGs in innate immunity outside of the regulation of GKS IRGs, remains largely unfulfilled. However, the results of our studies do contribute to the working model of overall IRG function in

other ways. For example, although GKS IRGs are known to localize to pathogen-containing compartments, the mechanisms whereby IRG proteins recognize and are trafficked to these vesicles are currently a mystery. We have presented here the intriguing finding that the GKS IRGs Irga6 and Irgb6 are polyubiquitinated (possibly through K63 linkages) in wild-type cells, and that this ubiquitination increases in the case of GMS IRG deficiency. We additionally demonstrated that these ubiquitinated proteins colocalize with macroautophagic markers, implying that the ubiquitination tag targets these GKS IRGs to the macroautophagic system. One interpretation of these findings is that macroautophagy is utilized to degrade large aggregate inclusions, which GKS IRGs are predisposed to form. However, we also propose an alternative interpretation: that ubiquitination of GKS IRGs mediates their trafficking to pathogen-containing compartments, a process that utilizes the macroautophagic machinery of the cell. In this scenario, the ubiquitinated GKS IRGs would not be present as aggregates inside degradative autophagic vacuoles, but rather would be present on the surface of the autophagic vacuole where they would presumably enact their function. This hypothesis is supported by a previous study that indicates that Irga6 fails to localize to the pathogen-containing vacuole in the presence of GMS IRGs but the absence of a functional autophagic system [221]. Additionally, a second study indicates that Irgb6 fails to localize to pathogen-containing vacuoles in the absence of the chromosome 3 guanylate-binding protein locus [95], which, when combined with previous data

indicating that GBPs play a role in specific macroautophagy, suggests that GBP-mediated autophagic trafficking is responsible for the correct targeting of Irgb6 to the pathogen-containing vacuole.

An additional benefit of the research presented in this dissertation is that we were able to contribute to understanding the mechanism of action of the guanylate-binding proteins, an interferon-induced GTPase family which has been less well-studied. Our data suggest that Gbp2 plays a role in the specific autophagic clearance of protein aggregates, as we demonstrated both that Gbp2 punctate structures form in the presence of generic protein aggregates, and that the murine chromosome 3 GBP locus is involved in the degradation of Irga6 protein aggregates. These data add to a previous study indicating a role for certain chromosome 3 GBPs in macroautophagic processes [85]. Further, these findings raise the interesting question of how macroautophagy of cellular aggregates could contribute to innate immunity. One possibility is that Gbp2 is involved in the targeting of substrates marked with a particular signal, such as K63-linked ubiquitination, to autophagosomes. Considering that many pathogen-containing compartments accumulate autophagosomal markers, this Gbp2-mediated targeting could be used to traffic anti-microbial effectors, including GKS IRGs, to phagosomes. Additionally, certain pathogens may employ survival strategies within the cell that promote the formation of defective protein products, such as viral interference with host translation; Gbp2 may function to lessen toxic effects on cells as a result of such

pathogenic effectors. Further research is necessary to fully elucidate the role of Gbp2 in cell-autonomous defense against intracellular pathogens.

In summary, we have presented research in this dissertation which increases our overall understanding of the functions of the immunity-related GTPases in innate immunity. While we were not able to establish a role for GMS IRGs outside of control of GKS IRGs, we were able to relate the GKS IRGs Irga6 and Irgb6 to the macroautophagic system, a finding which suggests a trafficking mechanism to the pathogen-containing compartment for these proteins. Additionally, we demonstrated that Gbp2 is involved in the macroautophagic clearance of protein aggregates, which has important implications for the understanding of the functions of the guanylate-binding proteins. Together, these findings contribute to our overall scientific understanding of interferon-induced innate immunity.

Appendix A: Proteins Identified in TUBE1 Pull-down Proteomic Screen

Immunity Related Proteins

Name	Reference Number	Peptide Count	Fold Change (KO v WT)
Gbp2	NP_034390.1	3	1.2
Gbp6	NP_919317.2	3	-1.5
Gvin1 / Vlig1	NP_001229969.1	1	1.1
IFITM3	NP_079654.1	1	-2.1
Irga6	NP_068564.4	4	3.6
Irgb6	NP_001138636.1	2	1.5
MIF	NP_034928.1	1	-2.0
Peroxiredoxin-1	NP_035164.1	2	-1.1
Stat1 (isoform 2)	NP_001192243.1	1	-2.8
TOLLIP	NP_076253.1	1	-1.1

Protein Degradation

Name	Reference Number	Peptide Count	Fold Change (KO v WT)
p62	NP_035148.1	3	-1.1
PLAA / PLAP	NP_766283.2	2	1.0
Polyubiquitin-C	NP_062613.3	14	-1.1
Trypsin 10 (Precursor)	NP_001034085.1	1	1.9
Serine Protease 1 (precursor)	NP_444473.1	1	-1.0

SUMO3 (precursor)	NP_064313.1	2	-1.2
Trypsinogen 7 (precursor)	NP_075822.3	1	1.1
Ubiquilin-1 (isoform 1)	NP_081118.4	4	1.2
UBR2 (isoform 1)	NP_666190.2	1	-2.1

Proteasome Catalytic Subunits

Name	Reference Number	Peptide Count	Fold Change (KO v WT)
α1	NP_036095.1	1	-1.5
α3	NP_035314.3	2	-1.5
α4	NP_036096.1	2	1.0
α6	NP_036098.1	1	-2.0
α7	NP_036099.1	3	1.2
β3	NP_036101.1	2	1.3
β6 (precursor)	NP_032972.3	1	-1.3
β10 (precursor)	NP_038668.2	1	-1.7

Proteasome Regulatory Subunits

Name	Reference Number	Peptide Count	Fold Change (KO v WT)
1	NP_081633.1	2	1.3
2	NP_598862.1	5	1.0
3	NP_033465.1	1	-1.1

4	NP_032973.1	4	-1.2
6A	NP_032974.2	1	-1.1
7	NP_035318.1	2	-1.0
10B	NP_080235.2	1	1.2
11	NP_848731.2	2	1.3
12	NP_080170.1	2	-1.2
14	NP_067501.2	1	-1.3

E2/E3 Ubiquitin Ligases

Name	Reference Number	Peptide Count	Fold Change (KO v WT)
Birc6	NP_031592.3	11	1.3
Hectd1	NP_659037.2	7	1.0
Huwe1	NP_067498.4	29	-1.1
Nedd4	NP_035020.2	2	-1.4
RLIM	NP_035406.3	3	-2.0
Ube2n	XP_001475660.2	2	1.1
Ube3A (isoform 1)	NP_766598.1	2	-1.3
Ubr4	NP_001153791.1	2	1.9
Ubr5 (isoform 2)	NP_001106192.1	3	1.3

Transcription / Splicing / Translation Factors

Name	Reference Number	Peptide Count	Fold Change (KO v WT)
Eef1-α1-like (isoform 3)	XP_003946343.1	5	-1.2

Eef2	NP_031933.1	1	1.7
EF-Tu (mitochondrial isoform 1)	NP_766333.1	1	2.2
Parp10	NP_001157048.1	1	-1.0
PCBP2 (isoform 1)	NP_001096635.1	1	-1.5
Ptrf	NP_033012.1	2	-1.0
RBM14	NP_063922.2	4	-1.5
SAM synthase (isoform type-2)	NP_663544.1	1	1.0
Sub1	NP_035424.1	1	1.0
U2AF 65 kDa subunit-like	XP_003085312.1	2	-1.0

Ribosomal Proteins

Name	Reference Number	Peptide Count	Fold Change (KO v WT)
40S RPS3	NP_036182.1	5	-1.1
40S RPS11	NP_038753.1	1	-1.1
40S RPS15a	NP_733769.1	1	-1.7
40S RPS16-like	XP_003688797.1	2	1.6
40S RPS18	NP_035426.1	1	-1.8
40S RPS20	NP_080423.1	2	-2.1
40S RPS27-like	NP_001177187.1	1	-1.5
40S RPS27a-like	XP_001002242.1	1	-1.4
60S RPL23-like	XP_003689266.1	3	-1.0
60S RPL38	NP_001041522.1	1	-1.1

Trafficking/Targeting

Name	Reference Number	Peptide Count	Fold Change (KO v WT)
Annexin A1	NP_034860.2	2	-1.4
Annexin A2	NP_031611.1	1	-1.6
Arf4	NP_031505.1	3	-1.0
Asap2 (isoform b)	NP_001004364.2	1	1.0
Get4 homolog (isoform 1)	NP_080545.2	4	-1.1
TER ATPase / Vcp	NP_033529.3	15	1.0
UBL4A	NP_663380.1	3	-2.3
Myosin-9 (isoform 1)	NP_071855.2	9	1.8
Unconventional Myosin-Ic (isoform b)	NP_001074243.1	1	10.7

Chaperones

Name	Reference Number	Peptide Count	Fold Change (KO v WT)
Bag2	NP_663367.1	1	1.8
Bag6 (isoform 2)	NP_001239397.1	16	-1.1
GRP-78	NP_001156906.1	8	1.2
Hsc70	NP_112442.2	11	1.0
HSP 90β	NP_032328.2	10	-1.5
PDIA6 (precursor)	NP_082235.1	1	-1.2
STCH (mitochondrial)	NP_034611.2	6	1.3

Metabolism

Name	Reference Number	Peptide Count	Fold Change (KO v WT)
Adh1	P00330	1	-1.3
ADP/ATP Translocase 1	NP_031476.3	4	1.1
ADP/ATP Translocase 2	NP_031477.1	3	-1.4
ATP Synthase, subunit E	NP_031533.2	1	-1.4
ATP Synthase, subunit α (mitochondrial precursor)	NP_031531.1	1	2.0
Carnitine O-Palmitoyltransferase 2 (mitochondrial precursor)	NP_034079.2	1	-1.0
GAPDH-like (isoform 2)	XP_001476757.1	10	-1.3
LDHA chain (isoform 1)	NP_034829.1	2	-1.9
NADH dehydrogenase 1 α subcomplex, subunit 4	NP_035016.1	1	-2.2
Phosphate Carrier Protein, mitochondrial-like (isoform 1)	XP_001475977.1	2	-1.1
Thioredoxin	NP_035790.1	1	-1.5

Cytoskeletal Components and Modulators

Name	Reference Number	Peptide Count	Fold Change (KO v WT)
Actin (cytoplasmic 2)	NP_033739.1	2	2.4
Actin (α skeletal muscle)	NP_033736.1	6	1.3
Fascin	NP_032010.2	1	1.5
Fibronectin (Precursor)	NP_034363.1	38	2.1
Fibulin-2 (isoform a)(Precursor)	NP_032018.2	3	2.5
Filamin-A	NP_034357.2	1	1.3
Keratin, type I (cytoskeletal 10)	NP_034790.2	8	-1.1
Keratin, type I (cytoskeletal 16)	NP_032496.1	3	1.1
Keratin, type I (cytoskeletal 17)	NP_034793.1	4	1.5
Keratin, type I (cytoskeletal 42)	NP_997648.2	1	-1.1
Keratin, type II (cytoskeletal 1)	NP_032499.2	3	1.1
Keratin, type II (cytoskeletal 2 epidermal)	NP_034798.2	4	1.1
Keratin, type II (cytoskeletal 5)	NP_081287.1	4	1.2
Keratin, type II (cytoskeletal 73)	NP_997650.1	1	1.7

Keratin, type II (cytoskeletal 78-like)	XP_003086989.1	1	1.3
Keratin, type II (cytoskeletal 79)	NP_666175.1	1	1.4
Lysyl Oxidase homolog 1 (precursor)	NP_034859.2	1	-1.3
Lysyl Oxidase (Precursor)	NP_034858.2	1	1.8
Mxra8 (precursor)	NP_077225.4	1	-1.1
Nestin	NP_057910.3	1	2.0
Pdlim7 (isoform a)	NP_001107560.1	1	-1.1
Prelamin-A/C (isoform A)	NP_001002011.2	5	-2.7
Thrombospondin-1 (Precursor)	NP_035710.2	1	2.9
Tubulin α-1B chain	NP_035784.1	1	-2.0
Tubulin α-1C chain	NP_033474.1	11	-1.1
Tubulin β-4B chain	NP_666228.1	1	-1.1
Tubulin β-5 chain	NP_035785.1	11	-1.3
Tubulin β-6 chain	NP_080749.2	2	-1.7
Vimentin	NP_035831.2	3	1.4
Zyxin	NP_035907.1	5	-1.0

Other

Name	Reference Number	Peptide Count	Fold Change (KO v WT)
Ankyrin Repeat Domain-Containing Protein 13A	NP_080994.2	4	-1.2
DDB1	NP_056550.1	6	-1.5
Fhl2	NP_034342.1	1	2.0
GPNMB (Precursor)	NP_444340.3	1	2.0
Iqca1	NP_083398.2	1	-1.1
ITM2B	NP_032436.1	1	-1.6
Nischarin	NP_073147.2	2	-1.4
Olfr976	NP_666479.1	1	-1.2
RNF213	XP_001476701.2	5	1.6
Spata7 homolog	NP_849245.2	1	-1.4
Teneurin-1	NP_035985.2	1	1.4
TGFβ1-induced transcript 1 protein	NP_033391.1	3	-1.2
ZNF334	NP_848498.2	1	1.0

References

1. Isaacs A, Lindenmann J: Virus interference. I. The interferon. *Proc R Soc Lond B Biol Sci* 1957, 147:258-267.

2. Pestka S, Krause CD, Walter MR: Interferons, interferon-like cytokines, and their receptors. *Immunol Rev* 2004, 202:8-32.

3. Ozato K, Tsujimura H, Tamura T: Toll-like receptor signaling and regulation of cytokine gene expression in the immune system. *Biotechniques* 2002, Suppl:66-68, 70, 72 passim.

4. Boehm U, Klamp T, Groot M, Howard JC: Cellular responses to interferon-gamma. *Annu Rev Immunol* 1997, 15:749-795.

5. Hardy KJ, Sawada T: Human gamma interferon strongly upregulates its own gene expression in peripheral blood lymphocytes. *J Exp Med* 1989, 170:1021-1026.

6. Ehrt S, Schnappinger D, Bekiranov S, Drenkow J, Shi S, Gingeras TR, Gaasterland T, Schoolnik G, Nathan C: Reprogramming of the macrophage transcriptome in response to interferon-gamma and Mycobacterium tuberculosis: signaling roles of nitric oxide synthase-2 and phagocyte oxidase. *J Exp Med* 2001, 194:1123-1140.

7. de Veer MJ, Holko M, Frevel M, Walker E, Der S, Paranjape JM, Silverman RH, Williams BR: Functional classification of interferon-stimulated genes identified using microarrays. *J Leukoc Biol* 2001, 69:912-920.

8. Kota RS, Rutledge JC, Gohil K, Kumar A, Enelow RI, Ramana CV: Regulation of gene expression in RAW 264.7 macrophage cell line by interferon-gamma. *Biochem Biophys Res Commun* 2006, 342:1137-1146.

9. Halonen SK, Woods T, McInnerney K, Weiss LM: Microarray analysis of IFN-gamma response genes in astrocytes. *J Neuroimmunol* 2006, 175:19-30.

10. Darnell JE, Jr., Kerr IM, Stark GR: Jak-STAT pathways and transcriptional activation in response to IFNs and other extracellular signaling proteins. *Science* 1994, 264:1415-1421.

11. Silvennoinen O, Ihle JN, Schlessinger J, Levy DE: Interferon-induced nuclear signalling by Jak protein tyrosine kinases. *Nature* 1993, 366:583-585.

12. Aaronson DS, Horvath CM: A road map for those who don't know JAK-STAT. *Science* 2002, 296:1653-1655.

13. Farrar JD, Smith JD, Murphy TL, Murphy KM: Recruitment of Stat4 to the human interferon-alpha/beta receptor requires activated Stat2. *J Biol Chem* 2000, 275:2693-2697.

14. Torpey N, Maher SE, Bothwell AL, Pober JS: Interferon alpha but not interleukin 12 activates STAT4 signaling in human vascular endothelial cells. *J Biol Chem* 2004, 279:26789-26796.

15. Matikainen S, Sareneva T, Ronni T, Lehtonen A, Koskinen PJ, Julkunen I: Interferon-alpha activates multiple STAT proteins and upregulates proliferation-associated IL-2Ralpha, c-myc, and pim-1 genes in human T cells. *Blood* 1999, 93:1980-1991.

16. Fasler-Kan E, Pansky A, Wiederkehr M, Battegay M, Heim MH: Interferon-alpha activates signal transducers and activators of transcription 5 and 6 in Daudi cells. *Eur J Biochem* 1998, 254:514-519.

17. Darnell JE, Jr.: STATs and gene regulation. *Science* 1997, 277:1630-1635.

18. Fu XY, Schindler C, Improta T, Aebersold R, Darnell JE, Jr.: The proteins of ISGF-3, the interferon alpha-induced transcriptional activator, define a gene family involved in signal transduction. *Proc Natl Acad Sci U S A* 1992, 89:7840-7843.

19. Schindler C, Shuai K, Prezioso VR, Darnell JE, Jr.: Interferon-dependent tyrosine phosphorylation of a latent cytoplasmic transcription factor. *Science* 1992, 257:809-813.

20. Pestka S, Kotenko SV, Muthukumaran G, Izotova LS, Cook JR, Garotta G: The interferon gamma (IFN-gamma) receptor: a paradigm for the multichain cytokine receptor. *Cytokine Growth Factor Rev* 1997, 8:189-206.

21. Bach EA, Aguet M, Schreiber RD: The IFN gamma receptor: a paradigm for cytokine receptor signaling. *Annu Rev Immunol* 1997, 15:563-591.

22. Watling D, Guschin D, Muller M, Silvennoinen O, Witthuhn BA, Quelle FW, Rogers NC, Schindler C, Stark GR, Ihle JN, et al.: Complementation by the protein tyrosine kinase JAK2 of a mutant cell line defective in the interferon-gamma signal transduction pathway. *Nature* 1993, 366:166-170.

23. Shuai K, Schindler C, Prezioso VR, Darnell JE, Jr.: Activation of transcription by IFN-gamma: tyrosine phosphorylation of a 91-kD DNA binding protein. *Science* 1992, 258:1808-1812.

24. Wen Z, Zhong Z, Darnell JE, Jr.: Maximal activation of transcription by Stat1 and Stat3 requires both tyrosine and serine phosphorylation. *Cell* 1995, 82:241-250.

25. Wen Z, Darnell JE, Jr.: Mapping of Stat3 serine phosphorylation to a single residue (727) and evidence that serine phosphorylation has no influence on DNA binding of Stat1 and Stat3. *Nucleic Acids Res* 1997, 25:2062-2067.

26. Varinou L, Ramsauer K, Karaghiosoff M, Kolbe T, Pfeffer K, Muller M, Decker T: Phosphorylation of the Stat1 transactivation domain is required for full-fledged IFN-gamma-dependent innate immunity. *Immunity* 2003, 19:793-802.

27. Nguyen H, Ramana CV, Bayes J, Stark GR: Roles of phosphatidylinositol 3-kinase in interferon-gamma-dependent phosphorylation of STAT1 on serine 727 and activation of gene expression. *J Biol Chem* 2001, 276:33361-33368.

28. Uddin S, Sassano A, Deb DK, Verma A, Majchrzak B, Rahman A, Malik AB, Fish EN, Platanias LC: Protein kinase C-delta (PKC-delta) is activated by type I interferons and mediates phosphorylation of Stat1 on serine 727. *J Biol Chem* 2002, 277:14408-14416.

29. Deb DK, Sassano A, Lekmine F, Majchrzak B, Verma A, Kambhampati S, Uddin S, Rahman A, Fish EN, Platanias LC: Activation of protein kinase C delta by IFN-gamma. *J Immunol* 2003, 171:267-273.

30. Cantley LC: The phosphoinositide 3-kinase pathway. *Science* 2002, 296:1655-1657.

31. Inoki K, Li Y, Zhu T, Wu J, Guan KL: TSC2 is phosphorylated and inhibited by Akt and suppresses mTOR signalling. *Nat Cell Biol* 2002, 4:648-657.

32. Yang Z, Klionsky DJ: Mammalian autophagy: core molecular machinery and signaling regulation. *Curr Opin Cell Biol* 22:124-131.

33. Noda T, Ohsumi Y: Tor, a phosphatidylinositol kinase homologue, controls autophagy in yeast. *J Biol Chem* 1998, 273:3963-3966.

34. Platanias LC: Mechanisms of type-I- and type-II-interferon-mediated signalling. *Nat Rev Immunol* 2005, 5:375-386.

35. Hu J, Roy SK, Shapiro PS, Rodig SR, Reddy SP, Platanias LC, Schreiber RD, Kalvakolanu DV: ERK1 and ERK2 activate CCAAAT/enhancer-binding protein-beta-dependent gene transcription in response to interferon-gamma. *J Biol Chem* 2001, 276:287-297.

36. Roy SK, Wachira SJ, Weihua X, Hu J, Kalvakolanu DV: CCAAT/enhancer-binding protein-beta regulates interferon-induced transcription through a novel element. *J Biol Chem* 2000, 275:12626-12632.

37. Gade P, Ramachandran G, Maachani UB, Rizzo MA, Okada T, Prywes R, Cross AS, Mori K, Kalvakolanu DV: An IFN-gamma-stimulated ATF6-C/EBP-beta-signaling pathway critical for the expression of Death Associated Protein Kinase 1 and induction of autophagy. *Proc Natl Acad Sci U S A* 2012, 109:10316-10321.

38. Bekpen C, Hunn JP, Rohde C, Parvanova I, Guethlein L, Dunn DM, Glowalla E, Leptin M, Howard JC: The interferon-inducible p47 (IRG) GTPases in vertebrates: loss of the cell autonomous resistance mechanism in the human lineage. *Genome Biol* 2005, 6:R92.

39. Bekpen C, Marques-Bonet T, Alkan C, Antonacci F, Leogrande MB, Ventura M, Kidd JM, Siswara P, Howard JC, Eichler EE: Death and resurrection of the human IRGM gene. *PLoS Genet* 2009, 5:e1000403.

40. Boehm U, Guethlein L, Klamp T, Ozbek K, Schaub A, Futterer A, Pfeffer K, Howard JC: Two families of GTPases dominate the complex cellular response to IFN-gamma. *J Immunol* 1998, 161:6715-6723.

41. Singh SB, Davis AS, Taylor GA, Deretic V: Human IRGM induces autophagy to eliminate intracellular mycobacteria. *Science* 2006, 313:1438-1441.

42. Ghosh A, Uthaiah R, Howard J, Herrmann C, Wolf E: Crystal structure of IIGP1: a paradigm for interferon-inducible p47 resistance GTPases. *Mol Cell* 2004, 15:727-739.

43. Danino D, Hinshaw JE: Dynamin family of mechanoenzymes. *Curr Opin Cell Biol* 2001, 13:454-460.

44. Praefcke GJ, McMahon HT: The dynamin superfamily: universal membrane tubulation and fission molecules? *Nat Rev Mol Cell Biol* 2004, 5:133-147.

45. Schafer DA: Regulating actin dynamics at membranes: a focus on dynamin. *Traffic* 2004, 5:463-469.

46. Cherfils J, Zeghouf M: Regulation of small GTPases by GEFs, GAPs, and GDIs. *Physiol Rev* 2013, 93:269-309.

47. Sever S, Muhlberg AB, Schmid SL: Impairment of dynamin's GAP domain stimulates receptor-mediated endocytosis. *Nature* 1999, 398:481-486.

48. Marks B, Stowell MH, Vallis Y, Mills IG, Gibson A, Hopkins CR, McMahon HT: GTPase activity of dynamin and resulting conformation change are essential for endocytosis. *Nature* 2001, 410:231-235.

49. Uthaiah RC, Praefcke GJ, Howard JC, Herrmann C: IIGP1, an interferon-gamma-inducible 47-kDa GTPase of the mouse, showing cooperative enzymatic activity and GTP-dependent multimerization. *J Biol Chem* 2003, 278:29336-29343.

50. Taylor GA, Stauber R, Rulong S, Hudson E, Pei V, Pavlakis GN, Resau JH, Vande Woude GF: The inducibly expressed GTPase localizes to the endoplasmic reticulum, independently of GTP binding. *J Biol Chem* 1997, 272:10639-10645.

51. Martens S, Sabel K, Lange R, Uthaiah R, Wolf E, Howard JC: Mechanisms regulating the positioning of mouse p47 resistance GTPases LRG-47 and IIGP1 on cellular membranes: retargeting to plasma membrane induced by phagocytosis. *J Immunol* 2004, 173:2594-2606.

52. Resh MD: Fatty acylation of proteins: new insights into membrane targeting of myristoylated and palmitoylated proteins. *Biochim Biophys Acta* 1999, 1451:1-16.

53. Maurer-Stroh S, Gouda M, Novatchkova M, Schleiffer A, Schneider G, Sirota FL, Wildpaner M, Hayashi N, Eisenhaber F: MYRbase: analysis of genome-wide glycine myristoylation enlarges the functional spectrum of eukaryotic myristoylated proteins. *Genome Biol* 2004, 5:R21.

54. Merrick BA, Dhungana S, Williams JG, Aloor JJ, Peddada S, Tomer KB, Fessler MB: Proteomic profiling of S-acylated macrophage proteins identifies a role for palmitoylation in mitochondrial targeting of phospholipid scramblase 3. *Mol Cell Proteomics* 2011, 10:M110 006007.

55. Butcher BA, Greene RI, Henry SC, Annecharico KL, Weinberg JB, Denkers EY, Sher A, Taylor GA: p47 GTPases regulate Toxoplasma gondii survival in activated macrophages. *Infect Immun* 2005, 73:3278-3286.

56. Zhao YO, Konen-Waisman S, Taylor GA, Martens S, Howard JC: Localisation and mislocalisation of the interferon-inducible immunity-related GTPase, Irgm1 (LRG-47) in mouse cells. *PLoS One* 2010, 5:e8648.

57. Springer HM, Schramm M, Taylor GA, Howard JC: Irgm1 (LRG-47), a Regulator of Cell-Autonomous Immunity, Does Not Localize to Mycobacterial or Listerial Phagosomes in IFN-gamma-Induced Mouse Cells. *J Immunol* 2013, 191:1765-1774.

58. Chang CP, Yang MC, Lei HY: Concanavalin A/IFN-gamma triggers autophagy-related necrotic hepatocyte death through IRGM1-mediated lysosomal membrane disruption. *PLoS One* 2011, 6:e28323.

59. Bougneres L, Helft J, Tiwari S, Vargas P, Chang BH, Chan L, Campisi L, Lauvau G, Hugues S, Kumar P, et al.: A role for lipid bodies in the cross-presentation of phagocytosed antigens by MHC class I in dendritic cells. *Immunity* 2009, 31:232-244.

60. Henry SC, Daniell XG, Burroughs AR, Indaram M, Howell DN, Coers J, Starnbach MN, Hunn JP, Howard JC, Feng CG, et al.: Balance of Irgm protein activities determines IFN-{gamma}-induced host defense. *J Leukoc Biol* 2009, 85:877-885.

61. Martens S, Parvanova I, Zerrahn J, Griffiths G, Schell G, Reichmann G, Howard JC: Disruption of Toxoplasma gondii parasitophorous vacuoles by the mouse p47-resistance GTPases. *PLoS Pathogens* 2005, 1:e24

62. Hunn JP, Koenen-Waisman S, Papic N, Schroeder N, Pawlowski N, Lange R, Kaiser F, Zerrahn J, Martens S, Howard JC: Regulatory interactions between IRG resistance GTPases in the cellular response to Toxoplasma gondii. *EMBO J* 2008, 27:2495-2509.

63. Collazo CM, Yap GS, Sempowski GD, Lusby KC, Tessarollo L, Woude GF, Sher A, Taylor GA: Inactivation of LRG-47 and IRG-47 reveals a family of interferon gamma-inducible genes with essential, pathogen-specific roles in resistance to infection. *J Exp Med* 2001, 194:181-188.

64. Henry SC, Daniell X, Indaram M, Whitesides JF, Sempowski GD, Howell D, Oliver T, Taylor GA: Impaired Macrophage Function Underscores Susceptibility to Salmonella in Mice Lacking Irgm1 (LRG-47). *J Immunol* 2007, 179:6963-6972.

65. Coers J, Bernstein-Hanley I, Grotsky D, Parvanova I, Howard JC, Taylor GA, Dietrich WF, Starnbach MN: Chlamydia muridarum evades growth restriction by the IFN-gamma-inducible host resistance factor Irgb10. *J Immunol* 2008, 180:6237-6245.

66. Vignola MJ, Kashatus DF, Taylor GA, Counter CM, Valdivia RH: cPLA2 regulates the expression of type I interferons and intracellular immunity to Chlamydia trachomatis. *J Biol Chem* 285:21625-21635.

67. Feng CG, Collazo-Custodio CM, Eckhaus M, Hieny S, Belkaid Y, Elkins K, Jankovic D, Taylor GA, Sher A: Mice deficient in LRG-47 display increased susceptibility to mycobacterial infection associated with the induction of lymphopenia. *J Immunol* 2004, 172:1163-1168.

68. MacMicking JD, Taylor GA, McKinney JD: Immune control of tuberculosis by IFN-gamma-inducible LRG-47. *Science* 2003, 302:654-659.

69. Taylor GA, Collazo CM, Yap GS, Nguyen K, Gregorio TA, Taylor LS, Eagleson B, Secrest L, Southon EA, Reid SW, et al.: Pathogen-specific loss of host resistance in mice lacking the IFN-gamma-inducible gene IGTP. *Proc Natl Acad Sci U S A* 2000, 97:751-755.

70. Collazo CM, Yap GS, Hieny S, Caspar P, Feng CG, Taylor GA, Sher A: The function of gamma interferon-inducible GTP-binding protein IGTP in host resistance to Toxoplasma gondii is Stat1 dependent and requires expression in both hematopoietic and nonhematopoietic cellular compartments. *Infect Immun* 2002, 70:6933-6939.

71. Papic N, Hunn JP, Pawlowski N, Zerrahn J, Howard JC: Inactive and active states of the interferon-inducible resistance GTPase, Irga6, in vivo. *J Biol Chem* 2008, 283:32143-32151.

72. Al-Zeer MA, Al-Younes HM, Braun PR, Zerrahn J, Meyer TF: IFN-gamma-inducible Irga6 mediates host resistance against Chlamydia trachomatis via autophagy. *PLoS One* 2009, 4:e4588.

73. Haldar AK, Saka HA, Piro AS, Dunn JD, Henry SC, Taylor GA, Frickel EM, Valdivia RH, Coers J: IRG and GBP host resistance factors target aberrant, "non-self" vacuoles characterized by the missing of "self" IRGM proteins. *PLoS Pathog* 2013, 9:e1003414.

74. Olszewski MA, Gray J, Vestal DJ: In silico genomic analysis of the human and murine guanylate-binding protein (GBP) gene clusters. *J Interferon Cytokine Res* 2006, 26:328-352.

75. Schwemmle M, Kaspers B, Irion A, Staeheli P, Schultz U: Chicken guanylate-binding protein. Conservation of GTPase activity and induction by cytokines. *J Biol Chem* 1996, 271:10304-10308.

76. Asundi VK, Stahl RC, Showalter L, Conner KJ, Carey DJ: Molecular cloning and characterization of an isoprenylated 67 kDa protein. *Biochim Biophys Acta* 1994, 1217:257-265.

77. Degrandi D, Konermann C, Beuter-Gunia C, Kresse A, Wurthner J, Kurig S, Beer S, Pfeffer K: Extensive characterization of IFN-induced GTPases mGBP1 to mGBP10 involved in host defense. *J Immunol* 2007, 179:7729-7740.

78. Cheng YS, Colonno RJ, Yin FH: Interferon induction of fibroblast proteins with guanylate binding activity. *J Biol Chem* 1983, 258:7746-7750.

79. Cheng YS, Becker-Manley MF, Chow TP, Horan DC: Affinity purification of an interferon-induced human guanylate-binding protein and its characterization. *J Biol Chem* 1985, 260:15834-15839.

80. Nguyen TT, Hu Y, Widney DP, Mar RA, Smith JB: Murine GBP-5, a new member of the murine guanylate-binding protein family, is coordinately regulated with other GBPs in vivo and in vitro. *J Interferon Cytokine Res* 2002, 22:899-909.

81. Prakash B, Praefcke GJ, Renault L, Wittinghofer A, Herrmann C: Structure of human guanylate-binding protein 1 representing a unique class of GTP-binding proteins. *Nature* 2000, 403:567-571.

82. Cheng YS, Patterson CE, Staeheli P: Interferon-induced guanylate-binding proteins lack an N(T)KXD consensus motif and bind GMP in addition to GDP and GTP. *Mol Cell Biol* 1991, 11:4717-4725.

83. Schwemmle M, Staeheli P: The interferon-induced 67-kDa guanylate-binding protein (hGBP1) is a GTPase that converts GTP to GMP. *J Biol Chem* 1994, 269:11299-11305.

84. Prakash B, Renault L, Praefcke GJ, Herrmann C, Wittinghofer A: Triphosphate structure of guanylate-binding protein 1 and implications for nucleotide binding and GTPase mechanism. *Embo J* 2000, 19:4555-4564.

85. Kim BH, Shenoy AR, Kumar P, Das R, Tiwari S, MacMicking JD: A family of IFN-gamma-inducible 65-kD GTPases protects against bacterial infection. *Science* 2011, 332:717-721.

86. Britzen-Laurent N, Bauer M, Berton V, Fischer N, Syguda A, Reipschlager S, Naschberger E, Herrmann C, Sturzl M: Intracellular trafficking of guanylate-binding proteins is regulated by heterodimerization in a hierarchical manner. *PLoS One* 2010, 5:e14246.

87. Modiano N, Lu YE, Cresswell P: Golgi targeting of human guanylate-binding protein-1 requires nucleotide binding, isoprenylation, and an IFN-gamma-inducible cofactor. *Proc Natl Acad Sci U S A* 2005, 102:8680-8685.

88. Tripal P, Bauer M, Naschberger E, Mortinger T, Hohenadl C, Cornali E, Thurau M, Sturzl M: Unique features of different members of the human guanylate-binding protein family. *J Interferon Cytokine Res* 2007, 27:44-52.

89. Vestal DJ, Gorbacheva VY, Sen GC: Different subcellular localizations for the related interferon-induced GTPases, MuGBP-1 and MuGBP-2: implications for different functions? *J Interferon Cytokine Res* 2000, 20:991-1000.

90. Carter CC, Gorbacheva VY, Vestal DJ: Inhibition of VSV and EMCV replication by the interferon-induced GTPase, mGBP-2: differential requirement for wild-type GTP binding domain. *Arch Virol* 2005, 150:1213-1220.

91. Anderson SL, Carton JM, Lou J, Xing L, Rubin BY: Interferon-induced guanylate binding protein-1 (GBP-1) mediates an antiviral effect against vesicular stomatitis virus and encephalomyocarditis virus. *Virology* 1999, 256:8-14.

92. Itsui Y, Sakamoto N, Kakinuma S, Nakagawa M, Sekine-Osajima Y, Tasaka-Fujita M, Nishimura-Sakurai Y, Suda G, Karakama Y, Mishima K, et al.: Antiviral effects of the interferon-induced protein guanylate binding protein 1 and its interaction with the hepatitis C virus NS5B protein. *Hepatology* 2009, 50:1727-1737.

93. Nordmann A, Wixler L, Boergeling Y, Wixler V, Ludwig S: A new splice variant of the human guanylate-binding protein 3 mediates anti-influenza activity through inhibition of viral transcription and replication. *FASEB J* 2012, 26:1290-1300.

94. Tietzel I, El-Haibi C, Carabeo RA: Human guanylate binding proteins potentiate the anti-chlamydia effects of interferon-gamma. *PLoS One* 2009, 4:e6499.

95. Yamamoto M, Okuyama M, Ma JS, Kimura T, Kamiyama N, Saiga H, Ohshima J, Sasai M, Kayama H, Okamoto T, et al.: A cluster of interferon-gamma-inducible p65 GTPases plays a critical role in host defense against Toxoplasma gondii. *Immunity* 2012, 37:302-313.

96. Vladimer GI, Marty-Roix R, Ghosh S, Weng D, Lien E: Inflammasomes and host defenses against bacterial infections. *Curr Opin Microbiol* 2013, 16:23-31.

97. Shenoy AR, Wellington DA, Kumar P, Kassa H, Booth CJ, Cresswell P, MacMicking JD: GBP5 promotes NLRP3 inflammasome assembly and immunity in mammals. *Science* 2012, 336:481-485.

98. Hershko A: The ubiquitin system for protein degradation and some of its roles in the control of the cell division cycle. *Cell Death Differ* 2005, 12:1191-1197.

99. Wang J, Maldonado MA: The ubiquitin-proteasome system and its role in inflammatory and autoimmune diseases. *Cell Mol Immunol* 2006, 3:255-261.

100. Voges D, Zwickl P, Baumeister W: The 26S proteasome: a molecular machine designed for controlled proteolysis. *Annu Rev Biochem* 1999, 68:1015-1068.

101. Liu CW, Li X, Thompson D, Wooding K, Chang TL, Tang Z, Yu H, Thomas PJ, DeMartino GN: ATP binding and ATP hydrolysis play distinct roles in the function of 26S proteasome. *Mol Cell* 2006, 24:39-50.

102. Komander D, Rape M: The ubiquitin code. *Annu Rev Biochem* 2012, 81:203-229.

103. Chau V, Tobias JW, Bachmair A, Marriott D, Ecker DJ, Gonda DK, Varshavsky A: A multiubiquitin chain is confined to specific lysine in a targeted short-lived protein. *Science* 1989, 243:1576-1583.

104. Shringarpure R, Grune T, Mehlhase J, Davies KJ: Ubiquitin conjugation is not required for the degradation of oxidized proteins by proteasome. *J Biol Chem* 2003, 278:311-318.

105. Zhang M, Pickart CM, Coffino P: Determinants of proteasome recognition of ornithine decarboxylase, a ubiquitin-independent substrate. *EMBO J* 2003, 22:1488-1496.

106. Settembre C, Fraldi A, Medina DL, Ballabio A: Signals from the lysosome: a control centre for cellular clearance and energy metabolism. *Nat Rev Mol Cell Biol* 2013, 14:283-296.

107. Pandey UB, Nie Z, Batlevi Y, McCray BA, Ritson GP, Nedelsky NB, Schwartz SL, DiProspero NA, Knight MA, Schuldiner O, et al.: HDAC6 rescues neurodegeneration and provides an essential link between autophagy and the UPS. *Nature* 2007, 447:859-863.

108. Li WW, Li J, Bao JK: Microautophagy: lesser-known self-eating. *Cell Mol Life Sci* 2012, 69:1125-1136.

109. Kaushik S, Cuervo AM: Chaperone-mediated autophagy: a unique way to enter the lysosome world. *Trends Cell Biol* 2012, 22:407-417.

110. Loewith R, Jacinto E, Wullschleger S, Lorberg A, Crespo JL, Bonenfant D, Oppliger W, Jenoe P, Hall MN: Two TOR complexes, only one of which is rapamycin sensitive, have distinct roles in cell growth control. *Mol Cell* 2002, 10:457-468.

111. Chan EY, Kir S, Tooze SA: siRNA screening of the kinome identifies ULK1 as a multidomain modulator of autophagy. *J Biol Chem* 2007, 282:25464-25474.

112. Jung CH, Jun CB, Ro SH, Kim YM, Otto NM, Cao J, Kundu M, Kim DH: ULK-Atg13-FIP200 complexes mediate mTOR signaling to the autophagy machinery. *Mol Biol Cell* 2009, 20:1992-2003.

113. Tee AR, Manning BD, Roux PP, Cantley LC, Blenis J: Tuberous sclerosis complex gene products, Tuberin and Hamartin, control mTOR signaling by acting as a GTPase-activating protein complex toward Rheb. *Curr Biol* 2003, 13:1259-1268.

114. Inoki K, Li Y, Xu T, Guan KL: Rheb GTPase is a direct target of TSC2 GAP activity and regulates mTOR signaling. *Genes Dev* 2003, 17:1829-1834.

115. Zhang Y, Gao X, Saucedo LJ, Ru B, Edgar BA, Pan D: Rheb is a direct target of the tuberous sclerosis tumour suppressor proteins. *Nat Cell Biol* 2003, 5:578-581.

116. Garami A, Zwartkruis FJ, Nobukuni T, Joaquin M, Roccio M, Stocker H, Kozma SC, Hafen E, Bos JL, Thomas G: Insulin activation of Rheb, a mediator of mTOR/S6K/4E-BP signaling, is inhibited by TSC1 and 2. *Mol Cell* 2003, 11:1457-1466.

117. Shaw RJ, Kosmatka M, Bardeesy N, Hurley RL, Witters LA, DePinho RA, Cantley LC: The tumor suppressor LKB1 kinase directly activates AMP-activated kinase and regulates apoptosis in response to energy stress. *Proc Natl Acad Sci U S A* 2004, 101:3329-3335.

118. Hawley SA, Boudeau J, Reid JL, Mustard KJ, Udd L, Makela TP, Alessi DR, Hardie DG: Complexes between the LKB1 tumor suppressor, STRAD alpha/beta and MO25 alpha/beta are upstream kinases in the AMP-activated protein kinase cascade. *J Biol* 2003, 2:28.

119. Woods A, Johnstone SR, Dickerson K, Leiper FC, Fryer LG, Neumann D, Schlattner U, Wallimann T, Carlson M, Carling D: LKB1 is the upstream kinase in the AMP-activated protein kinase cascade. *Curr Biol* 2003, 13:2004-2008.

120. Corradetti MN, Inoki K, Bardeesy N, DePinho RA, Guan KL: Regulation of the TSC pathway by LKB1: evidence of a molecular link between tuberous sclerosis complex and Peutz-Jeghers syndrome. *Genes Dev* 2004, 18:1533-1538.

121. Hoyer-Hansen M, Bastholm L, Szyniarowski P, Campanella M, Szabadkai G, Farkas T, Bianchi K, Fehrenbacher N, Elling F, Rizzuto R, et al.: Control of macroautophagy by calcium, calmodulin-dependent kinase kinase-beta, and Bcl-2. *Mol Cell* 2007, 25:193-205.

122. Feng Z, Zhang H, Levine AJ, Jin S: The coordinate regulation of the p53 and mTOR pathways in cells. *Proc Natl Acad Sci U S A* 2005, 102:8204-8209.

123. Margolis B, Skolnik EY: Activation of Ras by receptor tyrosine kinases. *J Am Soc Nephrol* 1994, 5:1288-1299.

124. Furuta S, Hidaka E, Ogata A, Yokota S, Kamata T: Ras is involved in the negative control of autophagy through the class I PI3-kinase. *Oncogene* 2004, 23:3898-3904.

125. Ma L, Chen Z, Erdjument-Bromage H, Tempst P, Pandolfi PP: Phosphorylation and functional inactivation of TSC2 by Erk implications for tuberous sclerosis and cancer pathogenesis. *Cell* 2005, 121:179-193.

126. Ganley IG, Lam du H, Wang J, Ding X, Chen S, Jiang X: ULK1.ATG13.FIP200 complex mediates mTOR signaling and is essential for autophagy. *J Biol Chem* 2009, 284:12297-12305.

127. Hosokawa N, Hara T, Kaizuka T, Kishi C, Takamura A, Miura Y, Iemura S, Natsume T, Takehana K, Yamada N, et al.: Nutrient-dependent mTORC1 association with the ULK1-Atg13-FIP200 complex required for autophagy. *Mol Biol Cell* 2009, 20:1981-1991.

128. Hara T, Takamura A, Kishi C, Iemura S, Natsume T, Guan JL, Mizushima N: FIP200, a ULK-interacting protein, is required for autophagosome formation in mammalian cells. *J Cell Biol* 2008, 181:497-510.

129. Mercer CA, Kaliappan A, Dennis PB: A novel, human Atg13 binding protein, Atg101, interacts with ULK1 and is essential for macroautophagy. *Autophagy* 2009, 5:649-662.

130. Yla-Anttila P, Vihinen H, Jokitalo E, Eskelinen EL: 3D tomography reveals connections between the phagophore and endoplasmic reticulum. *Autophagy* 2009, 5:1180-1185.

131. Hayashi-Nishino M, Fujita N, Noda T, Yamaguchi A, Yoshimori T, Yamamoto A: A subdomain of the endoplasmic reticulum forms a cradle for autophagosome formation. *Nat Cell Biol* 2009, 11:1433-1437.

132. Chen Y, Klionsky DJ: The regulation of autophagy - unanswered questions. *J Cell Sci* 2011, 124:161-170.

133. Mizushima N, Yamamoto A, Hatano M, Kobayashi Y, Kabeya Y, Suzuki K, Tokuhisa T, Ohsumi Y, Yoshimori T: Dissection of autophagosome formation using Apg5-deficient mouse embryonic stem cells. *J Cell Biol* 2001, 152:657-668.

134. Itakura E, Kishi C, Inoue K, Mizushima N: Beclin 1 forms two distinct phosphatidylinositol 3-kinase complexes with mammalian Atg14 and UVRAG. *Mol Biol Cell* 2008, 19:5360-5372.

135. Sun Q, Fan W, Chen K, Ding X, Chen S, Zhong Q: Identification of Barkor as a mammalian autophagy-specific factor for Beclin 1 and class III phosphatidylinositol 3-kinase. *Proc Natl Acad Sci U S A* 2008, 105:19211-19216.

136. Liang C, Feng P, Ku B, Dotan I, Canaani D, Oh BH, Jung JU: Autophagic and tumour suppressor activity of a novel Beclin1-binding protein UVRAG. *Nat Cell Biol* 2006, 8:688-699.

137. Zhong Y, Wang QJ, Li X, Yan Y, Backer JM, Chait BT, Heintz N, Yue Z: Distinct regulation of autophagic activity by Atg14L and Rubicon associated with Beclin 1-phosphatidylinositol-3-kinase complex. *Nat Cell Biol* 2009, 11:468-476.

138. Matsunaga K, Saitoh T, Tabata K, Omori H, Satoh T, Kurotori N, Maejima I, Shirahama-Noda K, Ichimura T, Isobe T, et al.: Two Beclin 1-binding proteins, Atg14L and Rubicon, reciprocally regulate autophagy at different stages. *Nat Cell Biol* 2009, 11:385-396.

139. Takahashi Y, Coppola D, Matsushita N, Cualing HD, Sun M, Sato Y, Liang C, Jung JU, Cheng JQ, Mule JJ, et al.: Bif-1 interacts with Beclin 1 through UVRAG and regulates autophagy and tumorigenesis. *Nat Cell Biol* 2007, 9:1142-1151.

140. Takahashi Y, Meyerkord CL, Wang HG: Bif-1/endophilin B1: a candidate for crescent driving force in autophagy. *Cell Death Differ* 2009, 16:947-955.

141. Liang C, Lee JS, Inn KS, Gack MU, Li Q, Roberts EA, Vergne I, Deretic V, Feng P, Akazawa C, et al.: Beclin1-binding UVRAG targets the class C Vps complex to coordinate autophagosome maturation and endocytic trafficking. *Nat Cell Biol* 2008, 10:776-787.

142. Weidberg H, Shvets E, Shpilka T, Shimron F, Shinder V, Elazar Z: LC3 and GATE-16/GABARAP subfamilies are both essential yet act differently in autophagosome biogenesis. *EMBO J* 2010, 29:1792-1802.

143. von Muhlinen N, Akutsu M, Ravenhill BJ, Foeglein A, Bloor S, Rutherford TJ, Freund SM, Komander D, Randow F: LC3C, Bound Selectively by a Noncanonical LIR Motif in NDP52, Is Required for Antibacterial Autophagy. *Mol Cell* 2012.

144. Kabeya Y, Mizushima N, Ueno T, Yamamoto A, Kirisako T, Noda T, Kominami E, Ohsumi Y, Yoshimori T: LC3, a mammalian homologue of yeast Apg8p, is localized in autophagosome membranes after processing. *EMBO J* 2000, 19:5720-5728.

145. Kabeya Y, Mizushima N, Yamamoto A, Oshitani-Okamoto S, Ohsumi Y, Yoshimori T: LC3, GABARAP and GATE16 localize to autophagosomal membrane depending on form-II formation. *J Cell Sci* 2004, 117:2805-2812.

146. Suzuki K, Kirisako T, Kamada Y, Mizushima N, Noda T, Ohsumi Y: The pre-autophagosomal structure organized by concerted functions of APG genes is essential for autophagosome formation. *EMBO J* 2001, 20:5971-5981.

147. Kim J, Huang WP, Stromhaug PE, Klionsky DJ: Convergence of multiple autophagy and cytoplasm to vacuole targeting components to a perivacuolar membrane compartment prior to de novo vesicle formation. *J Biol Chem* 2002, 277:763-773.

148. Kirisako T, Ichimura Y, Okada H, Kabeya Y, Mizushima N, Yoshimori T, Ohsumi M, Takao T, Noda T, Ohsumi Y: The reversible modification regulates the membrane-binding state of Apg8/Aut7 essential for autophagy and the cytoplasm to vacuole targeting pathway. *J Cell Biol* 2000, 151:263-276.

149. Hemelaar J, Lelyveld VS, Kessler BM, Ploegh HL: A single protease, Apg4B, is specific for the autophagy-related ubiquitin-like proteins GATE-16, MAP1-LC3, GABARAP, and Apg8L. *J Biol Chem* 2003, 278:51841-51850.

150. Tanida I, Mizushima N, Kiyooka M, Ohsumi M, Ueno T, Ohsumi Y, Kominami E: Apg7p/Cvt2p: A novel protein-activating enzyme essential for autophagy. *Mol Biol Cell* 1999, 10:1367-1379.

151. Shintani T, Mizushima N, Ogawa Y, Matsuura A, Noda T, Ohsumi Y: Apg10p, a novel protein-conjugating enzyme essential for autophagy in yeast. *EMBO J* 1999, 18:5234-5241.

152. Mizushima N, Noda T, Yoshimori T, Tanaka Y, Ishii T, George MD, Klionsky DJ, Ohsumi M, Ohsumi Y: A protein conjugation system essential for autophagy. *Nature* 1998, 395:395-398.

153. Kuma A, Mizushima N, Ishihara N, Ohsumi Y: Formation of the approximately 350-kDa Apg12-Apg5.Apg16 multimeric complex, mediated by Apg16 oligomerization, is essential for autophagy in yeast. *J Biol Chem* 2002, 277:18619-18625.

154. Tanida I, Tanida-Miyake E, Komatsu M, Ueno T, Kominami E: Human Apg3p/Aut1p homologue is an authentic E2 enzyme for multiple substrates,

GATE-16, GABARAP, and MAP-LC3, and facilitates the conjugation of hApg12p to hApg5p. *J Biol Chem* 2002, 277:13739-13744.

155. Yang Z, Klionsky DJ: An overview of the molecular mechanism of autophagy. *Curr Top Microbiol Immunol* 2009, 335:1-32.

156. Ichimura Y, Kirisako T, Takao T, Satomi Y, Shimonishi Y, Ishihara N, Mizushima N, Tanida I, Kominami E, Ohsumi M, et al.: A ubiquitin-like system mediates protein lipidation. *Nature* 2000, 408:488-492.

157. Sou YS, Waguri S, Iwata J, Ueno T, Fujimura T, Hara T, Sawada N, Yamada A, Mizushima N, Uchiyama Y, et al.: The Atg8 conjugation system is indispensable for proper development of autophagic isolation membranes in mice. *Mol Biol Cell* 2008, 19:4762-4775.

158. Fujita N, Hayashi-Nishino M, Fukumoto H, Omori H, Yamamoto A, Noda T, Yoshimori T: An Atg4B mutant hampers the lipidation of LC3 paralogues and causes defects in autophagosome closure. *Mol Biol Cell* 2008, 19:4651-4659.

159. Fujita N, Noda T, Yoshimori T: Atg4B(C74A) hampers autophagosome closure: a useful protein for inhibiting autophagy. *Autophagy* 2009, 5:88-89.

160. Chakrama FZ, Seguin-Py S, Le Grand JN, Fraichard A, Delage-Mourroux R, Despouy G, Perez V, Jouvenot M, Boyer-Guittaut M: GABARAPL1 (GEC1) associates with autophagic vesicles. *Autophagy* 2010, 6:495-505.

161. Tanida I, Komatsu M, Ueno T, Kominami E: GATE-16 and GABARAP are authentic modifiers mediated by Apg7 and Apg3. *Biochem Biophys Res Commun* 2003, 300:637-644.

162. Tanida I, Sou YS, Minematsu-Ikeguchi N, Ueno T, Kominami E: Atg8L/Apg8L is the fourth mammalian modifier of mammalian Atg8 conjugation mediated by human Atg4B, Atg7 and Atg3. *FEBS J* 2006, 273:2553-2562.

163. Young AR, Chan EY, Hu XW, Kochl R, Crawshaw SG, High S, Hailey DW, Lippincott-Schwartz J, Tooze SA: Starvation and ULK1-dependent cycling of mammalian Atg9 between the TGN and endosomes. *J Cell Sci* 2006, 119:3888-3900.

164. Reggiori F, Tucker KA, Stromhaug PE, Klionsky DJ: The Atg1-Atg13 complex regulates Atg9 and Atg23 retrieval transport from the pre-autophagosomal structure. *Dev Cell* 2004, 6:79-90.

165. Ropolo A, Grasso D, Pardo R, Sacchetti ML, Archange C, Lo Re A, Seux M, Nowak J, Gonzalez CD, Iovanna JL, et al.: The pancreatitis-induced vacuole membrane protein 1 triggers autophagy in mammalian cells. *J Biol Chem* 2007, 282:37124-37133.

166. Nowak J, Archange C, Tardivel-Lacombe J, Pontarotti P, Pebusque MJ, Vaccaro MI, Velasco G, Dagorn JC, Iovanna JL: The TP53INP2 protein is required for autophagy in mammalian cells. *Mol Biol Cell* 2009, 20:870-881.

167. Berg TO, Fengsrud M, Stromhaug PE, Berg T, Seglen PO: Isolation and characterization of rat liver amphisomes. Evidence for fusion of autophagosomes with both early and late endosomes. *J Biol Chem* 1998, 273:21883-21892.

168. Tooze J, Hollinshead M, Ludwig T, Howell K, Hoflack B, Kern H: In exocrine pancreas, the basolateral endocytic pathway converges with the autophagic pathway immediately after the early endosome. *J Cell Biol* 1990, 111:329-345.

169. Jager S, Bucci C, Tanida I, Ueno T, Kominami E, Saftig P, Eskelinen EL: Role for Rab7 in maturation of late autophagic vacuoles. *J Cell Sci* 2004, 117:4837-4848.

170. Atlashkin V, Kreykenbohm V, Eskelinen EL, Wenzel D, Fayyazi A, Fischer von Mollard G: Deletion of the SNARE vti1b in mice results in the loss of a single SNARE partner, syntaxin 8. *Mol Cell Biol* 2003, 23:5198-5207.

171. Itakura E, Mizushima N: Syntaxin 17: the autophagosomal SNARE. *Autophagy* 2013, 9:917-919.

172. Epple UD, Suriapranata I, Eskelinen EL, Thumm M: Aut5/Cvt17p, a putative lipase essential for disintegration of autophagic bodies inside the vacuole. *J Bacteriol* 2001, 183:5942-5955.

173. Teter SA, Eggerton KP, Scott SV, Kim J, Fischer AM, Klionsky DJ: Degradation of lipid vesicles in the yeast vacuole requires function of Cvt17, a putative lipase. *J Biol Chem* 2001, 276:2083-2087.

174. Sagne C, Agulhon C, Ravassard P, Darmon M, Hamon M, El Mestikawy S, Gasnier B, Giros B: Identification and characterization of a lysosomal transporter for small neutral amino acids. *Proc Natl Acad Sci U S A* 2001, 98:7206-7211.

175. Yang Z, Klionsky DJ: Eaten alive: a history of macroautophagy. *Nat Cell Biol* 2010, 12:814-822.

176. Levine B, Mizushima N, Virgin HW: Autophagy in immunity and inflammation. *Nature* 2011, 469:323-335.

177. Deretic V: Autophagy as an innate immunity paradigm: expanding the scope and repertoire of pattern recognition receptors. *Curr Opin Immunol* 2012, 24:21-31.

178. Johansen T, Lamark T: Selective autophagy mediated by autophagic adapter proteins. *Autophagy* 2011, 7:279-296.

179. Kirkin V, Lamark T, Sou YS, Bjorkoy G, Nunn JL, Bruun JA, Shvets E, McEwan DG, Clausen TH, Wild P, et al.: A role for NBR1 in autophagosomal degradation of ubiquitinated substrates. *Mol Cell* 2009, 33:505-516.

180. Pankiv S, Clausen TH, Lamark T, Brech A, Bruun JA, Outzen H, Overvatn A, Bjorkoy G, Johansen T: p62/SQSTM1 binds directly to Atg8/LC3 to facilitate degradation of ubiquitinated protein aggregates by autophagy. *J Biol Chem* 2007, 282:24131-24145.

181. Wild P, Farhan H, McEwan DG, Wagner S, Rogov VV, Brady NR, Richter B, Korac J, Waidmann O, Choudhary C, et al.: Phosphorylation of the autophagy receptor optineurin restricts Salmonella growth. *Science* 2011, 333:228-233.

182. Ichimura Y, Kumanomidou T, Sou YS, Mizushima T, Ezaki J, Ueno T, Kominami E, Yamane T, Tanaka K, Komatsu M: Structural basis for sorting mechanism of p62 in selective autophagy. *J Biol Chem* 2008, 283:22847-22857.

183. Seibenhener ML, Geetha T, Wong HC, Krishna NR, Wooten MW: Sequestosome 1/p62 Is a Polyubiquitin Chain Binding Protein Involved in Ubiquitin Proteasome Degradation. *Molecular and Cellular Biology* 2004, 24:8055-8068.

184. Waters S, Marchbank K, Solomon E, Whitehouse C, Gautel M: Interactions with LC3 and polyubiquitin chains link nbr1 to autophagic protein turnover. *FEBS Lett* 2009, 583:1846-1852.

185. Thurston TL, Ryzhakov G, Bloor S, von Muhlinen N, Randow F: The TBK1 adaptor and autophagy receptor NDP52 restricts the proliferation of ubiquitin-coated bacteria. *Nat Immunol* 2009, 10:1215-1221.

186. Sumimoto H, Kamakura S, Ito T: Structure and function of the PB1 domain, a protein interaction module conserved in animals, fungi, amoebas, and plants. *Sci STKE* 2007, 2007:re6.

187. Sanz L, Diaz-Meco MT, Nakano H, Moscat J: The atypical PKC-interacting protein p62 channels NF-kappaB activation by the IL-1-TRAF6 pathway. *EMBO J* 2000, 19:1576-1586.

188. Kim JY, Ozato K: The sequestosome 1/p62 attenuates cytokine gene expression in activated macrophages by inhibiting IFN regulatory factor 8 and TNF receptor-associated factor 6/NF-kappaB activity. *J Immunol* 2009, 182:2131-2140.

189. Morton S, Hesson L, Peggie M, Cohen P: Enhanced binding of TBK1 by an optineurin mutant that causes a familial form of primary open angle glaucoma. *FEBS Lett* 2008, 582:997-1002.

190. Fratti RA, Chua J, Vergne I, Deretic V: Mycobacterium tuberculosis glycosylated phosphatidylinositol causes phagosome maturation arrest. *Proc Natl Acad Sci U S A* 2003, 100:5437-5442.

191. Gutierrez MG, Master SS, Singh SB, Taylor GA, Colombo MI, Deretic V: Autophagy is a defense mechanism inhibiting BCG and Mycobacterium tuberculosis survival in infected macrophages. *Cell* 2004, 119:753-766.

192. Feng CG, Zheng L, Jankovic D, Bafica A, Cannons JL, Watford WT, Chaussabel D, Hieny S, Caspar P, Schwartzberg PL, et al.: The immunity-related GTPase Irgm1 promotes the expansion of activated CD4+ T cell populations by preventing interferon-gamma-induced cell death. *Nat Immunol* 2008, 9:1279-1287.

193. He S, Wang C, Dong H, Xia F, Zhou H, Jiang X, Pei C, Ren H, Li H, Li R, et al.: Immune-related GTPase M (IRGM1) regulates neuronal autophagy in a mouse model of stroke. *Autophagy* 2012, 8:1621-1627.

194. McCarroll SA, Huett A, Kuballa P, Chilewski SD, Landry A, Goyette P, Zody MC, Hall JL, Brant SR, Cho JH, et al.: Deletion polymorphism upstream of IRGM associated with altered IRGM expression and Crohn's disease. *Nat Genet* 2008, 40:1107-1112.

195. Lapaquette P, Bringer MA, Darfeuille-Michaud A: Defects in autophagy favour adherent-invasive Escherichia coli persistence within macrophages leading to increased pro-inflammatory response. *Cell Microbiol* 2012, 14:791-807.

196. Parkes M, Barrett JC, Prescott NJ, Tremelling M, Anderson CA, Fisher SA, Roberts RG, Nimmo ER, Cummings FR, Soars D, et al.: Sequence variants in the autophagy gene IRGM and multiple other replicating loci contribute to Crohn's disease susceptibility. *Nat Genet* 2007, 39:830-832.

197. Prescott NJ, Dominy KM, Kubo M, Lewis CM, Fisher SA, Redon R, Huang N, Stranger BE, Blaszczyk K, Hudspith B, et al.: Independent and population-specific association of risk variants at the IRGM locus with Crohn's disease. *Hum Mol Genet* 2010, 19:1828-1839.

198. Porter EM, Bevins CL, Ghosh D, Ganz T: The multifaceted Paneth cell. *Cell Mol Life Sci* 2002, 59:156-170.

199. Hampe J, Franke A, Rosenstiel P, Till A, Teuber M, Huse K, Albrecht M, Mayr G, De La Vega FM, Briggs J, et al.: A genome-wide association scan of nonsynonymous SNPs identifies a susceptibility variant for Crohn disease in ATG16L1. *Nat Genet* 2007, 39:207-211.

200. Cadwell K, Liu JY, Brown SL, Miyoshi H, Loh J, Lennerz JK, Kishi C, Kc W, Carrero JA, Hunt S, et al.: A key role for autophagy and the autophagy gene Atg16l1 in mouse and human intestinal Paneth cells. *Nature* 2008, 456:259-263.

201. Liu B, Gulati AS, Cantillana V, Henry SC, Schmidt EA, Daniell X, Grossniklaus E, Schoenborn AA, Sartor RB, Taylor GA: Irgm1-deficient mice exhibit Paneth cell abnormalities and increased susceptibility to acute intestinal inflammation. *Am J Physiol Gastrointest Liver Physiol* 2013.

202. Matsuzawa T, Kim BH, Shenoy AR, Kamitani S, Miyake M, Macmicking JD: IFN-gamma elicits macrophage autophagy via the p38 MAPK signaling pathway. *J Immunol* 2012, 189:813-818.

203. Gavrilescu LC, Butcher BA, Del Rio L, Taylor GA, Denkers EY: STAT1 is essential for antimicrobial effector function but dispensable for gamma interferon production during Toxoplasma gondii infection. *Infect Immun* 2004, 72:1257-1264.

204. Thachil E, Hugot JP, Arbeille B, Paris R, Grodet A, Peuchmaur M, Codogno P, Barreau F, Ogier-Denis E, Berrebi D, et al.: Abnormal activation of autophagy-

induced crinophagy in Paneth cells from patients with Crohn's disease. *Gastroenterology* 2012, 142:1097-1099 e1094.

205. Kuma A, Matsui M, Mizushima N: LC3, an autophagosome marker, can be incorporated into protein aggregates independent of autophagy: caution in the interpretation of LC3 localization. *Autophagy* 2007, 3:323-328.

206. Szeto J, Kaniuk NA, Canadien V, Nisman R, Mizushima N, Yoshimori T, Bazett-Jones DP, Brumell JH: ALIS are stress-induced protein storage compartments for substrates of the proteasome and autophagy. *Autophagy* 2006, 2:189-199.

207. Komatsu M, Waguri S, Koike M, Sou YS, Ueno T, Hara T, Mizushima N, Iwata J, Ezaki J, Murata S, et al.: Homeostatic levels of p62 control cytoplasmic inclusion body formation in autophagy-deficient mice. *Cell* 2007, 131:1149-1163.

208. Clague MJ, Urbe S: Ubiquitin: same molecule, different degradation pathways. *Cell* 143:682-685.

209. Jacobson AD, Zhang NY, Xu P, Han KJ, Noone S, Peng J, Liu CW: The lysine 48 and lysine 63 ubiquitin conjugates are processed differently by the 26 s proteasome. *J Biol Chem* 2009, 284:35485-35494.

210. Geisler S, Holmstrom KM, Skujat D, Fiesel FC, Rothfuss OC, Kahle PJ, Springer W: PINK1/Parkin-mediated mitophagy is dependent on VDAC1 and p62/SQSTM1. *Nat Cell Biol* 12:119-131.

211. Waguri S, Komatsu M: Biochemical and morphological detection of inclusion bodies in autophagy-deficient mice. *Methods Enzymol* 2009, 453:181-196.

212. Johnston JA, Ward CL, Kopito RR: Aggresomes: a cellular response to misfolded proteins. *J Cell Biol* 1998, 143:1883-1898.

213. Klionsky DJ, Abdalla FC, Abeliovich H, Abraham RT, Acevedo-Arozena A, Adeli K, Agholme L, Agnello M, Agostinis P, Aguirre-Ghiso JA, et al.: Guidelines for the use and interpretation of assays for monitoring autophagy. *Autophagy* 2012, 8:445-544.

214. Tiwari S, Choi HP, Matsuzawa T, Pypaert M, MacMicking JD: Targeting of the GTPase Irgm1 to the phagosomal membrane via PtdIns(3,4)P(2) and PtdIns(3,4,5)P(3) promotes immunity to mycobacteria. *Nat Immunol* 2009, 10:907-917.

215. Collazo CM, Yap GS, Sempowski GD, Lusby KC, Tessarollo L, Vande Woude GF, Sher A, Taylor GA: Inactivation of LRG-47 and IRG-47 reveals a family of interferon gamma-inducible genes with essential, pathogen-specific roles in resistance to infection. *J Exp Med* 2001, 194:181-188.

216. Todaro GJ, Green H: Quantitative studies of the growth of mouse embryo cells in culture and their development into established lines. *J Cell Biol* 1963, 17:299-313.

217. Linares JF, Amanchy R, Greis K, Diaz-Meco MT, Moscat J: Phosphorylation of p62 by cdk1 controls the timely transit of cells through mitosis and tumor cell proliferation. *Mol Cell Biol* 2011, 31:105-117.

218. Kelliher MA, Grimm S, Ishida Y, Kuo F, Stanger BZ, Leder P: The death domain kinase RIP mediates the TNF-induced NF-kappaB signal. *Immunity* 1998, 8:297-303.

219. Komatsu M, Kurokawa H, Waguri S, Taguchi K, Kobayashi A, Ichimura Y, Sou YS, Ueno I, Sakamoto A, Tong KI, et al.: The selective autophagy substrate p62 activates the stress responsive transcription factor Nrf2 through inactivation of Keap1. *Nat Cell Biol* 2010, 12:213-223.

220. Lau A, Wang XJ, Zhao F, Villeneuve NF, Wu T, Jiang T, Sun Z, White E, Zhang DD: A noncanonical mechanism of Nrf2 activation by autophagy deficiency: direct interaction between Keap1 and p62. *Mol Cell Biol* 2010, 30:3275-3285.

221. Zhao Z, Fux B, Goodwin M, Dunay IR, Strong D, Miller BC, Cadwell K, Delgado MA, Ponpuak M, Green KG, et al.: Autophagosome-independent essential function for the autophagy protein Atg5 in cellular immunity to intracellular pathogens. *Cell Host Microbe* 2008, 4:458-469.

222. Wilm M, Shevchenko A, Houthaeve T, Breit S, Schweigerer L, Fotsis T, Mann M: Femtomole sequencing of proteins from polyacrylamide gels by nano-electrospray mass spectrometry. *Nature* 1996, 379:466-469.

223. Goldberg AL: Development of proteasome inhibitors as research tools and cancer drugs. *J Cell Biol* 2012, 199:583-588.

224. Yarmolinsky MB, Haba GL: INHIBITION BY PUROMYCIN OF AMINO ACID INCORPORATION INTO PROTEIN. *Proc Natl Acad Sci U S A* 1959, 45:1721-1729.

225. Nathans D: PUROMYCIN INHIBITION OF PROTEIN SYNTHESIS: INCORPORATION OF PUROMYCIN INTO PEPTIDE CHAINS. *Proc Natl Acad Sci U S A* 1964, 51:585-592.

226. Lelouard H, Ferrand V, Marguet D, Bania J, Camosseto V, David A, Gatti E, Pierre P: Dendritic cell aggresome-like induced structures are dedicated areas for ubiquitination and storage of newly synthesized defective proteins. *J Cell Biol* 2004, 164:667-675.

227. Degrandi D, Kravets E, Konermann C, Beuter-Gunia C, Klumpers V, Lahme S, Wischmann E, Mausberg AK, Beer-Hammer S, Pfeffer K: Murine guanylate binding protein 2 (mGBP2) controls Toxoplasma gondii replication. *Proc Natl Acad Sci U S A* 2013, 110:294-299.

228. Taylor GA, Jeffers M, Largaespada DA, Jenkins NA, Copeland NG, Woude GF: Identification of a novel GTPase, the inducibly expressed GTPase, that accumulates in response to interferon gamma. *J Biol Chem* 1996, 271:20399-20405.

229. Zhao YO, Khaminets A, Hunn JP, Howard JC: Disruption of the Toxoplasma gondii parasitophorous vacuole by IFNgamma-inducible immunity-related GTPases (IRG proteins) triggers necrotic cell death. *PLoS Pathog* 2009, 5:e1000288.

Biography

Maria Kathleen Traver was born the second of three children to Mark and Laura Happel in Newport News, VA. Following family tradition, she attended the College of William and Mary in Williamsburg, VA. While there, she studied with Dr. John C Poutsma (and later with Dr. Paul Wenthold of Purdue University), researching the thermochemical properties of gas-phase amino acids as a Howard Hughes Undergraduate Research Scholar and Beckman Scholar. She eventually graduated summa cum laude with highest honors with a BS degree in Chemistry in May 2007.

Upon graduation, Maria received a James B Duke fellowship to pursue a doctoral education at Duke University in Durham, NC, in Molecular Genetics and Microbiology, joining the laboratory of Dr. Gregory Taylor. While at Duke, Maria participated in the Society for Duke Fellows and became a Duke Scholar in Infectious Diseases. She has published her early work in the Journal of Biological Chemistry ("Immunity-related GTPase M (IRGM) Proteins Influence the Localization of Guanylate-binding Protein 2 (GBP2) by Modulating Macroautophagy," Sept 2, 2011, 286(35): 30471), and contributed to a chapter in the Encyclopedia of Signaling Molecules ("IRG: Immunity-related GTPases," Springer 2013).

Outside of the laboratory, Maria enjoys reading science fiction and fantasy novels; she is also an avid Irish stepdancer, competing at local and regional competitions across the southern United States as a preliminary champion.